

Electronic Supplementary Information for:

**Maximizing the Thiol-Activated Photodynamic and
Fluorescence Imaging Functionalities of Theranostic
Reagents by Modularization of the Bodipy-based Dyad
Triplet Photosensitizers**

Jianzhang Zhao,^{a,} Ling Huang,^a Xiaoneng Cui,^a Shujing Li^b and Huijian Wu^{b,*}*

^a State Key Laboratory of Fine Chemicals, School of Chemical Engineering, Dalian University of
Technology, Dalian 116024, P. R. China. E-mail: zhaojzh@dlut.edu.cn

Web: <http://finechem2.dlut.edu.cn/photochem>

^b School of Life Science and Biotechnology, Dalian University of Technology, Dalian 116024, P. R.
China. E-mail: wuhj@dlut.edu.cn

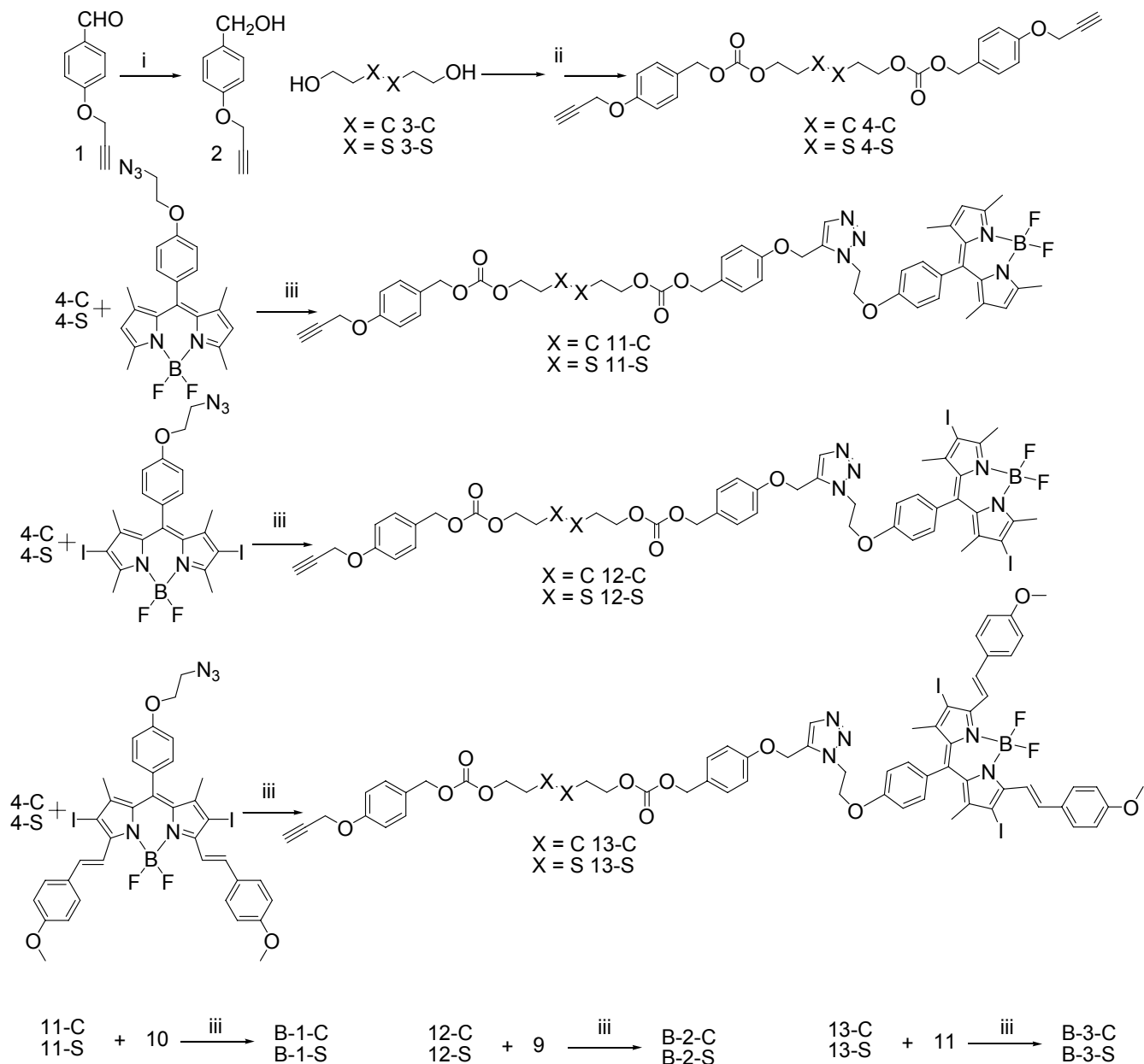
Index

General information.....	S3
Synthesis procedure and characterization data	S4–1
Figure S1-S47. ¹ H NMR, ¹³ C NMR and HRMS.....	S14–38
Figure S48-S49. UV-vis absorption and fluorescence spectra for B-1-C–B-3-C	S38–3
Figure S50-S51. Fluorescence spectra and the kinetics of 9 in presence of Cys.....	S39–40
Figure S52. the kinetics of B-3-S in presence of Cys.....	S40
Figure S53. The fluorescence excitation spectra of B-1-S and 10 in the presence of Cys.....	S41
Figure S54. Response of B-3-S to different analytes.....	S41
Figure S55-S58. UV-vis absorption and fluorescence spectra of 10, 11, B-3-S, B-3-C	S42–4
Figure S59-S70. Nanosecond time-resolved transient absorption spectra	S44–54
Figure S71. The fluorescence spectra of B-3-S and 11 in toluene.....	S55
Figure S72-73. The fluorescence excitation spectra of B-3-C, B-3-S	S55–56
Figure S74-S76. CV of B-1-S, B-3-S, 15 and the process of calculation.....	S56–59
Scheme S4. The photophysical processes of B-3-S	S60
Figure S77-S80. Switch singlet oxygen in presence of Cys for B-1-C and B-4	S61–64
Figure S81. Confocal laser fluorescence microscopic images of HeLa cells of B-1-C	S65
Figure S82. PDT effect of in different condition.....	S65
Figure S83. MTT assay of the PDT studies.....	S65

General Information:

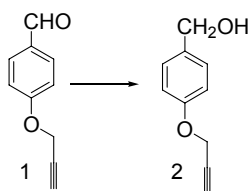
UV-Vis absorption spectra were taken on a HP8453 UV-visible spectrophotometer. Fluorescence spectra were recorded on a Shimadzu RF 5301PC spectrofluorometer. Luminescence lifetimes were measured on a OB920 fluorescence/phosphorescence lifetime spectrometer (Edinburgh Instruments, UK). The nanosecond time-resolved transient difference absorption spectra were detected by Edinburgh LP920 instruments (Edinburgh Instruments, UK). The signal was buffered on a Tektronix TDS 3012B oscilloscope and was analyzed by the LP900 software. All samples in flash photolysis experiments were deaerated with argon for ca. 15 min before measurement and the gas flow is kept during the measurement.

Scheme S1: The synthesis steps of target molecule and control compounds.^a



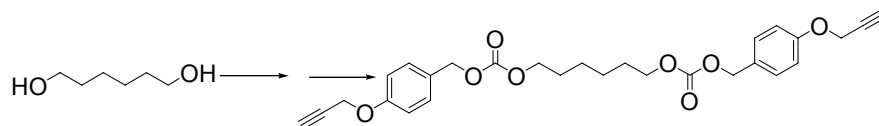
^a **Key:** (i) EtOH, NaBH₄, rt 98%; (ii) THF, DMAP, triphosgene, compound 2, 15%; (iii) CHCl₃/EtOH/H₂O = 12/1/1, CuSO₄·5H₂O, sodium ascorbate.

Preparation of compound 2



Compound 2: Compound 1 (1.6 g, 10 mmol) were dissolved in EtOH (50 mL), then NaBH_4 (12.0 mmol, 460 mg) was added during 10 min and TLC monitor the reaction in room temperature. After completion of the reaction, the reaction was quenched for acetic acid. The solution was extracted with dichloromethane (3×60 mL), and Na_2SO_4 dry the solution. After removal of the solvent under reduced pressure, This compound is applied directly to the next step. colorless oil liquid. Yield: (1.58 g, 98 %). $^1\text{H NMR}$ (500 MHz, CDCl_3): δ = 7.25 (d, 2H, J = 8.0 Hz), 6.94 (d, 2H, J = 7.6 Hz), 4.66 (s, 2H), 4.54 (s, 2H), 2.51 (s, 1H), 2.38 ppm (s, 2H).

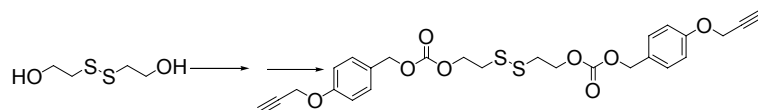
Preparation of 4-C



4-C: Under Ar atmosphere, a mixture of DMAP (61.0 mg, 0.5 mmol) and triphosgene (2.96 g, 10.0 mmol), were dissolved in dry THF (100 mL), and stir for 0.5 h in room temperature. And 1,6-dihexanediol (1.18 g, 10.0 mmol) was dissolved in 10 mL THF, The solution was added during 10 min and reacted in room temperature for 12 h. The solution was bubbled N_2 for an hour in order to removed the more phosgene. After removal of the solvent under reduced pressure and filter the white solid. The colorless oil was dissolved in 50 mL dry DCM in ice bath. And pyridine (5 mL) was added. Compound 2 (3.32 g, 20 mmol) also was dissolved DCM (20 mL). the compound 2 solution was added during 30 min. The mixture was stir for 24 h in room temperature, and TLC monitor the reaction. After completion of the reaction, the

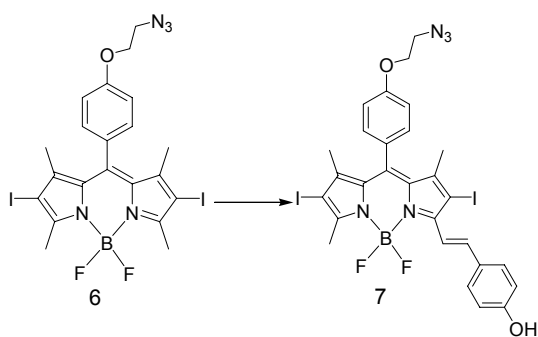
mixture was added 50 mL of water, and extracted with dichloromethane (3×60 mL), and Na₂SO₄ dry the solution. After removal of the solvent under reduced pressure, the mixture was purified by column chromatography (silica gel, DCM/ petroleum = 1:1 v/v) to give white solid. Yield: (1.49 g, 15 %). ¹H NMR (500 MHz, CDCl₃): δ = 7.35–7.32 (d, 4H, *J* = 10.5 Hz), 6.97 (d, 4H, *J* = 11.0 Hz), 5.09 (s, 4H), 4.69 (s, 4H), 4.14–4.10 (m, 4H), 2.51 (s, 2H), 1.67–1.64 (m, 4H), 1.38 ppm (m, 4H).

Preparation of 4-S



The same synthesis steps for **4-C**. ¹H NMR (500 MHz, CDCl₃): δ = 7.35 (d, 4H, *J* = 8.5 Hz), 6.97 (d, 4H, *J* = 8.5 Hz), 5.10 (s, 4H), 4.69 (s, 4H), 4.38–4.35 (m, 4H), 2.94–2.92 (m, 4H), 2.53 ppm (s, 2H).

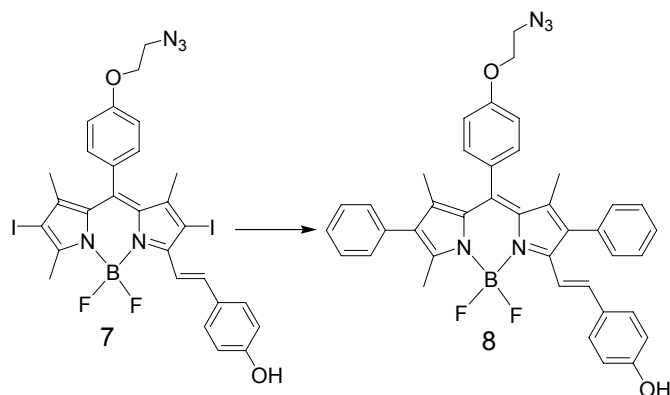
Preparation of Compound 7.



Compound 7: Under Ar atmosphere, a mixture of compound 6 (335.5 mg, 0.5 mmol) and 4-hydroxybenzaldehyde (120 mg, 1.0 mmol), were dissolved in dry toluene (50 mL), then 1.0 mL acetic acid and 1.0 mL piperidine was added. The mixture was refluxed for 0.5 h. After completion of the reaction, the mixture was cooled to room temperature, was added 50 mL of

water, and extracted with dichloromethane (3×100 mL), and Na₂SO₄ dry the solution. After removal of the solvent under reduced pressure, the mixture was purified by column chromatography (silica gel, DCM) to give deep purple solid. Yield: (45.9 mg, 12 %). ¹H NMR (500 MHz, CDCl₃): δ = 8.12 (d, 1H, *J* = 20.0 Hz), 7.55–7.50 (m, 3H), 7.19(d, 2H, *J* = 8.5 Hz), 7.08 (d, 2H, *J* = 8.5 Hz), 6.85 (d, 2H, *J* = 10.0 Hz), 5.06 (s, 1H), 4.24 (d, 2H, *J* = 9.5 Hz), 3.70 (d, 2H, *J* = 9.5 Hz), 2.74 (s, 3H), 1.49 (s, 3H), 1.45 ppm (s, 3H). HRMS (MALDI): *m/z* calcd for [C₂₈H₂₄BI₂F₂N₅]⁺: 765.0081; found 765.0089

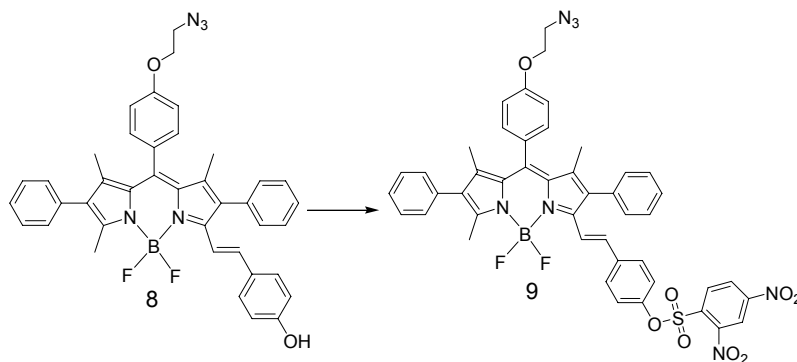
Preparation of Compound 8.



Compound 8: Under Ar atmosphere, a mixture of compound 7 (30.0 mg, 0.040 mmol) and phenylboronic acid (48 mg, 0.4 mmol), K₂CO₃ (16.8mg, 0.12 mmol), were dissolved in toluene/EtOH/H₂O (5/5/3, v/v/v, 13 mL). and Pd(PPh₃)₄ (0.004 mmol, 4.8 mg). The mixture was refluxed for 0.5 h. After completion of the reaction, the mixture was cooled to room temperature, was added 15 mL of water, and extracted with dichloromethane (3×10 mL), and Na₂SO₄ dry the solution. After removal of the solvent under reduced pressure, the mixture was purified by column chromatography (silica gel, DCM) to give deep purple solid. Yield: (25.6 mg, 95 %). ¹H NMR (500 MHz, CDCl₃): δ = 7.57 (d, 1H, *J* = 15.0 Hz), 7.42–7.36 (m, 5H), 7.35–7.27 (m, 3H), 7.25–7.24 (m, 2H), 7.19 (d, 2H, *J* = 10.5 Hz), 7.14 (d, 2H, *J* = 10.0 Hz), 7.05 (d, 2H, *J*

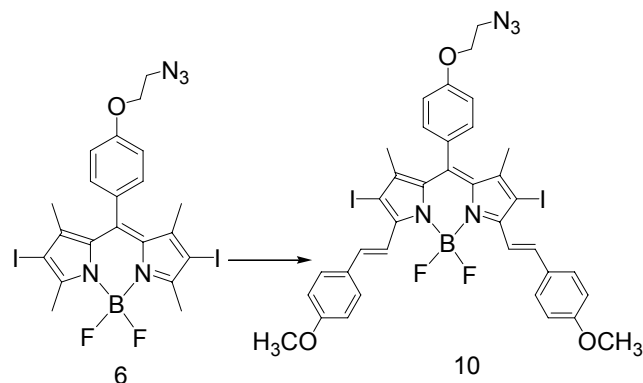
= 10.0 Hz), 6.73 (d, 2H, J = 10.5 Hz), 6.46 (d, 1H, J = 15.0 Hz), 5.06 (s, 1H), 4.20–4.18 (m, 3H), 3.66–3.64 (m, 2H), 2.58 (s, 3H), 1.38 (s, 3H), 1.27 ppm (s, 3H). HRMS (MALDI): m/z calcd for $[C_{40}H_{34}BF_2N_5O_2]^+$: 665.2774; found 665.2755.

Preparation of Compound 9.



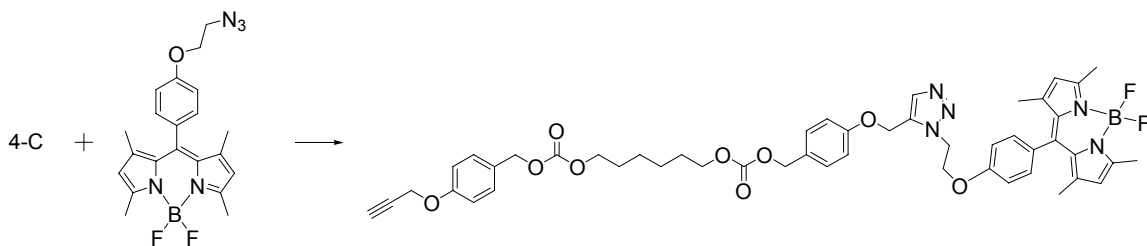
Compound 9: Under Ar atmosphere, a mixture of compound **8** (20.0 mg, 0.030 mmol) was dissolved in dry DCM (10 mL), and TEA (0.1 mL) was added in ice bath. 2,4-dinitrosulfonylchloride (19.3 mg, 0.050 mmol) was dissolved in DCM (5 mL) and was added during 5 min. the mixture was stirred 30 min. After completion of the reaction, the mixture was added 15 mL of water, and extracted with dichloromethane (3×10 mL), and Na₂SO₄ dry the solution. After removal of the solvent under reduced pressure, the mixture was purified by column chromatography (silica gel, DCM/PE = 1/1 v/v) to give deep purple solid. Yield: (25.5 mg, 95 %). ¹H NMR (500 MHz, CDCl₃): δ = 8.65 (s, 1H), 8.48–8.45 (m, 1H), 8.11 (d, 1H, J = 5.0 Hz), 7.62 (d, 1H, J = 15.0 Hz), 7.43–7.32 (m, 6H), 7.29 (d, 2H, J = 10.0 Hz), 7.24–7.21 (m, 4H), 7.18 (d, 2H, J = 10.0 Hz), 7.08–7.04 (m, 4H), 6.42 (d, 1H, J = 15.0 Hz), 4.21–4.19 (d, 2H, J = 10.0 Hz), 3.66–3.64 (m, 2H), 2.57 (s, 3H), 1.39 (s, 3H), 1.27 ppm (s, 3H). HRMS (MALDI): m/z calcd for $[C_{46}H_{36}BSF_2N_7O_2]^+$: 895.2407; found 895.2421, [M-DNS]⁺ 665.2816, DNS is 2,4-dinitrosulfonyl group.

Preparation of Compound 10.



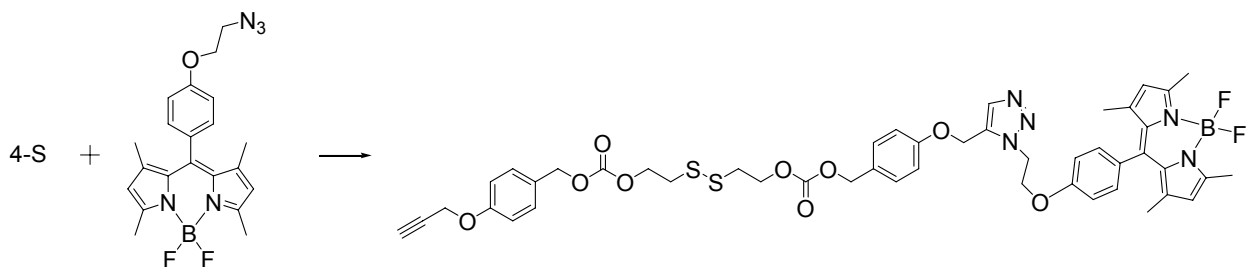
Compound 10: Under Ar atmosphere, a mixture of compound 6 (335.5 mg, 0.5 mmol) and 4-methoxybenzaldehyde (680.0 mg, 5.0 mmol), were dissolved in dry toluene (50 mL), then 1.0 mL acetic acid and 1.0 mL piperidine was added. The mixture was refluxed for 2 h. After completion of the reaction, the mixture was cooled to room temperature, was added 50 mL of water, and extracted with dichloromethane (3×100 mL), and Na₂SO₄ dry the solution. After removal of the solvent under reduced pressure, the mixture was purified by column chromatography (silica gel, DCM/PE = 2/1 v/v) to give deep black solid. Yield: (313.9 mg, 70 %). ¹H NMR (500 MHz, CDCl₃): δ = 8.15 (d, 2H, *J* = 15.0 Hz), 7.62–7.57 (m, 6H), 7.21 (d, 2H, *J* = 10.0 Hz), 7.08–7.05 (m, 2H), 6.98–6.95 (m, 4H), 4.24–4.22 (m, 2H), 3.87 (s, 6H), 3.69–3.68 (m, 2H), 1.43 ppm (s, 6H). HRMS (MALDI): *m/z* calcd for [C₃₇H₃₂BI₂F₂O₃N₅]⁺: 897.0656; found 897.0625.

Preparation of 11-C.



11-C: Under Ar atmosphere, a mixture of compound 5 (45.0 mg, 0.1 mmol), 4-C (149.1 mg, 0.3 mmol) and $\text{CuSO}_4 \cdot 5\text{H}_2\text{O}$ (0.05 mmol, 5.0 mg) were dissolved in $\text{CHCl}_3/\text{EtOH}/\text{H}_2\text{O}$ (12/1/1, v/v/v, 12 mL), then sodium ascorbate (0.05 mmol, 4.9 mg) was added. The mixture was stirred in room temperature for 24 h. After completion of the reaction, the mixture was added 50 mL of water, and extracted with dichloromethane (3×50 mL), and Na_2SO_4 dry the solution. After removal of the solvent under reduced pressure, the mixture was purified by column chromatography (silica gel, $\text{DCM}/\text{EtOAc} = 5/1$ v/v) to give orange solid. Yield: (36.1 mg, 42 %). $^1\text{H NMR}$ (500 Hz, CDCl_3): $\delta = 7.84$ (s, 1H), 7.34–7.32 (m, 4H), 7.19 (d, 2H, $J = 10.0$ Hz), 6.99–6.95 (m, 6H), 5.97 (s, 2H), 5.25 (s, 2H), 5.10 (d, 4H, $J = 7.6$ Hz), 4.82–4.81 (m, 2H), 4.69 (d, 2H, $J = 7.5$ Hz), 4.44–4.43 (m, 2H), 4.13–4.10 (m, 4H), 2.55 (s, 6H), 2.52 (s, 1H), 1.67–1.63 (m, 4H), 1.40 (s, 6H), 1.38–1.36 ppm (m, 4H). HRMS (MALDI): m/z calcd for $[\text{C}_{49}\text{H}_{52}\text{BF}_2\text{O}_9\text{N}_5]^+$: 903.3826; found 903.3870.

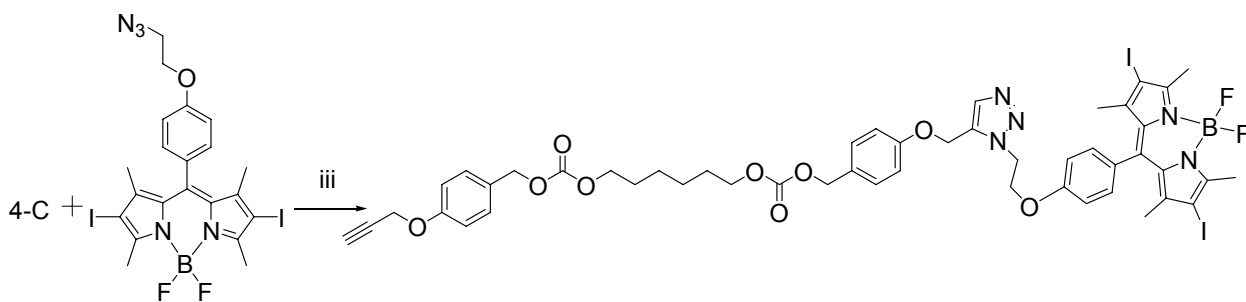
Preparation of 11-S.



11-S: The same synthesis steps for **11-S**. $^1\text{H NMR}$ (500 Hz, CDCl_3) $\delta = 7.88$ (s, 1H), 7.34 (d, 4H, $J = 10.0$ Hz), 7.19 (d, 2H, 5.0 Hz), 7.00–6.95 (m, 6H), 5.95 (s, 2H), 5.28 (s, 2H), 5.11–5.09 (m,

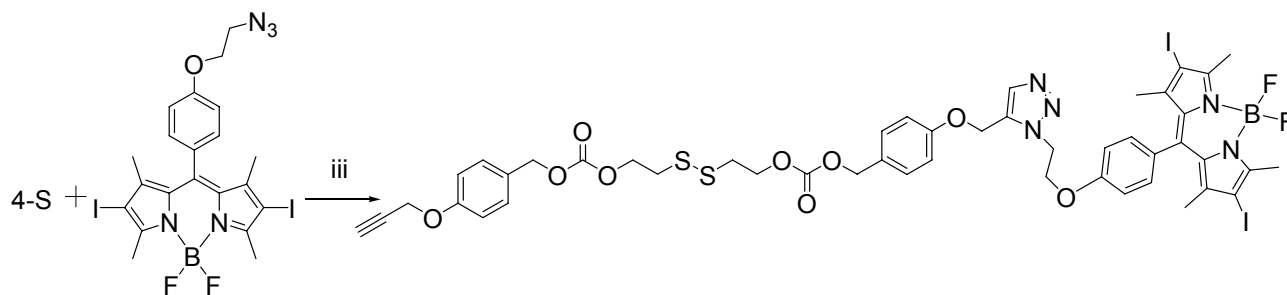
4H), 4.83 (s, 2H), 4.70–4.68 (m, 2H), 4.44 (s, 2H), 4.38–4.34 (m, 4H), 2.94–2.91(m, 4H), 2.54 (s, 6H), 2.52 (s, 1H), 1.39 ppm (s, 6H). HRMS (MALDI): m/z calcd for $[C_{47}H_{48}BSF_2O_9N_5]^+$: 939.2955; found 939.2978.

Preparation of 12-C.



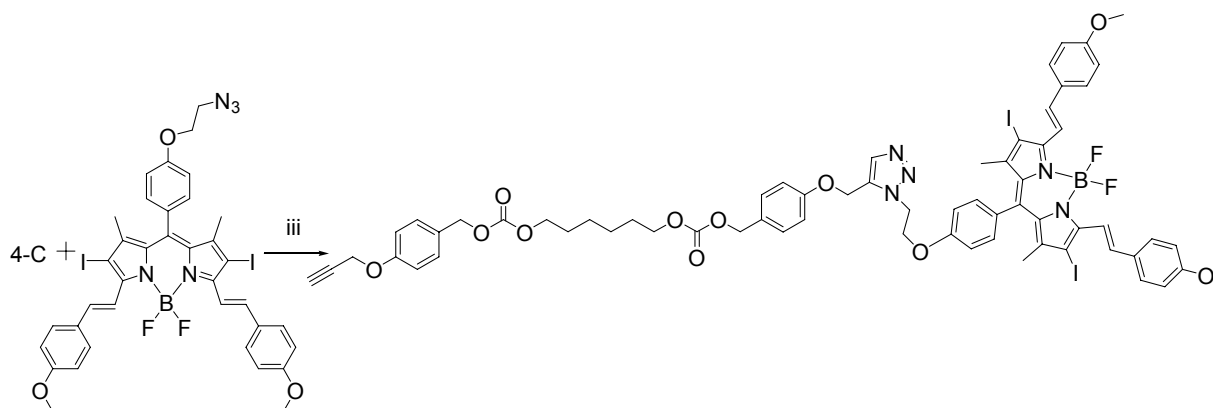
12-C: Under Ar atmosphere, a mixture of compound 6 (66.7 mg, 0.1 mmol), 4-C (149.1 mg, 0.3 mmol) and $CuSO_4 \cdot 5H_2O$ (0.05 mmol, 5.0 mg) were dissolved in $CHCl_3/EtOH/H_2O$ (12/1/1, v/v/v, 14 mL), then sodium ascorbate (0.05 mmol, 4.9 mg) was added. The mixture was stirred in room temperature for 24 h. After completion of the reaction, the mixture was added 50 mL of water, and extracted with dichloromethane (3×50 mL), and Na_2SO_4 dry the solution. After removal of the solvent under reduced pressure, the mixture was purified by column chromatography (silica gel, DCM/EtOAc = 5/1 v/v) to give orange solid. Yield: (53.0 mg, 45 %). 1H NMR (500 Hz, $CDCl_3$) δ = 7.83 (s, 1H), 7.34 (d, 4H, J = 5.0 Hz), 7.16 (d, 2H, J = 10.0 Hz), 7.00–6.95 (m, 6H), 5.25 (s, 2H), 5.08 (s, 4H), 4.84–4.82 (m, 2H), 4.47–4.45 (m, 2H), 4.13–4.10 (m, 4H), 2.64 (s, 6H), 2.52 (s, 1H), 1.65–1.64 (m, 4H), 1.41 (s, 6H), 1.38–1.36 ppm (m, 4H) HRMS (MALDI): m/z calcd for $[C_{49}H_{50}BF_2O_9N_5I_2 + Na]^+$: 1178.1657; found 1178.1621.

Preparation of 12-S.



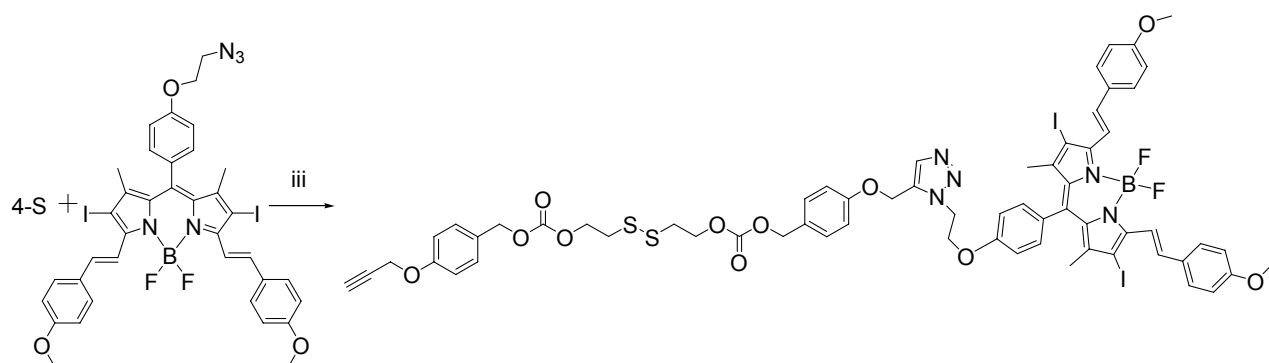
12-S: The same synthesis steps for **12-C**. Yield: 43.1 mg (39 %). $^1\text{H NMR}$ (500 Hz, CDCl_3) δ = 7.83 (s, 1H), 7.34 (d, 4H, J = 10.0 Hz), 7.16 (d, 2H, J = 10.5 Hz), 7.00–6.95 (m, 6H), 5.24 (s, 2H), 5.10 (d, 4H, J = 5 Hz), 4.84–4.82 (m, 2H), 4.70–4.68 (m, 2H), 4.47–4.45 (m, 2H), 4.38–4.34 (m, 4H), 2.94–2.91 (m, 4H), 2.63 (s, 6H), 2.52 (s, 1H), 1.41 ppm (s, 6H). HRMS (MALDI): m/z calcd for $[\text{C}_{47}\text{H}_{46}\text{BF}_2\text{O}_9\text{N}_5\text{I}_2\text{S}_2]^+$: 1191.0888; found 1191.0959.

Preparation of 13-C.



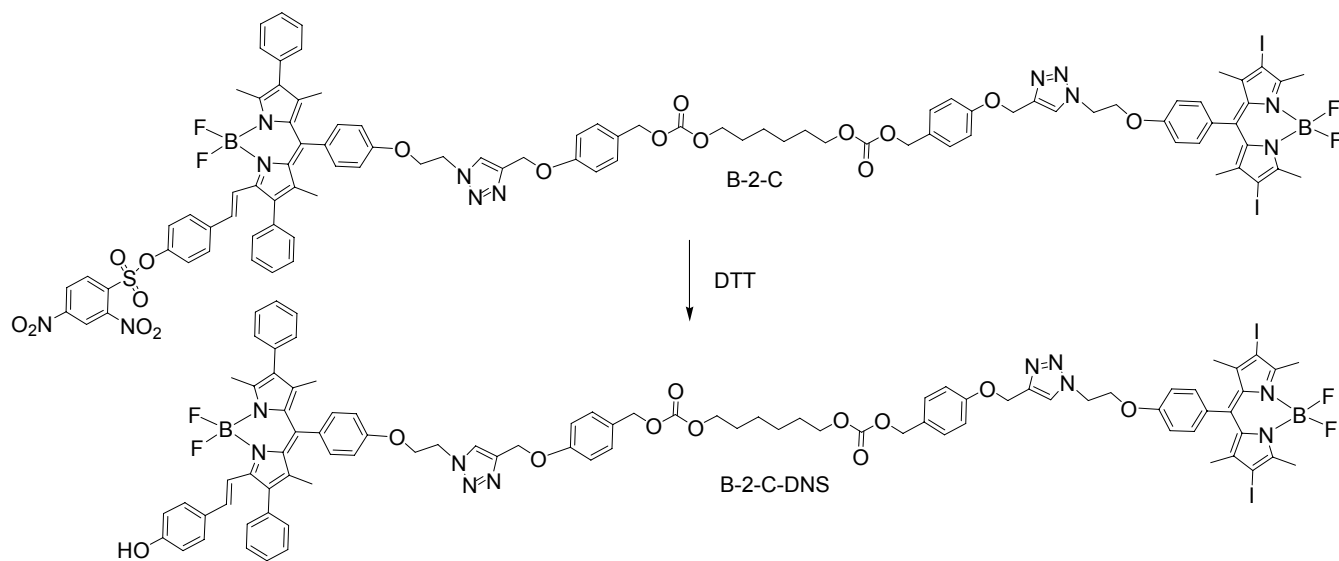
The same synthesis steps for **12-C**. Yield: (62.1 mg, 51 %). $^1\text{H NMR}$ (500 Hz, CDCl_3) δ = 8.15 (d, 2H, J =15.0 Hz), 7.84 (s, 1H), 7.62–7.60 (m, 6 H), 7.35–7.32 (m, 4H), 7.19–7.17 (d, 2H, J =10.0 Hz), 7.01–6.94 (m, 10 H), 5.25 (s, 2 H), 5.08 (s, 4H), 4.84–4.82(m, 2 H), 4.69 (s, 2H), 4.47–4.45 (m, 2 H), 4.12–4.10 (m, 4 H), 3.86 (s, 6H), 2.52 (s, 1H), 1.65–1.63 (m, 7H), 1.47 (s, 6H), 1.38–1.36 ppm (m, 4H). HRMS (MALDI): m/z calcd for $[\text{C}_{65}\text{H}_{61}\text{BF}_2\text{O}_{11}\text{N}_5\text{I}_2]^+$: 1391.2520; found 1391.2546.

Preparation of 13-S.



The same synthesis steps for **12-C**. Yield: (47.1 mg, 41 %). $^1\text{H NMR}$ (500 Hz, CDCl_3) δ = 8.15 (d, 2H, J = 15.0 Hz), 7.84 (s, 1H), 7.62–7.57 (m, 6 H), 7.34–7.32 (m, 4H), 7.19–7.17 (d, 2H, J = 10.0 Hz), 7.01–6.94 (m, 10 H), 5.25 (s, 2 H), 5.10 (s, 4H), 4.84–4.82 (m, 2 H), 4.69 (s, 2H), 4.47–4.45 (m, 2 H), 4.39–4.35 (m, 4 H), 3.86 (s, 6H), 2.94–2.91 (m, 4 H), 2.52 (s, 1H), 1.46 ppm (s, 6H). HRMS (MALDI): m/z calcd for $[\text{C}_{63}\text{H}_{57}\text{BF}_2\text{O}_{11}\text{N}_5\text{I}_2\text{S}_2]^+$: 1427.1650; found 1427.1642.

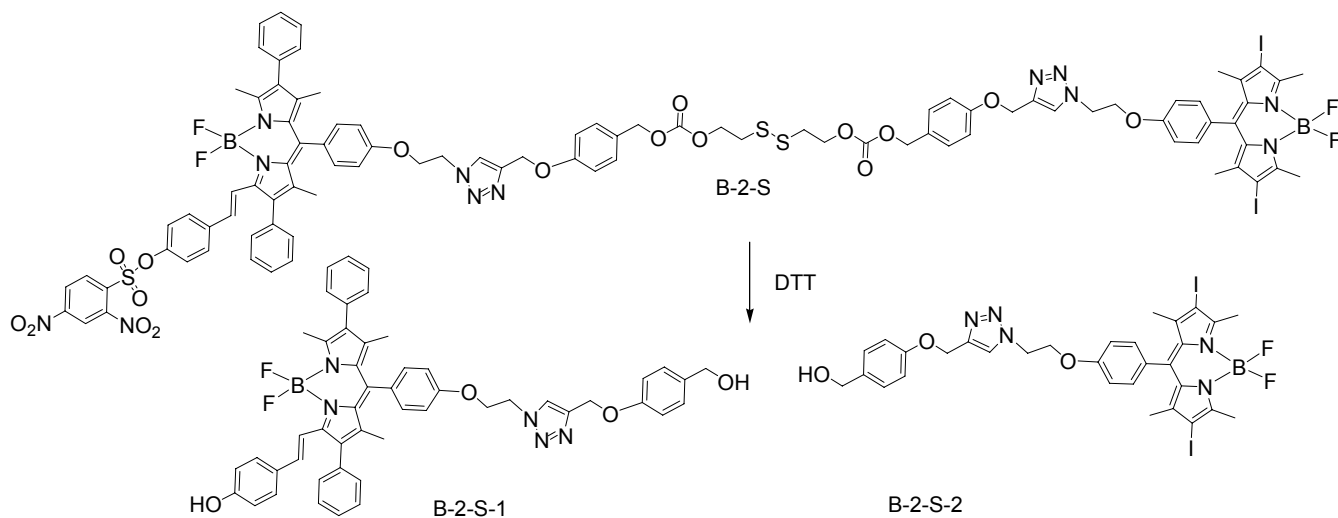
Scheme S2. The proof mechanism process of B-2-C and preparation of B-2-C-DNS



Preparation of B-2-C-DNS.

A mixture of compound B-2-C (20.1 mg, 0.01 mmol), DTT (10.2 mg, 0.05 mmol) were dissolved in EtOH (20 mL). The mixture was stirred in room temperature for 0.5 h. After completion of the reaction, the mixture was added 10 mL of water, and extracted with dichloromethane (3×20 mL), and Na₂SO₄ dry the solution. After removal of the solvent under reduced pressure, the mixture was purified by column chromatography (silica gel, DCM/EtOAc = 5/2 v/v) to give black solid. Yield: (15.6 mg, 85 %). ¹HNMR (500 Hz, CDCl₃) δ = 7.84 (d, 2H, *J* = 12.0 Hz), 7.73–7.70 (m, 2H), 7.56–7.52 (m, 3H), 7.40–7.29 (m, 10H), 7.23 (d, 2H, *J* = 5.0 Hz), 7.18 (d, 2H, *J* = 5.0 Hz), 7.14–7.12 (m, 2H), 6.99–6.94 (m, 8H), 6.74 (d, 2H, *J* = 10.0 Hz), 6.47 (d, 1H, *J* = 15.0 Hz), 6.05 (s, 1H), 5.23 (s, 2H), 5.20 (s, 2H), 5.05 (d, 4H, *J* = 5.0 Hz), 4.83–4.79 (m, 4H), 4.45–4.40 (m, 4H), 4.12–4.09 (m, 4H), 2.63 (s, 6H), 2.57 (s, 3H), 1.64 (s, 8H), 1.40 (s, 6H), 1.34 ppm (s, 6H). HRMS (MALDI): *m/z* calcd for [C₈₉H₈₄B₂F₄O₁₁N₁₀I₂]⁺: 1820.4533; found 1820.4510.

Scheme S3. The proof of mechanism process of B-2-S and preparation of B-2-C-DNS



Preparation of B-2-S-1 and B-2-S-2.

A mixture of compound B-2-S (20.6 mg, 0.01 mmol), DTT (10.2 mg, 0.05 mmol) were dissolved in EtOH (20 mL). The mixture was stirred in room temperature for 0.5 h. After completion of the reaction, the mixture was added 10 mL of water, and extracted with dichloromethane (3×20 mL), and Na₂SO₄ dry the solution. After removal of the solvent under reduced pressure, the mixture was purified by column chromatography (silica gel, DCM/EtOAc = 5/2 v/v) to give red solid and black solid. For **B-2-S-1** ¹H NMR (500 Hz, CDCl₃) δ = 7.81 (s, 1 H), 7.72–7.70 (m, 2H), 7.56–7.52 (m, 3H), 7.39–7.35 (m, 5H), 7.32–7.27 (m, 2H), 7.24–7.22 (m, 3H), 7.17 (d, 2H, *J* = 7.0 Hz), 7.12 (d, 2H, *J* = 8.5 Hz), 6.96–6.94 (m, 4H), 6.73–6.71 (d, 2H, *J* = 8.5 Hz), 6.47 (d, 1H, *J* = 15.0 Hz), 5.20 (s, 1H), 4.79–4.77 (m, 2H), 4.60 (s, 2H), 4.44–4.39 (m, 2H), 2.57 (s, 3H), 1.34 (s, 3H), 1.23 ppm (s, 3H). HRMS (MALDI): *m/z* calcd for [C₅₀H₄₄BF₂O₄N₅]⁺: 827.3454; found 827.3427.

For **B-2-S-2** ¹H NMR (500 Hz, CDCl₃) δ = 7.84 (s, 1H), 7.73–7.70, 7.54–7.51 (m, 1H), 7.31 (d, 2H, *J* = 8.5 Hz), 7.15 (d, 2H, *J* = 6.5 Hz), 7.01–6.97 (m, 4H), 5.25 (s, 2H), 4.84–4.82 (m, 2H), 4.63 (s, 2H), 4.47–4.45 (m, 3H), 2.64 (s, 3H), 1.41 ppm (s, 6 H). HRMS (MALDI): *m/z* calcd for [C₃₁H₃₀BF₂O₃N₅I₂]⁺: 823.0499; found 823.0515.

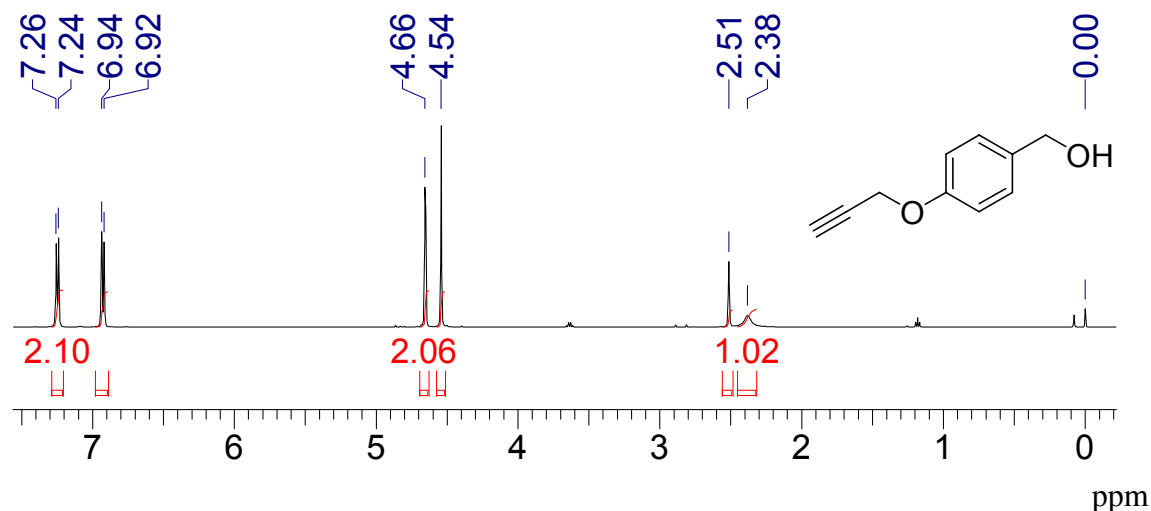


Figure S1. ¹H NMR of compound 2 (400 MHz, CDCl₃).

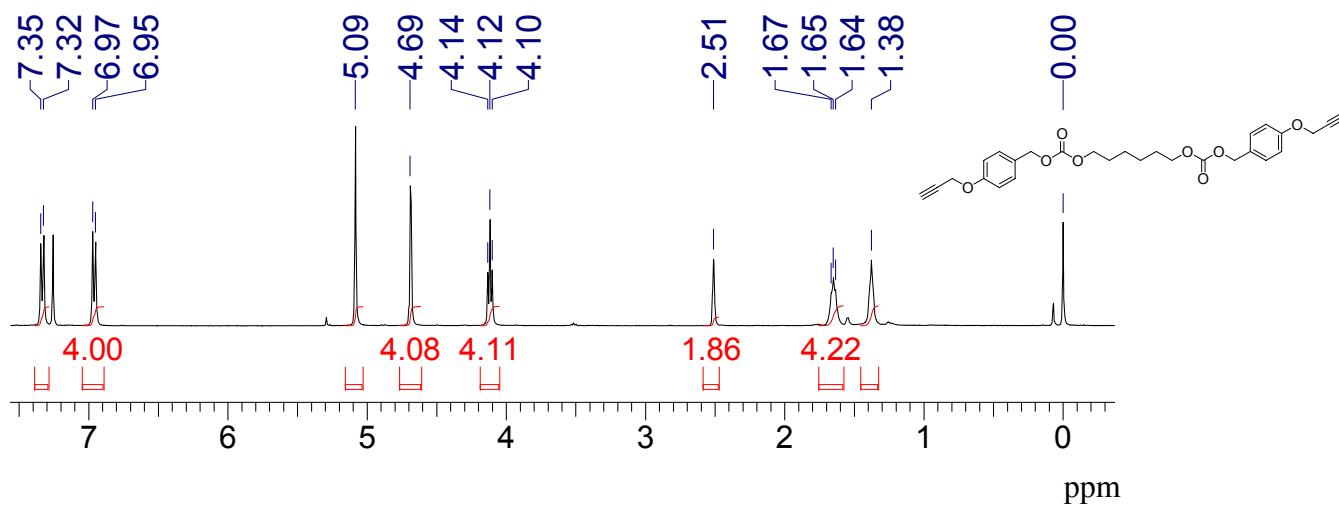


Figure S2. ^1H NMR of 4-C (400 MHz, CDCl_3).

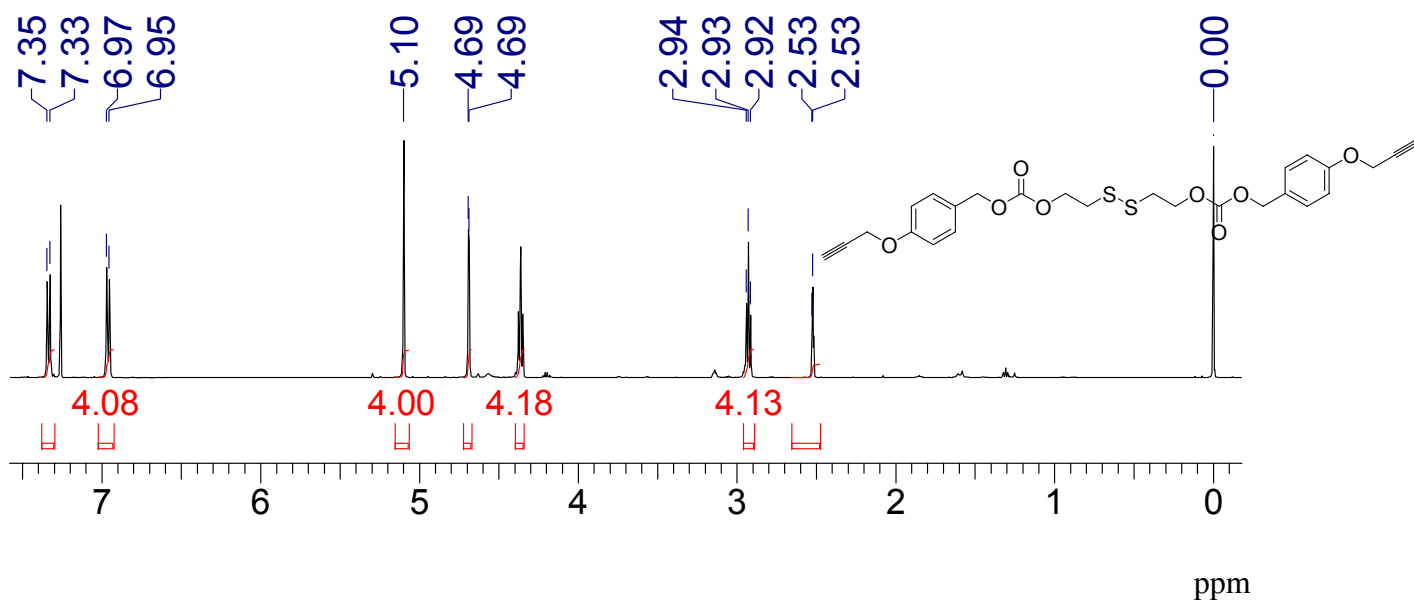


Figure S4. ^1H NMR of 4-S (500 MHz, CDCl_3).

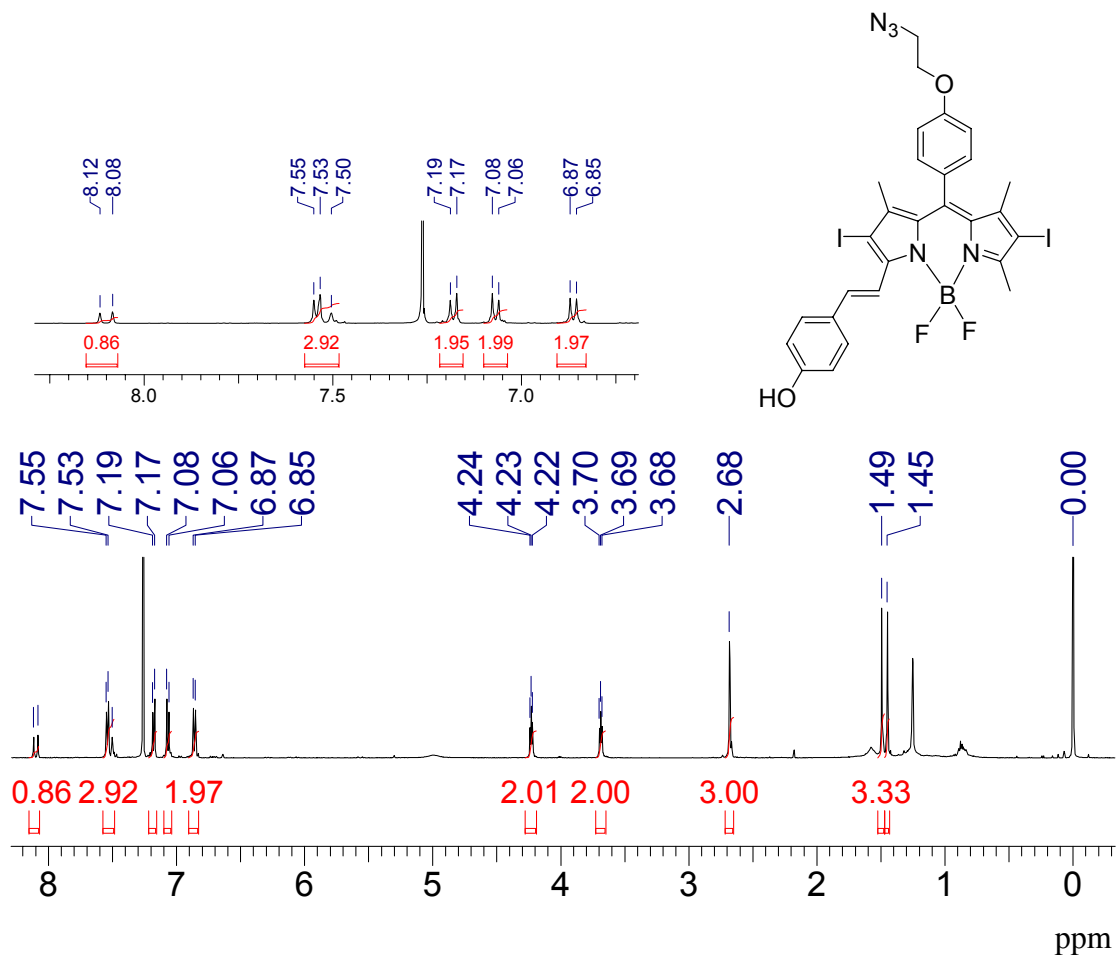


Figure S6. ¹H NMR of compound **7** (500 MHz, CDCl₃).

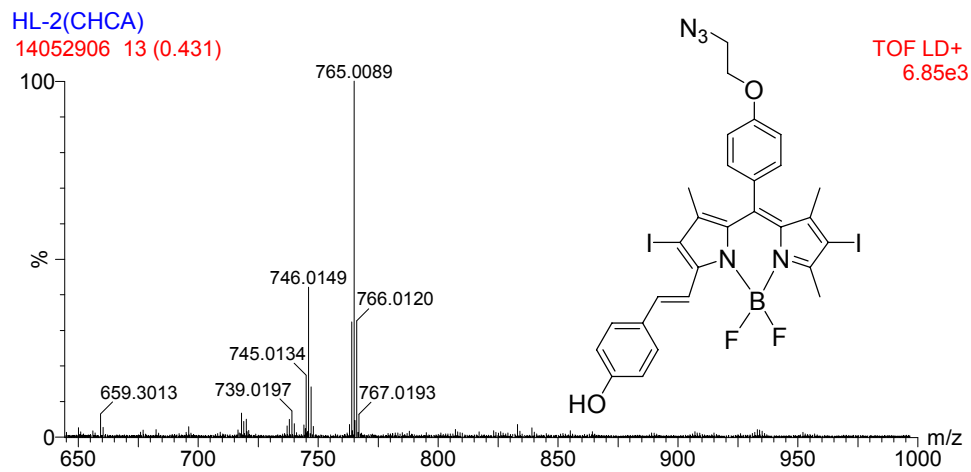


Figure S7. TOF HRMS (MALDI) of compound 7.

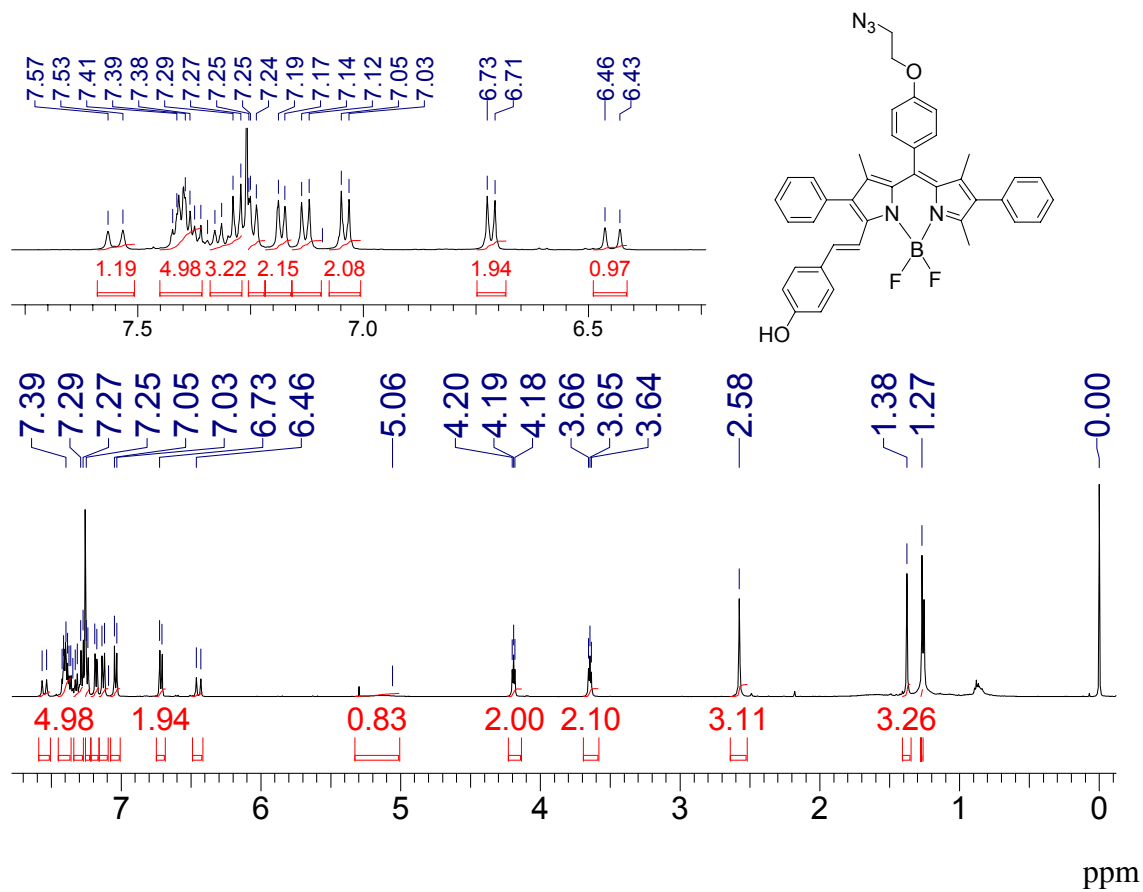


Figure S8. ¹H NMR of compound 8 (500 MHz, CDCl₃).

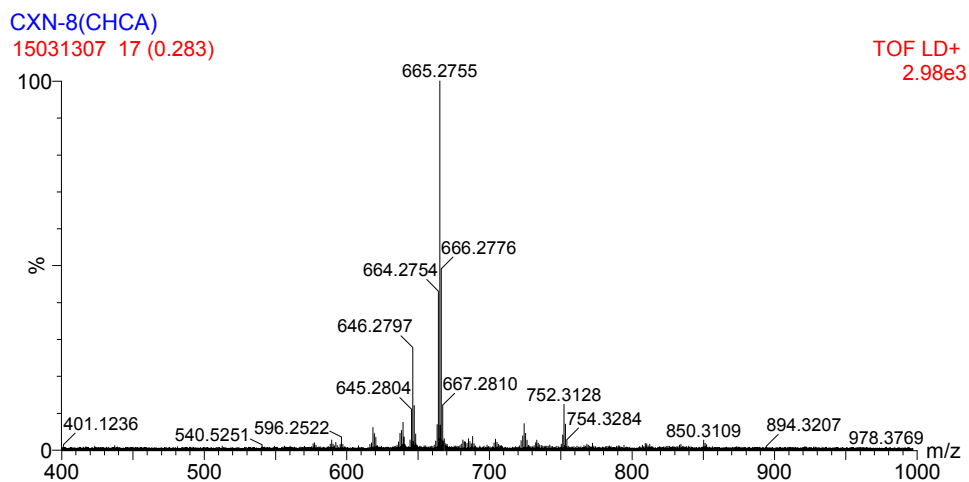


Figure S9. TOF HRMS (MALDI) of compound 8.

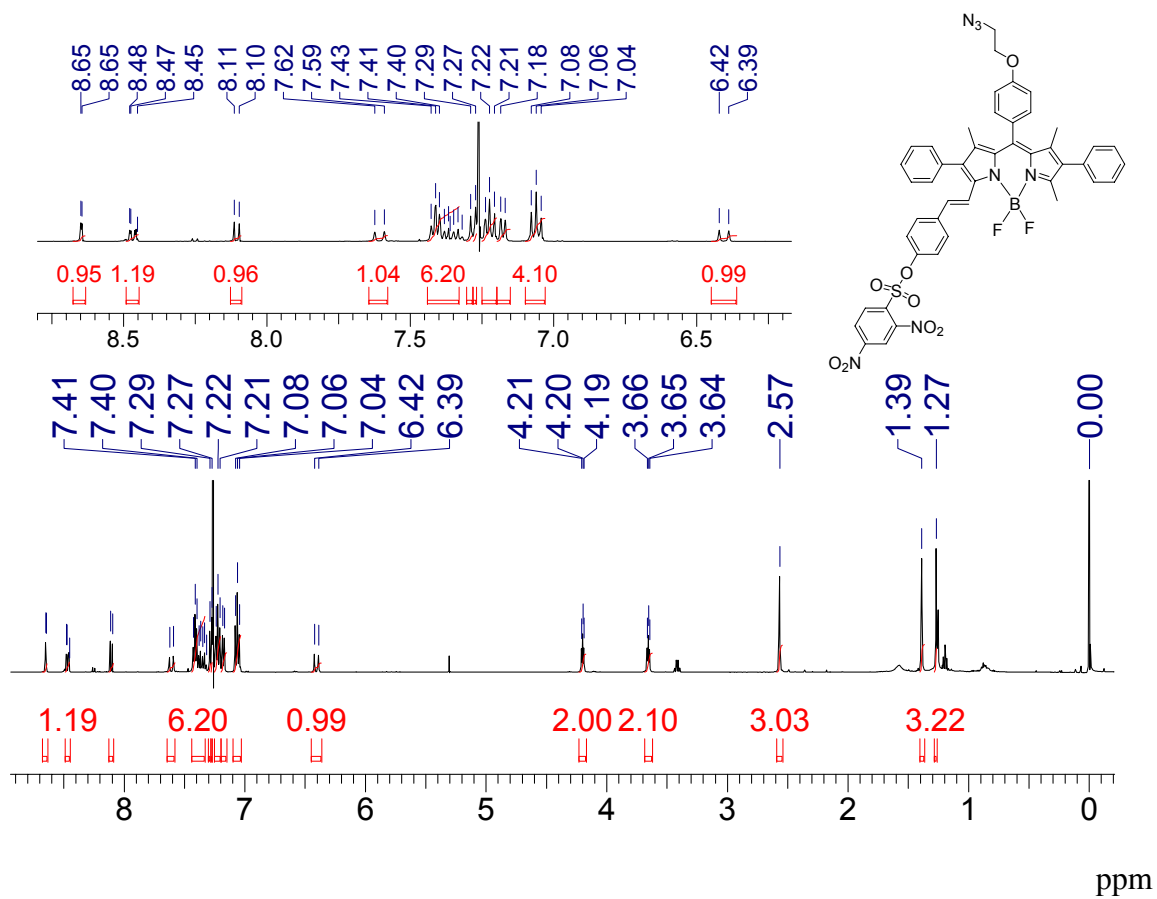


Figure S10. ^1H NMR of **9** (500 MHz, CDCl_3).

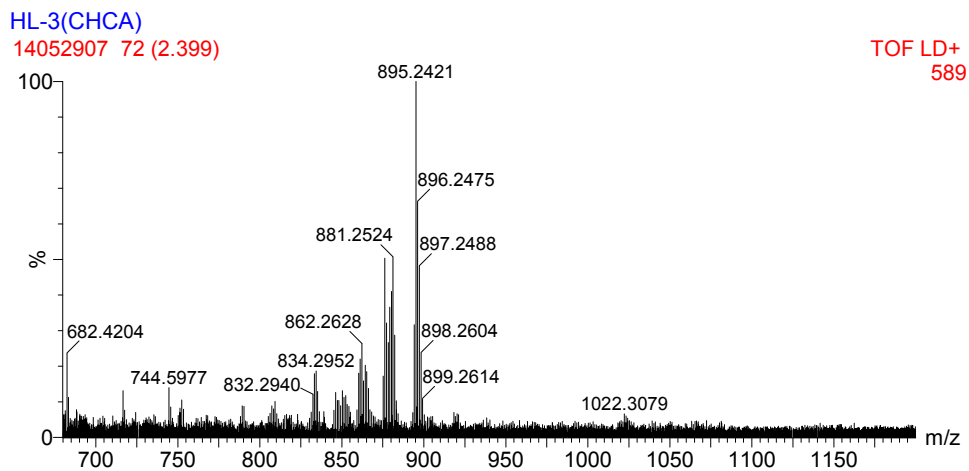


Figure S11. TOF HRMS (MALDI) of **9**.

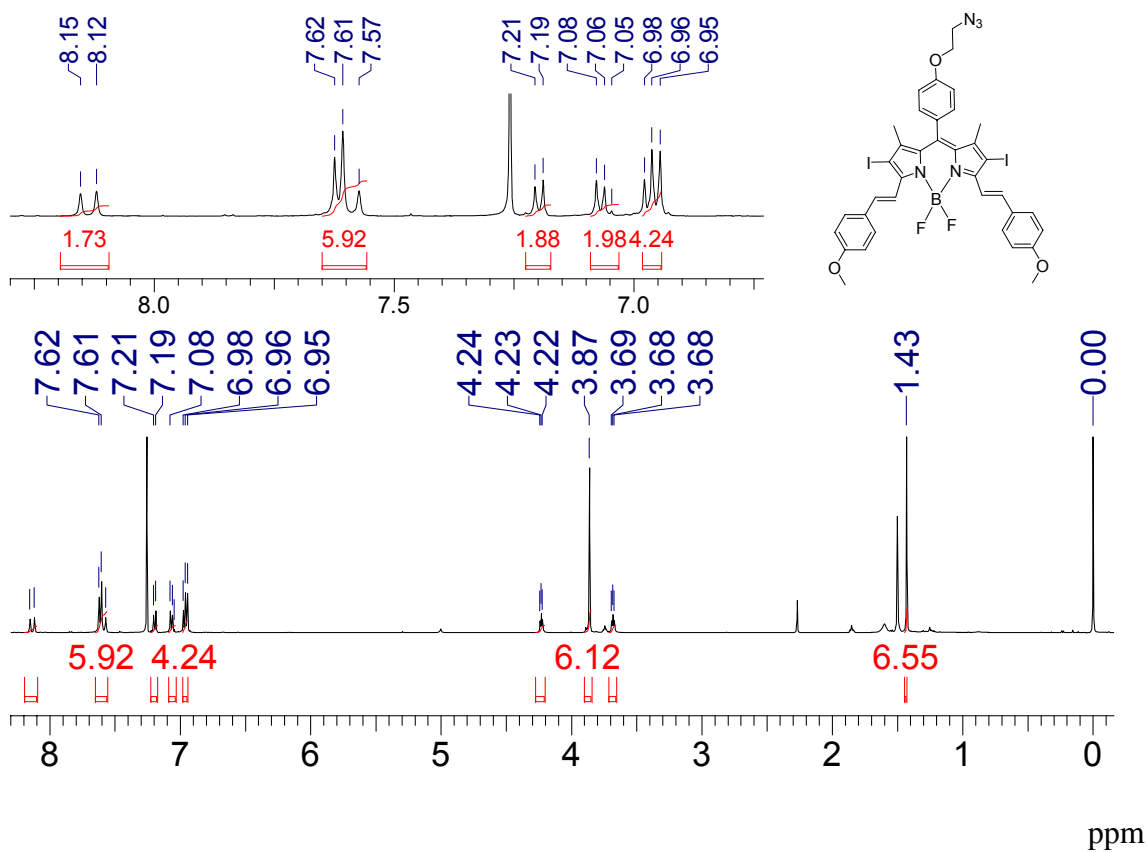


Figure S12. ^1H NMR of **10** (500 MHz, CDCl_3).

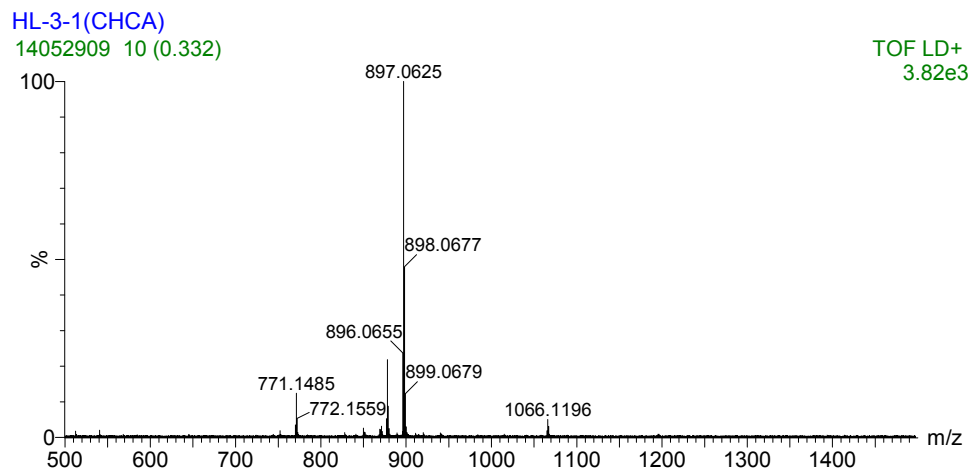


Figure S13. TOF HRMS (MALDI) of 10.

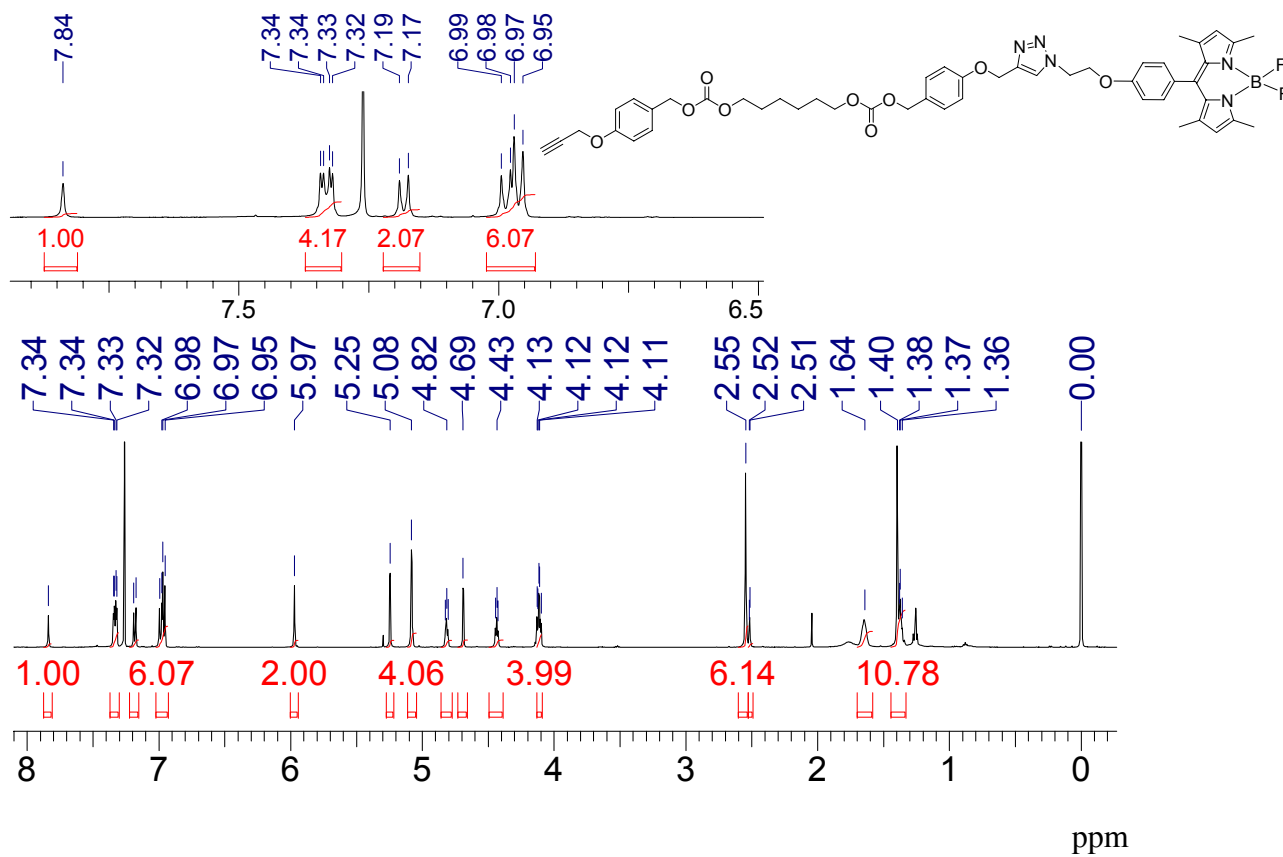


Figure S14. ¹H NMR of 11-C (500 MHz, CDCl₃).

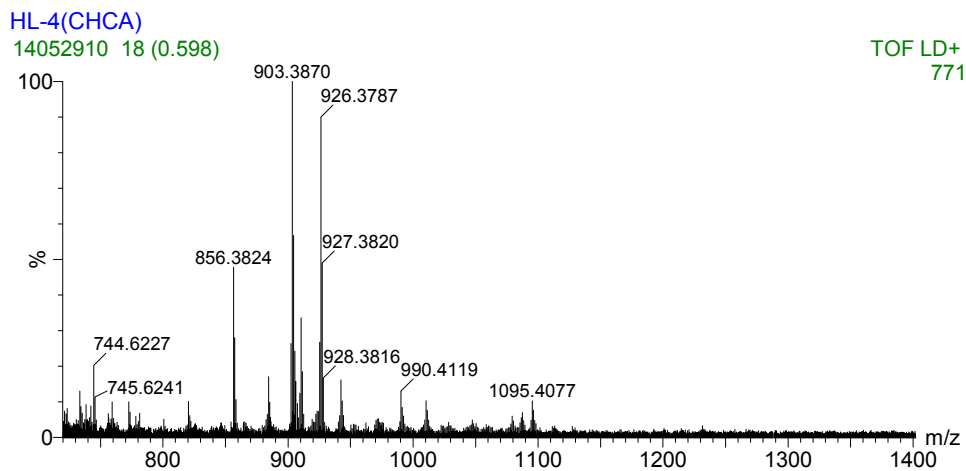


Figure S15. TOF HRMS (MALDI) of 11-C.

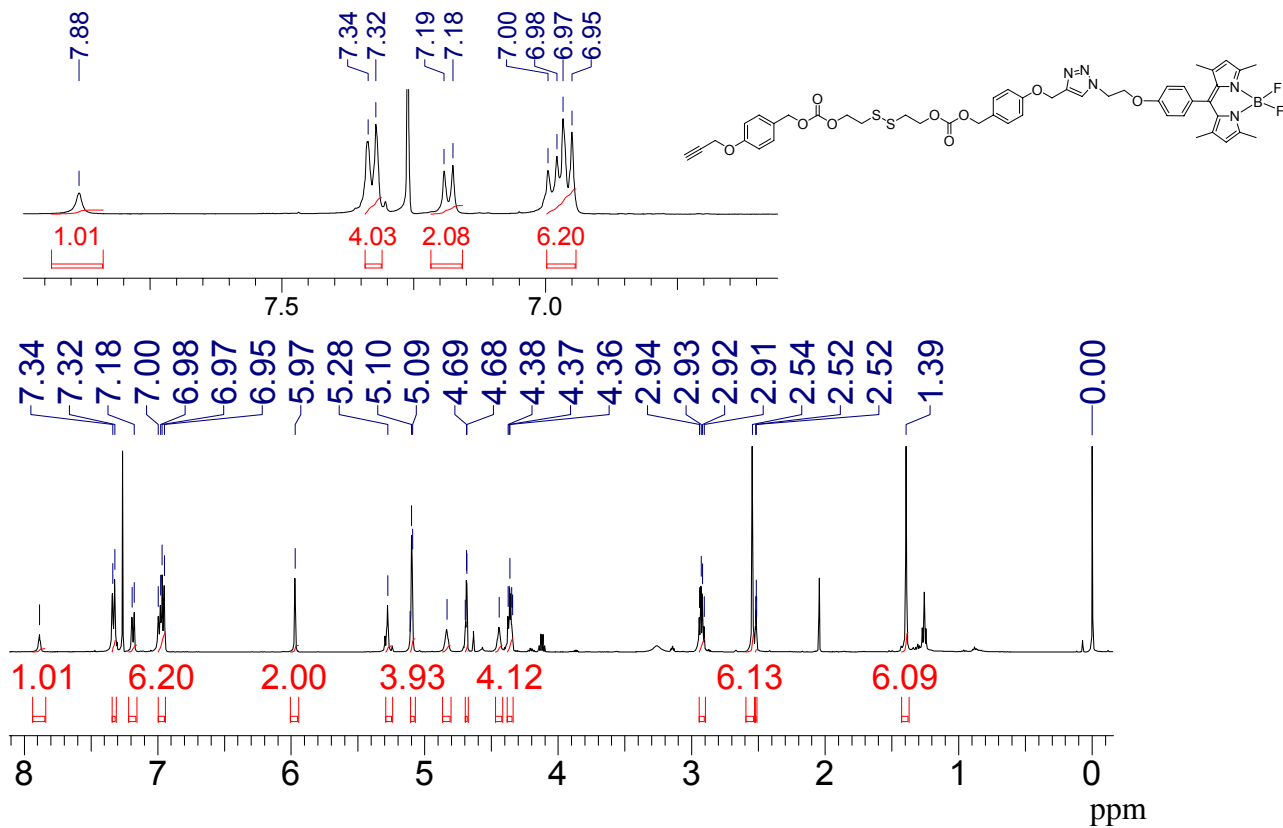


Figure S16. ^1H NMR of 11-S (500 MHz, CDCl_3).

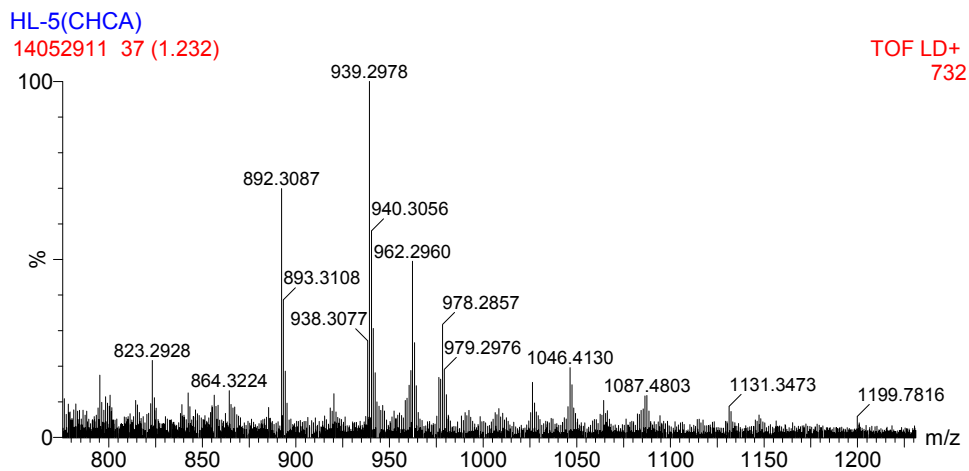


Figure S17. TOF HRMS (MALDI) of 11-S.

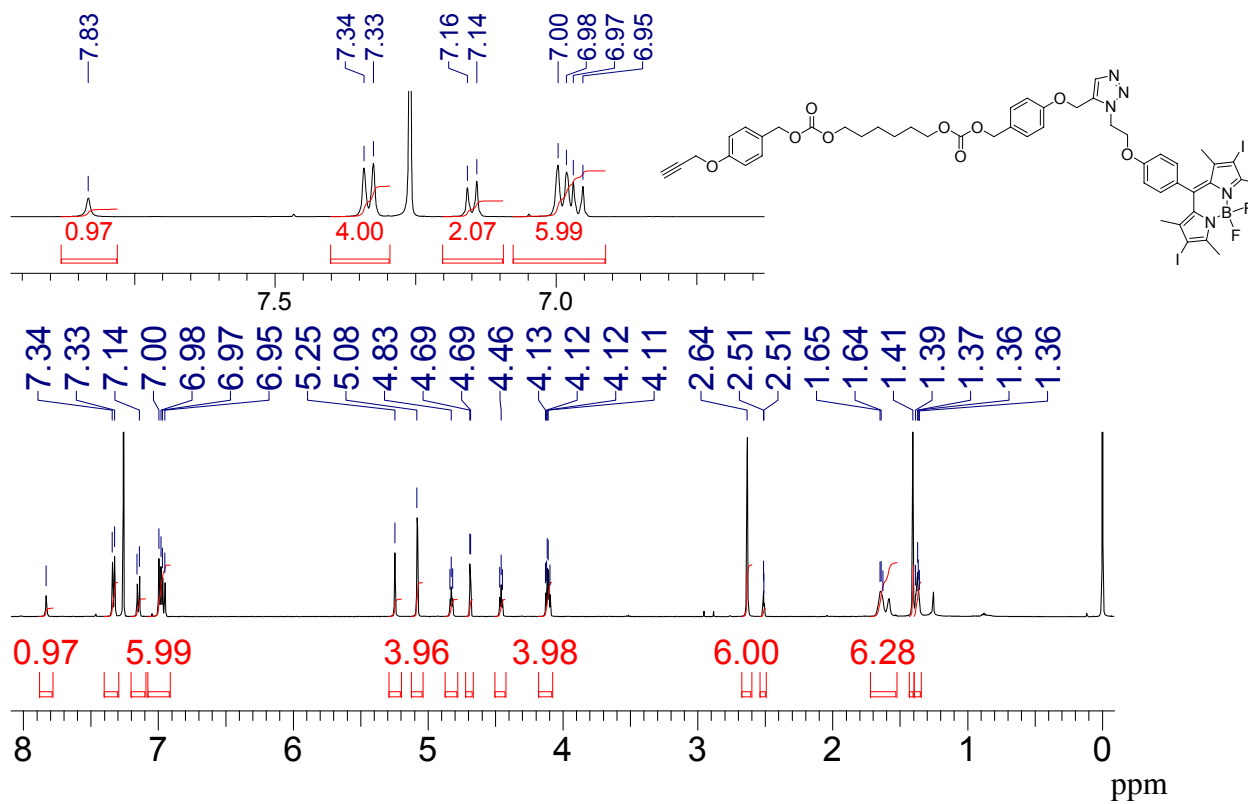


Figure S18. ¹H NMR of 12-C (500 MHz, CDCl₃).

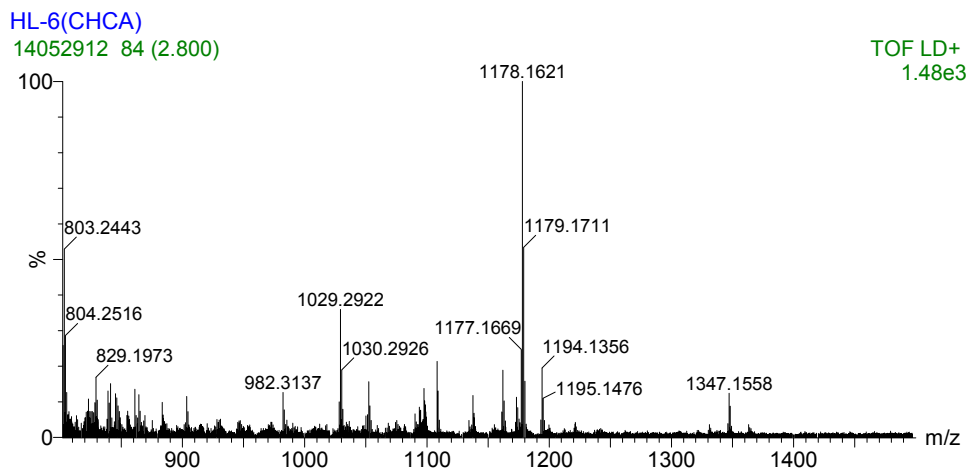


Figure S19. TOF HRMS (MALDI) of 12-C.

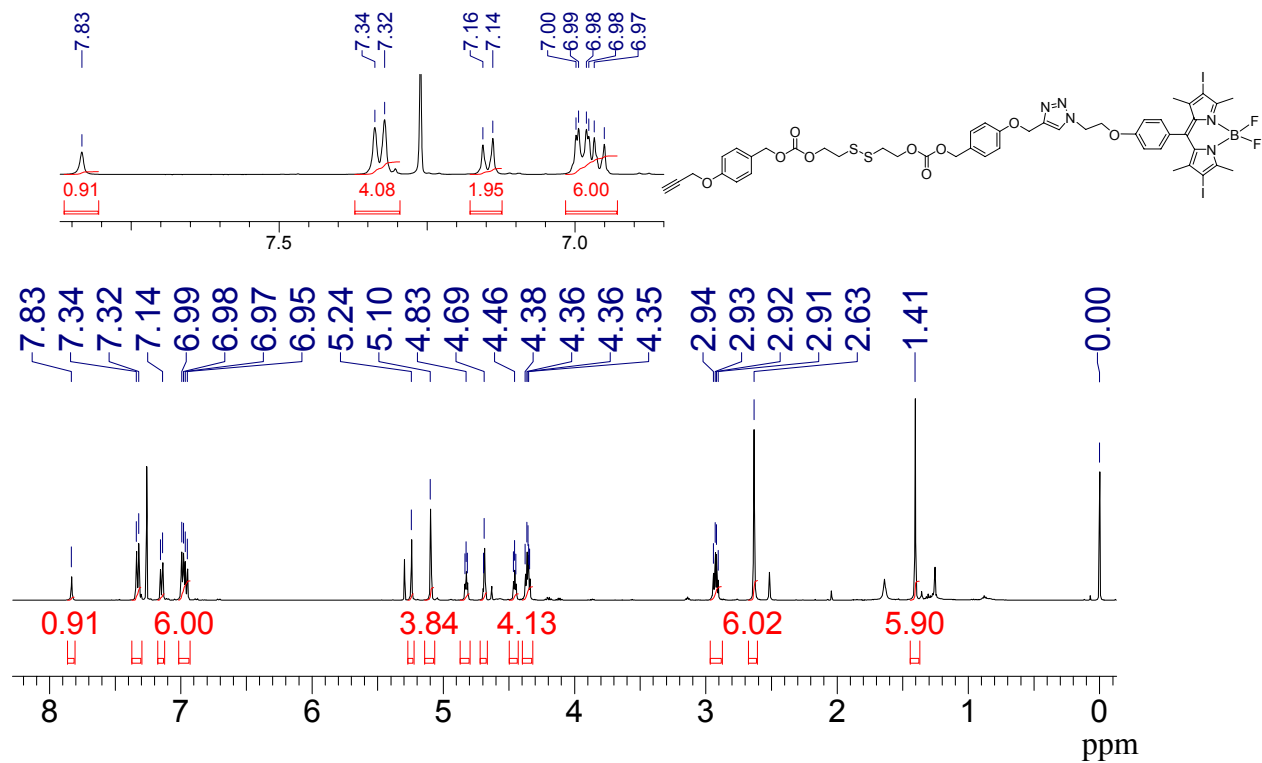


Figure S20. ^1H NMR of 12-S (500 MHz, CDCl_3).

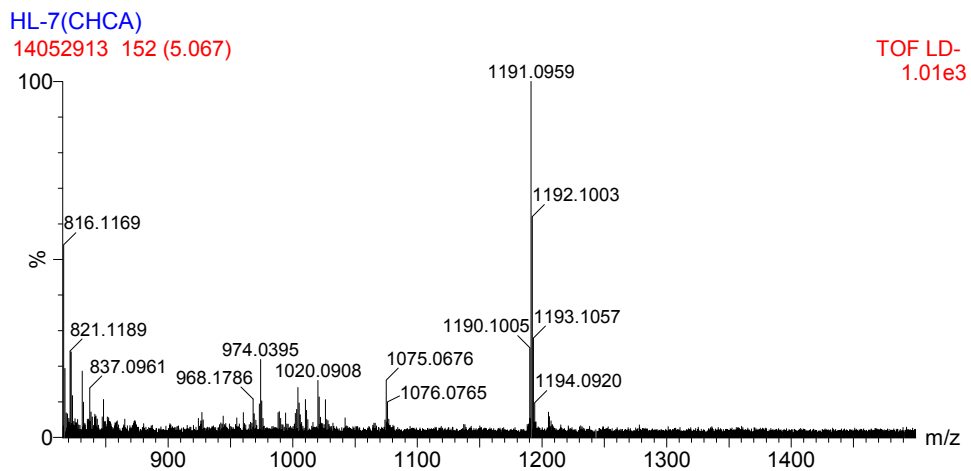


Figure S21. TOF HRMS (MALDI) of 12-S.

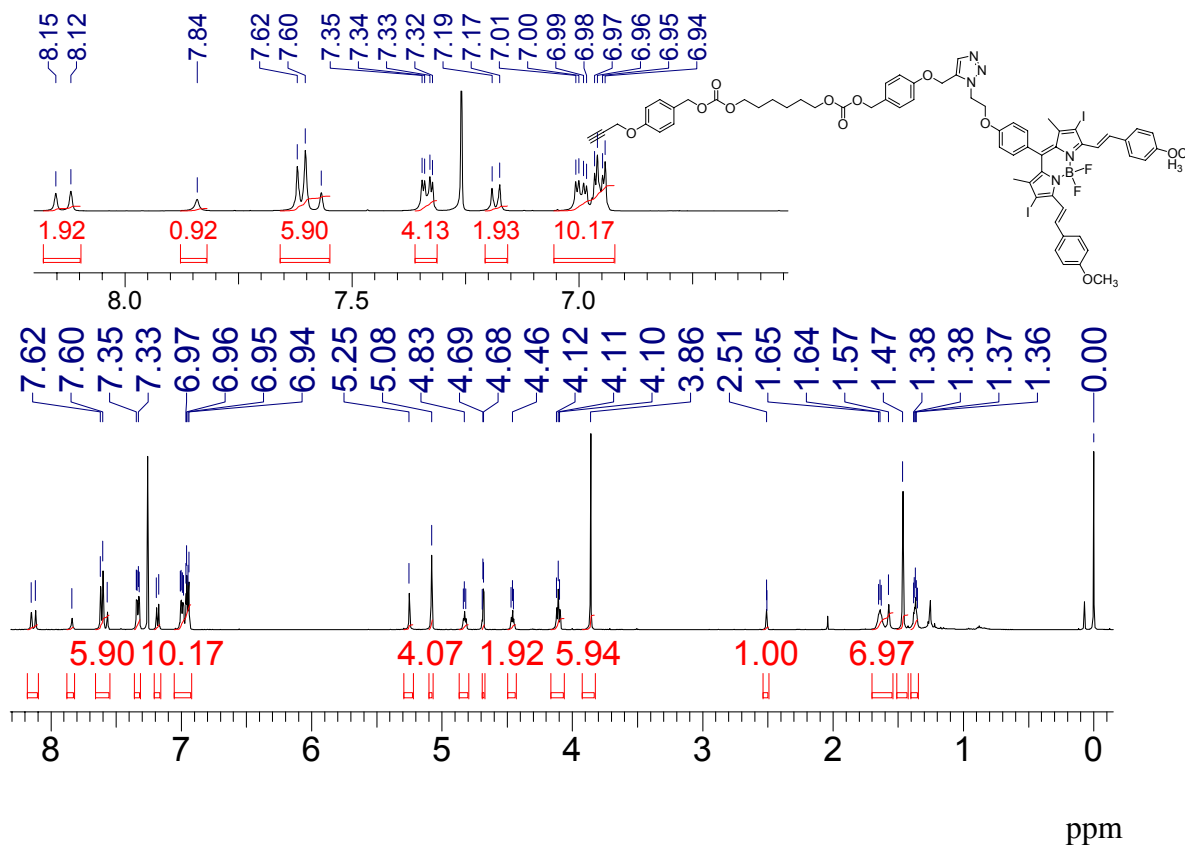


Figure S22. ^1H NMR of 13-C (500 MHz, CDCl_3).

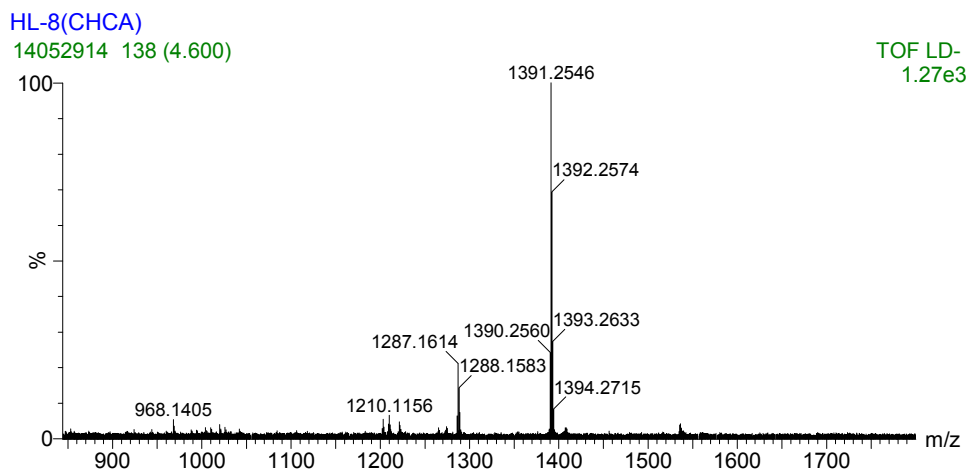


Figure S23. TOF HRMS (MALDI) of **13-C**

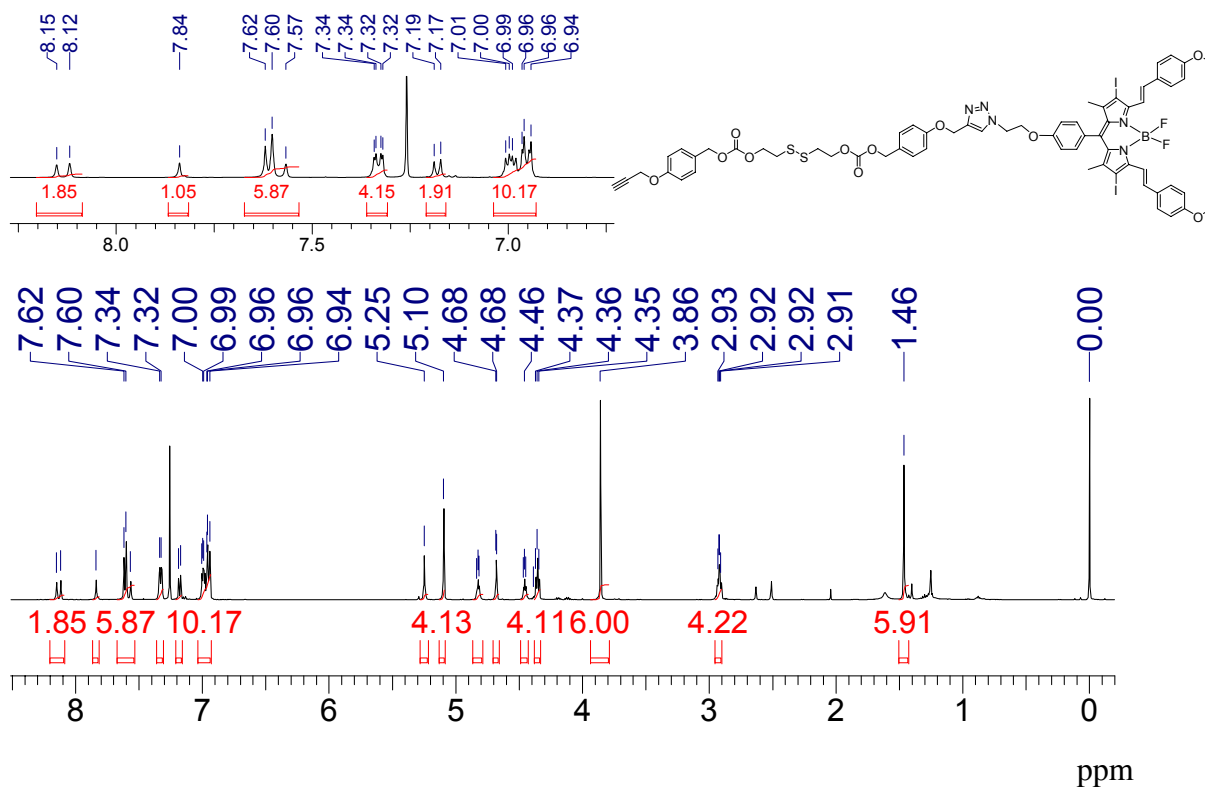


Figure S24. ^1H NMR of **13-S** (500 MHz, CDCl_3).

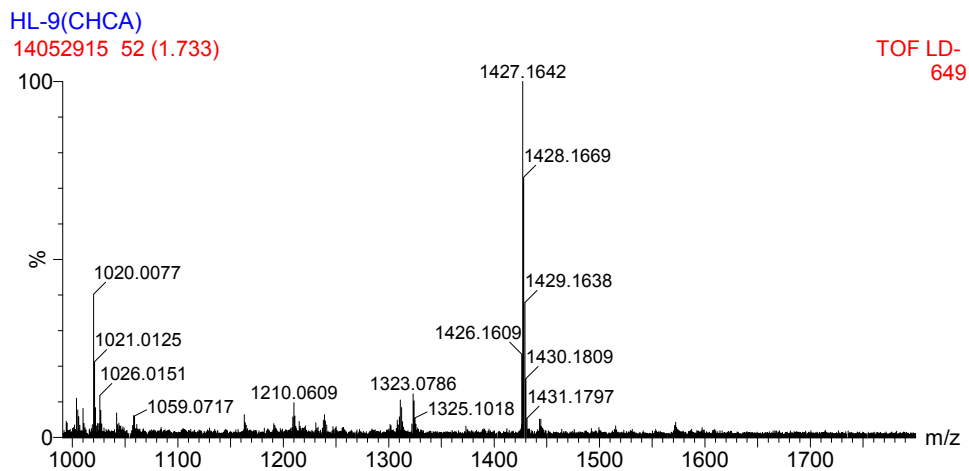


Figure S25. TOF HRMS (MALDI) of 13-S.

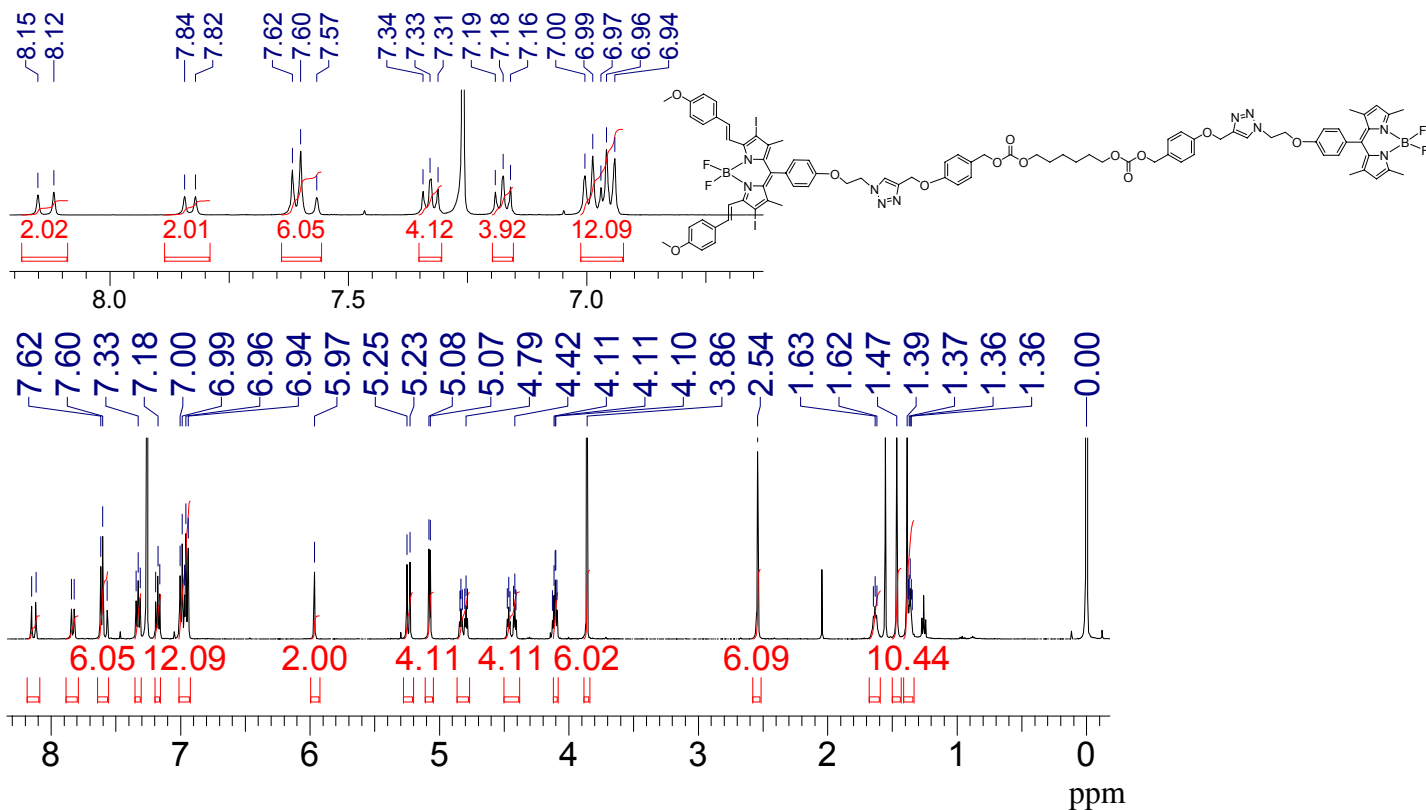


Figure S26. ^1H NMR of B-1-C (500 MHz, CDCl_3).

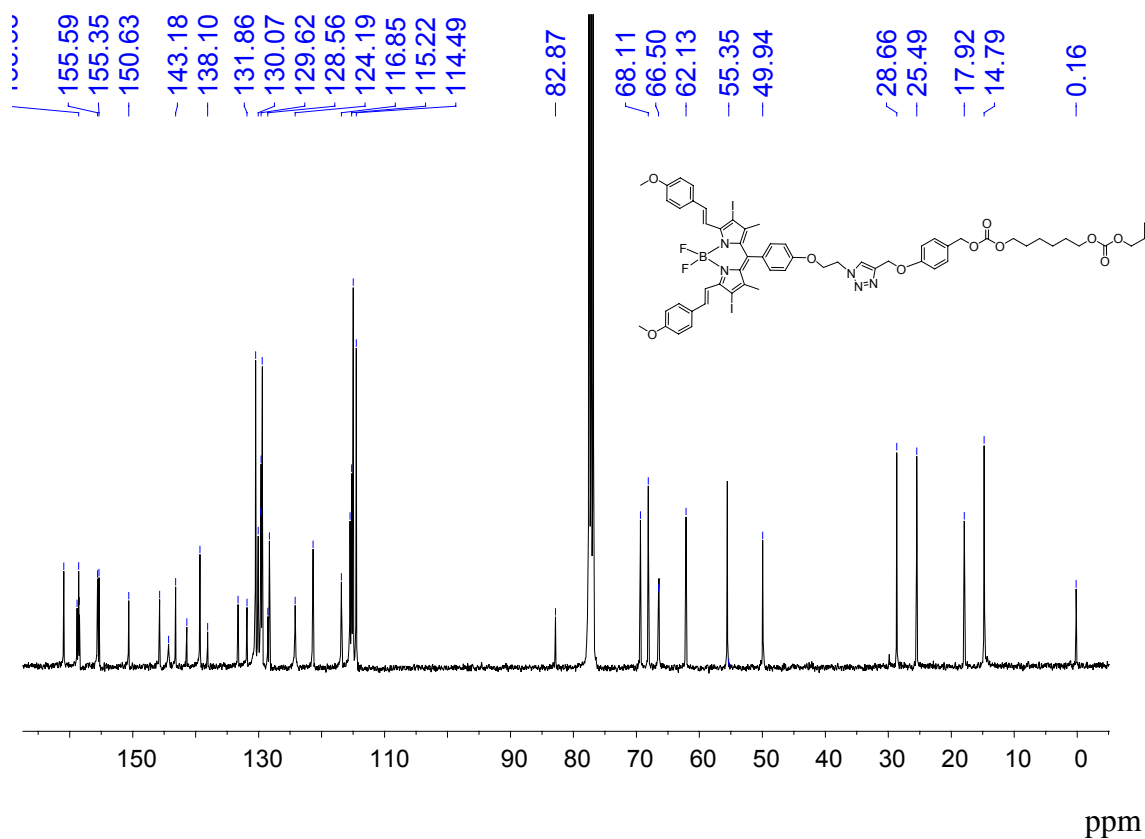


Figure S27. ^{13}C NMR of **B-1-C** (125 MHz, CDCl_3).

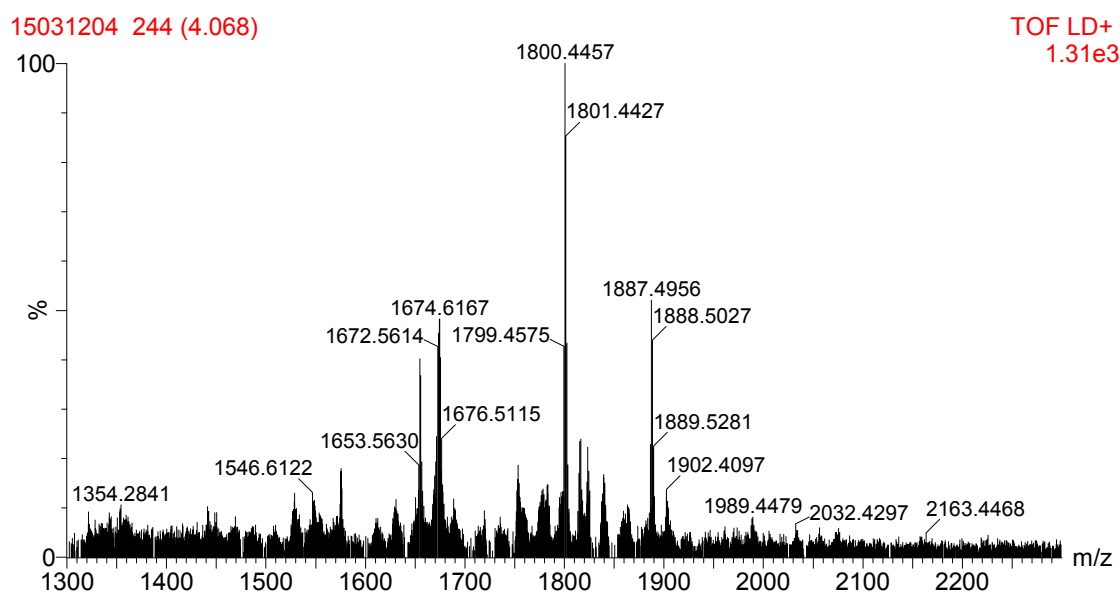


Figure S28. TOF HRMS (MALDI) of **B-1-C**.

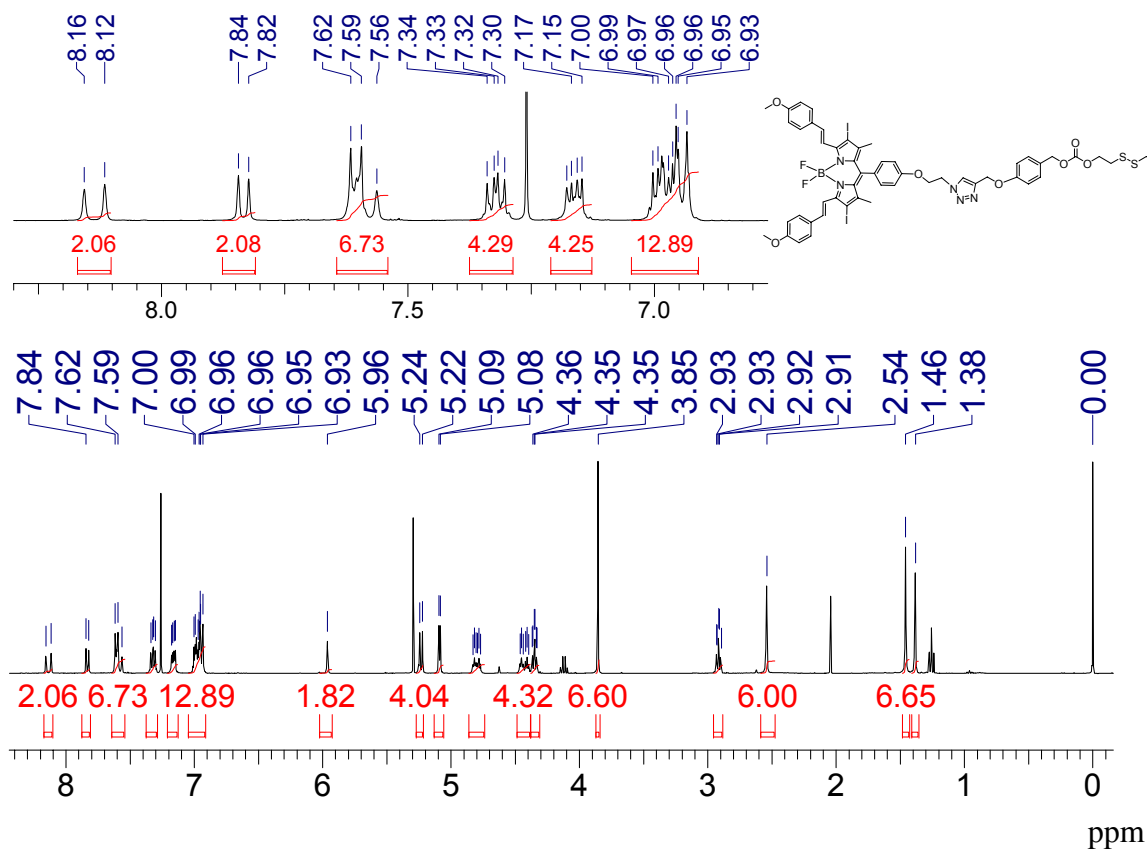


Figure S29. ¹H NMR of B-1-S (500 MHz, CDCl₃).

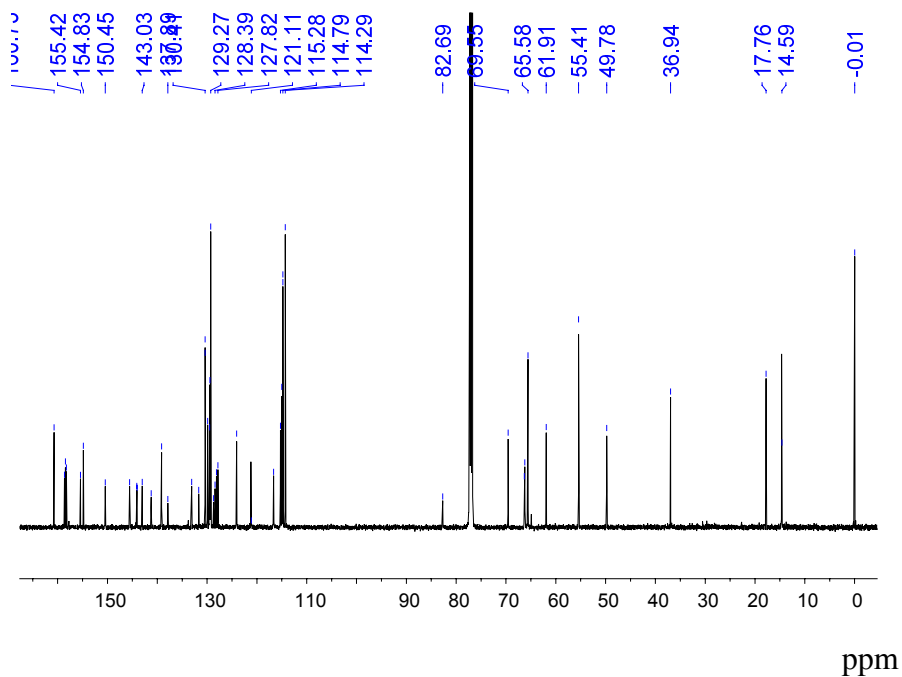


Figure S30. ¹³C NMR of B-1-S (125 MHz, CDCl₃).

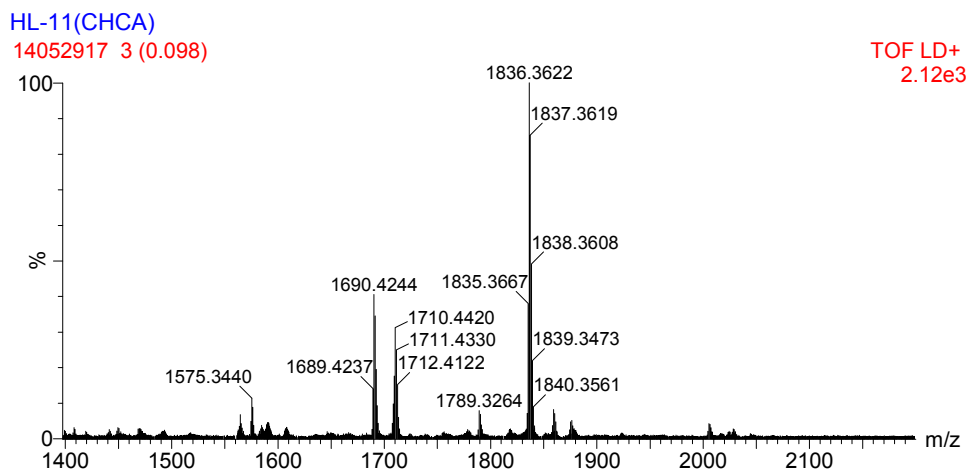


Figure S31. TOF HRMS (MALDI) of B-1-S.

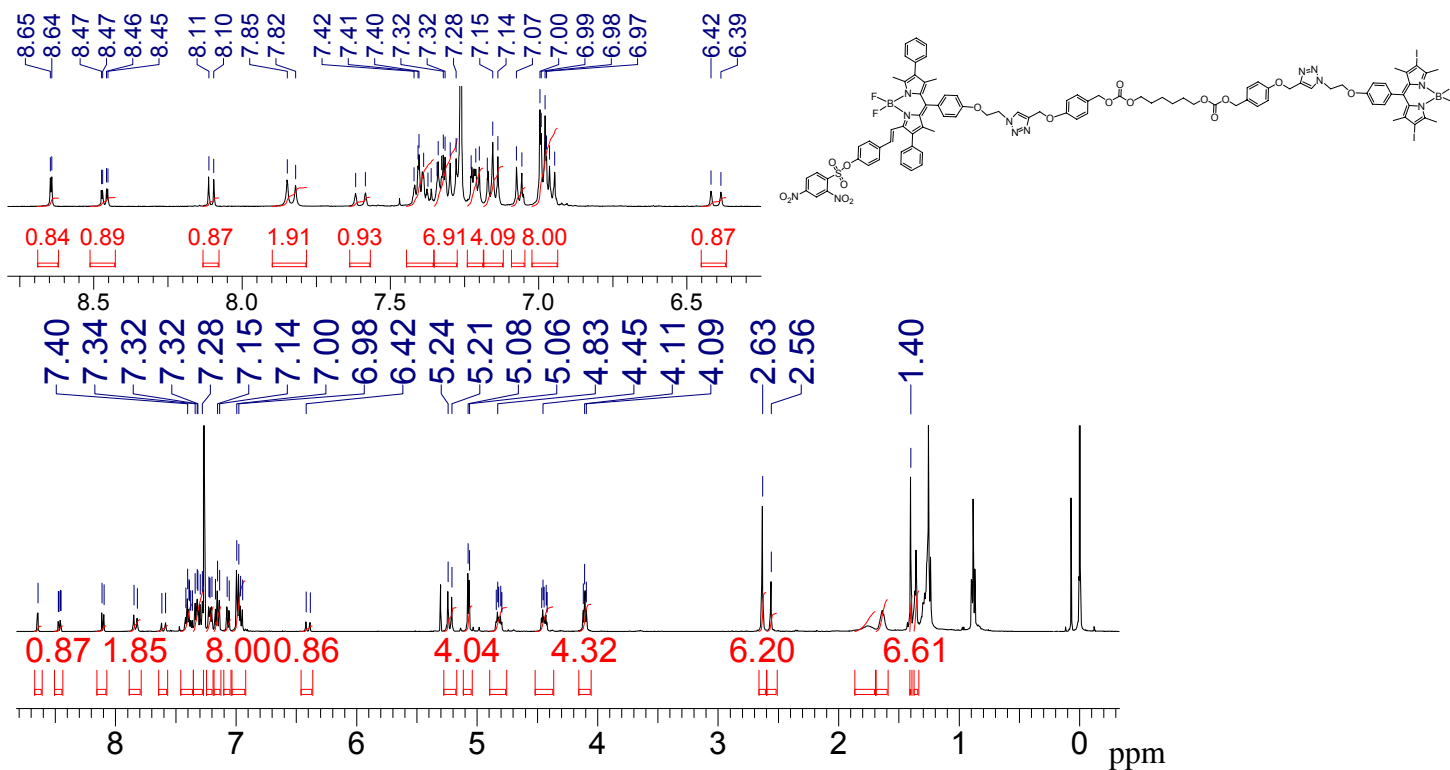


Figure S32. ^1H NMR of B-2-C (500 MHz, CDCl_3).

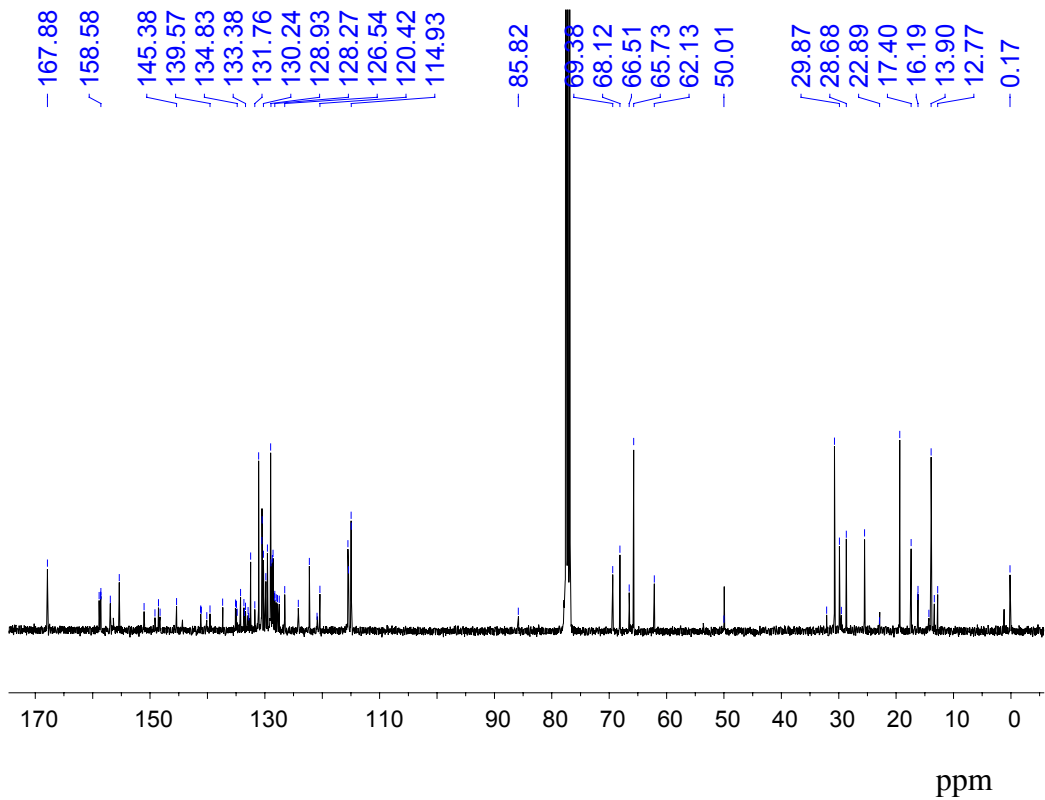


Figure S33. ^{13}C NMR of B-2-C (125 MHz, CDCl_3).

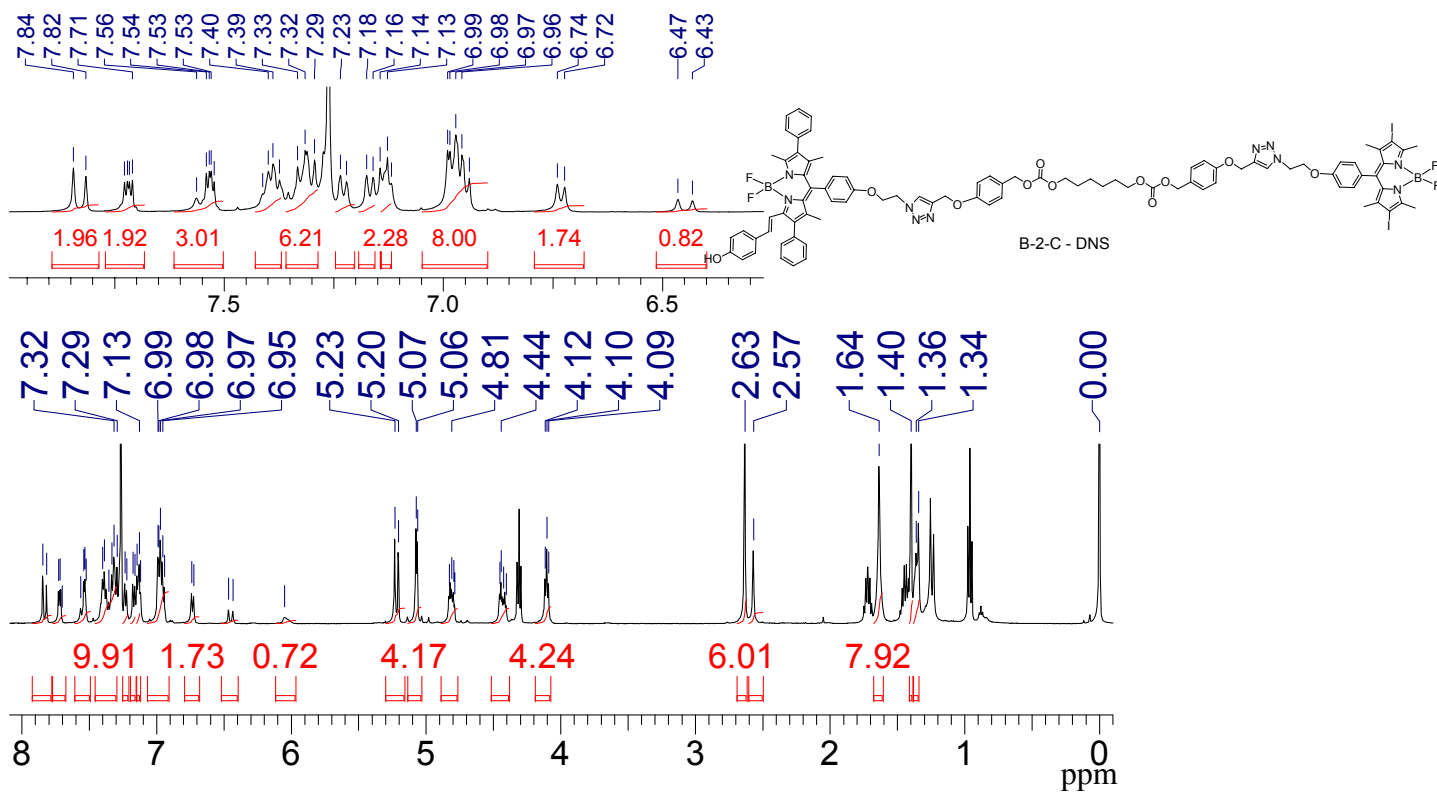


Figure S34. ^1H NMR of B-2-C-DNS (500 MHz, CDCl_3).

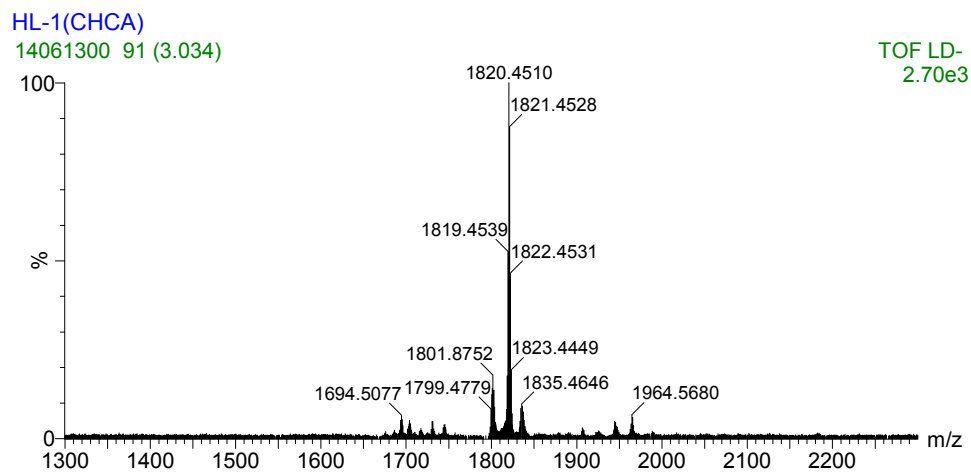


Figure S35. TOF HRMS (MALDI) of **B-2-C-DNS**.

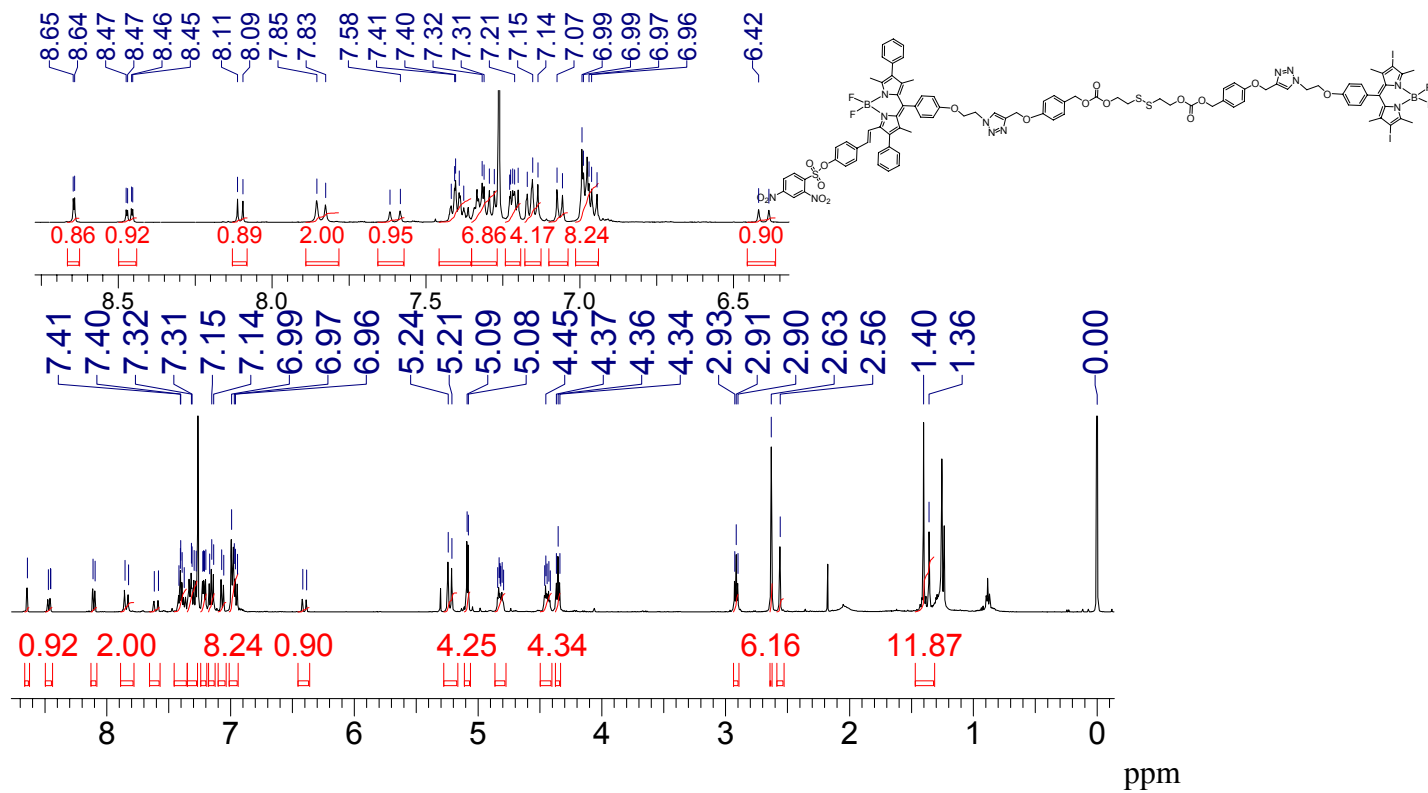


Figure S36. ^1H NMR of **B-2-S** (500 MHz, CDCl_3).

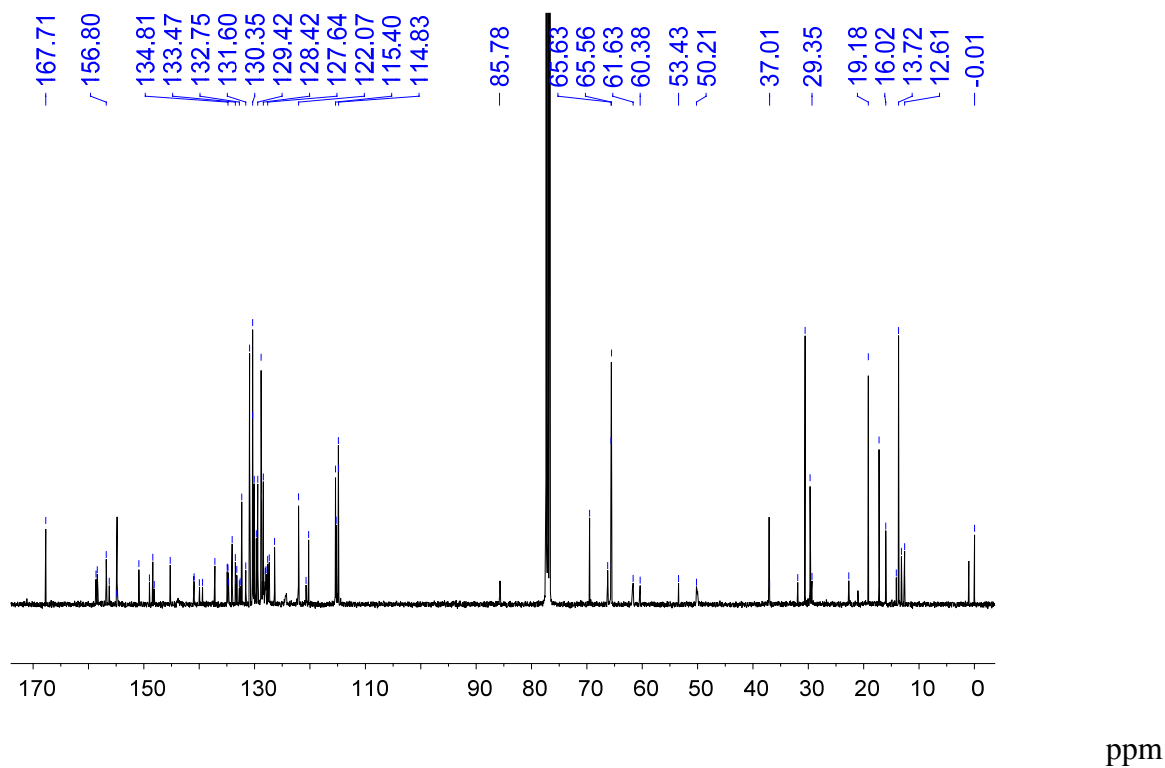


Figure S37. ¹³C NMR of B-2-S (125 MHz, CDCl₃).

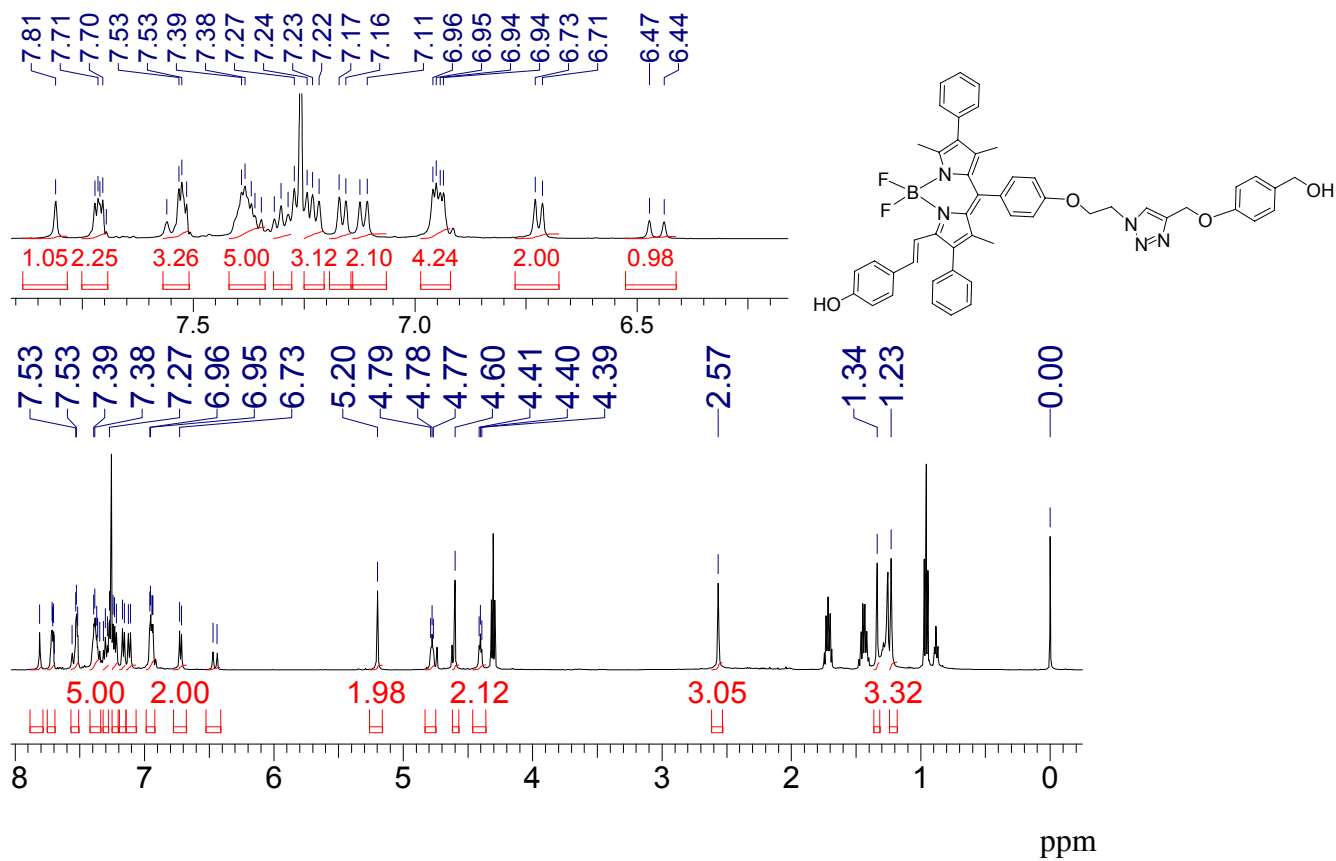


Figure S38. ¹H NMR of B-2-S-1 (500 MHz, CDCl₃).

CXN-B-2-S-1(CHCA)
15031306 157 (2.616)

TOF LD+
7.36e3

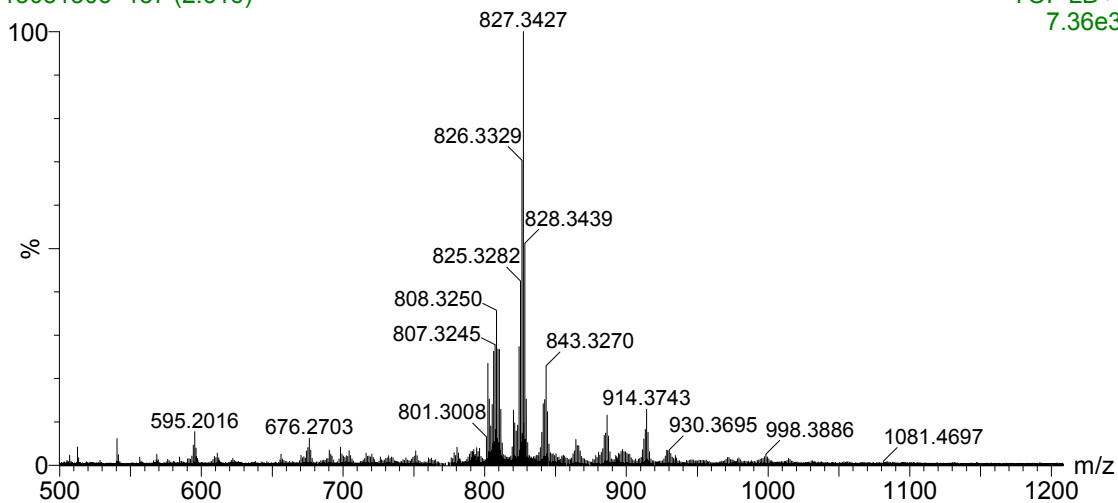


Figure S39. TOF HRMS (MALDI) of **B-2-S-1**

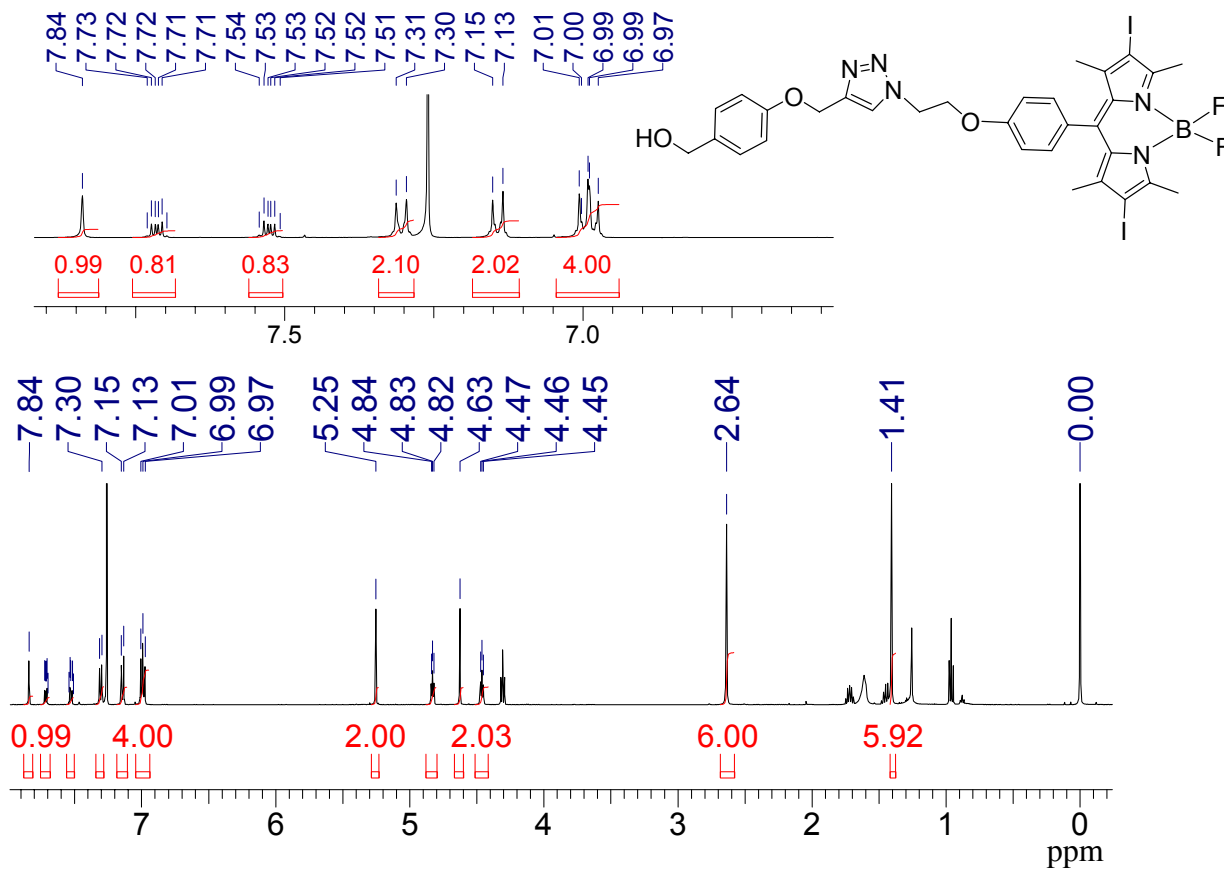


Figure S40. ^1H NMR of **B-2-S-2** (500 MHz, CDCl_3).

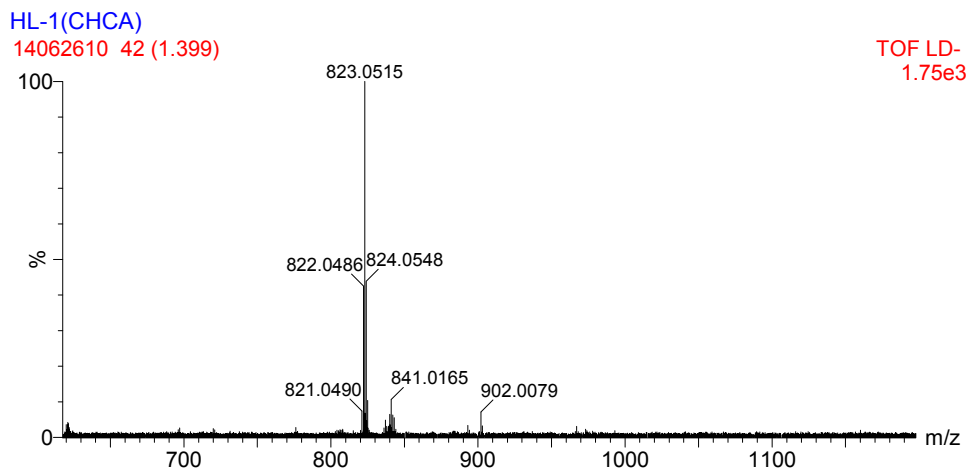


Figure S41. TOF HRMS (MALDI) of B-2-S-2

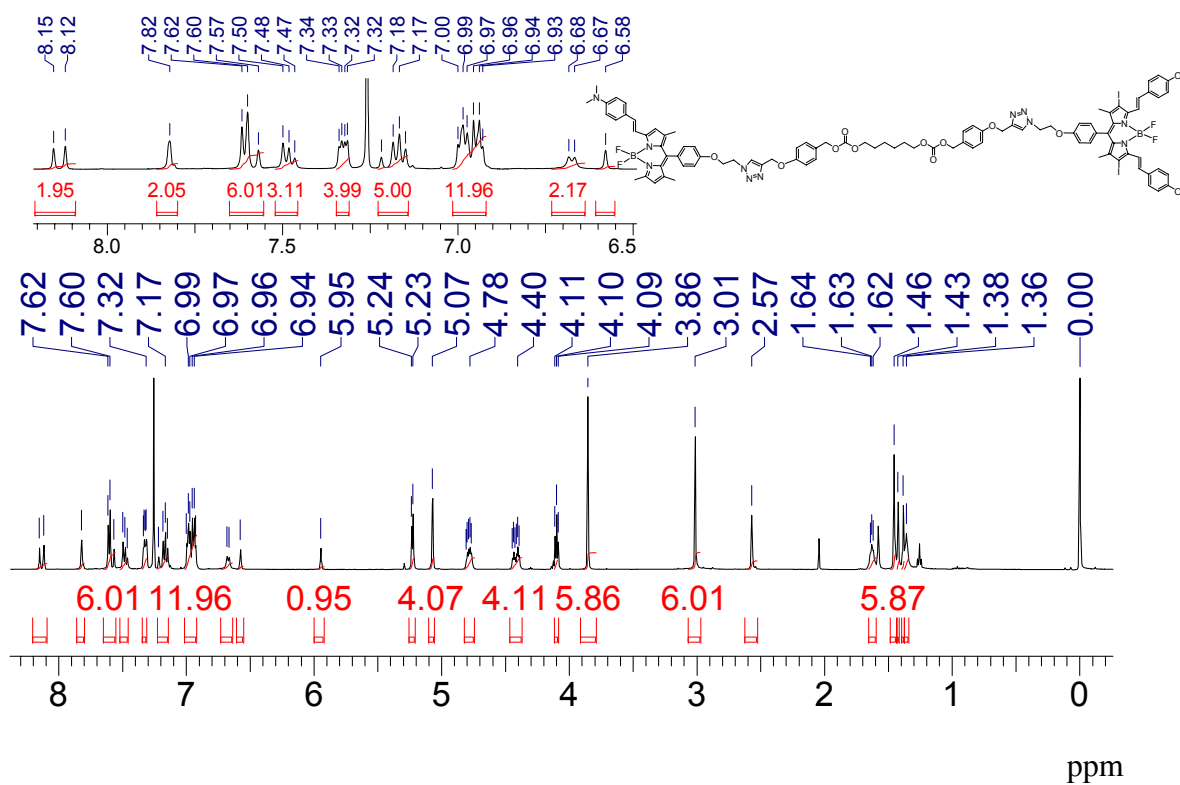


Figure S42. ^1H NMR of B-3-C (500 MHz, CDCl_3).

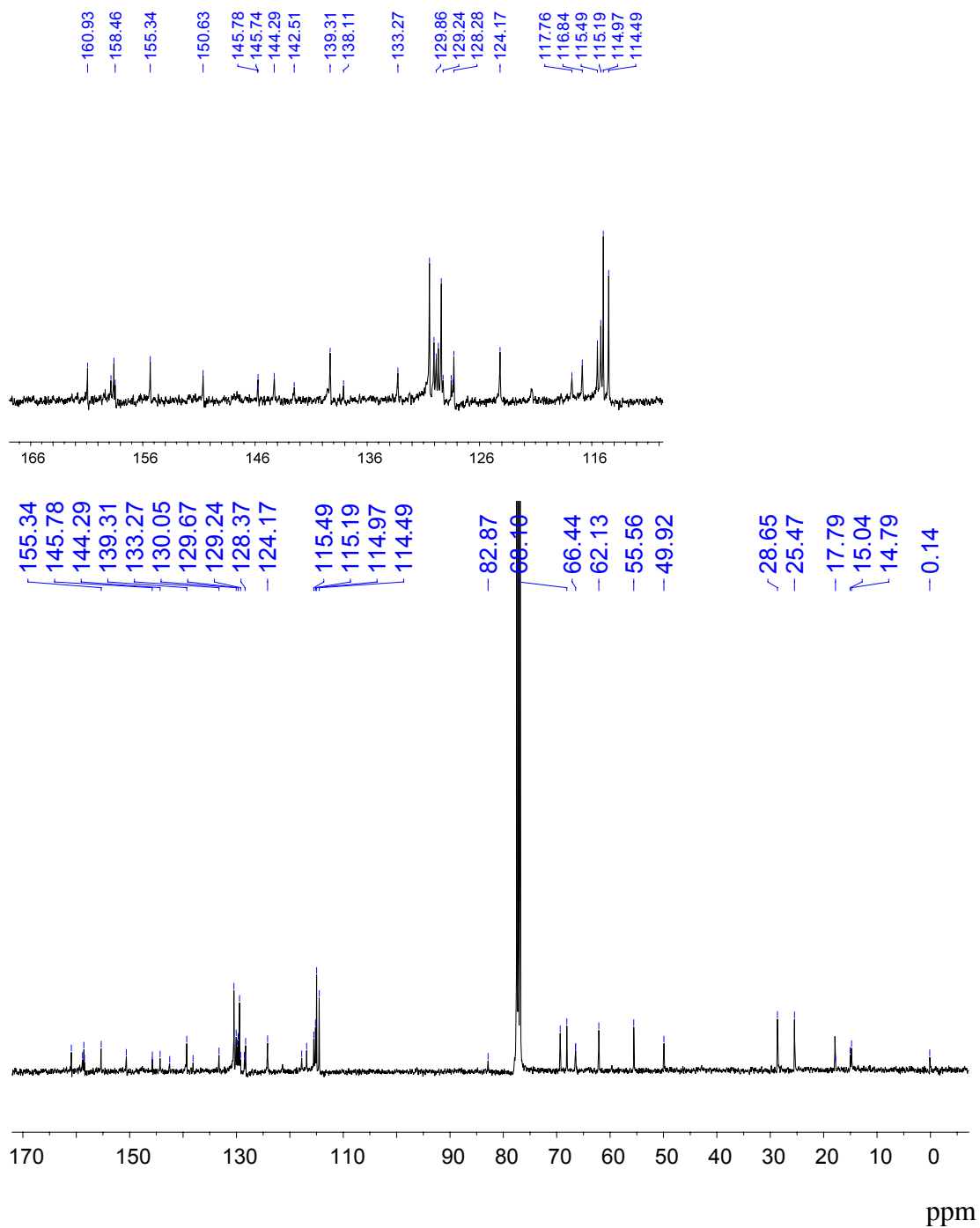


Figure S43. ^{13}C NMR of **B-3-C** (100 MHz, CDCl_3).

CXN-B-3-C(CHCA)
15031303 229 (3.816)

TOF LD+
2.34e3

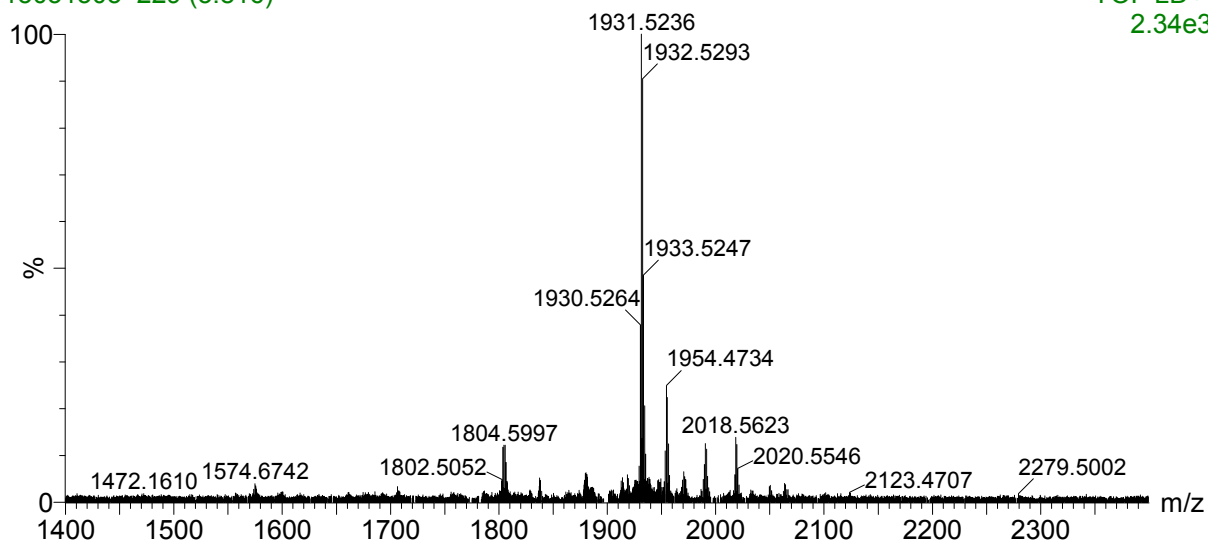


Figure S44. TOF HRMS (MALDI) of B-3-C

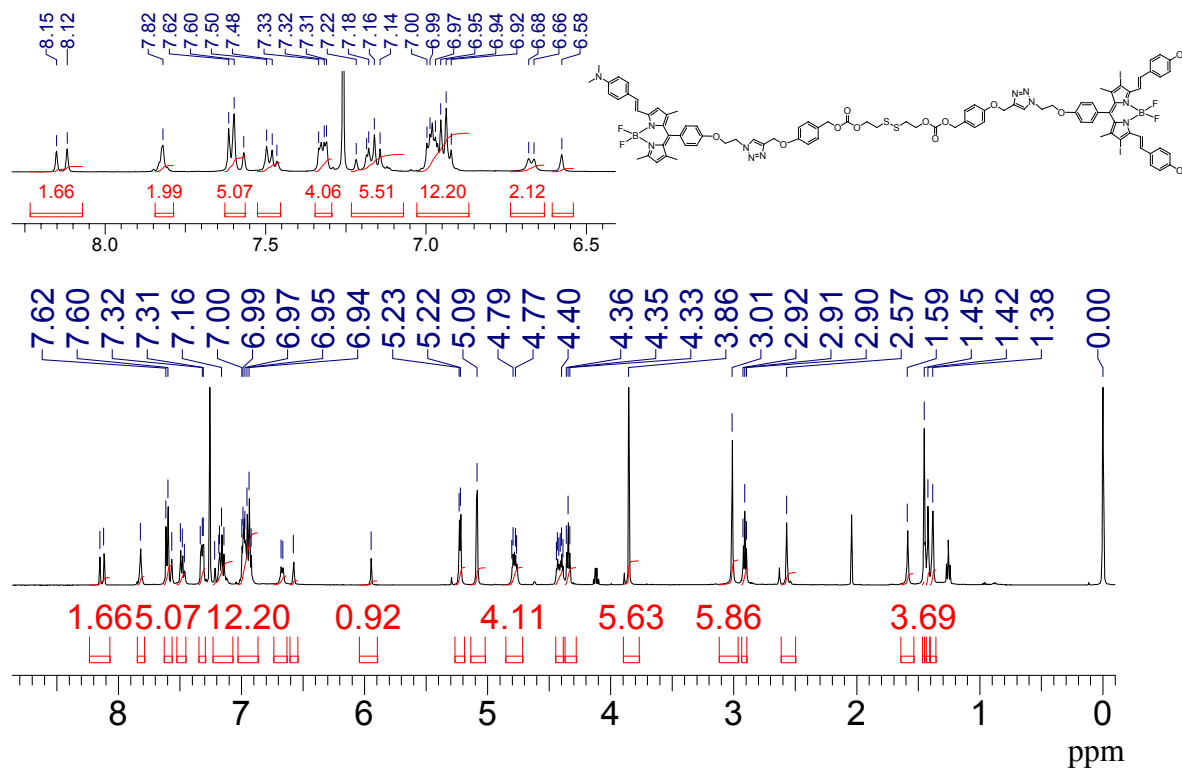


Figure S45. ¹H NMR of B-3-S (500 MHz, CDCl₃).

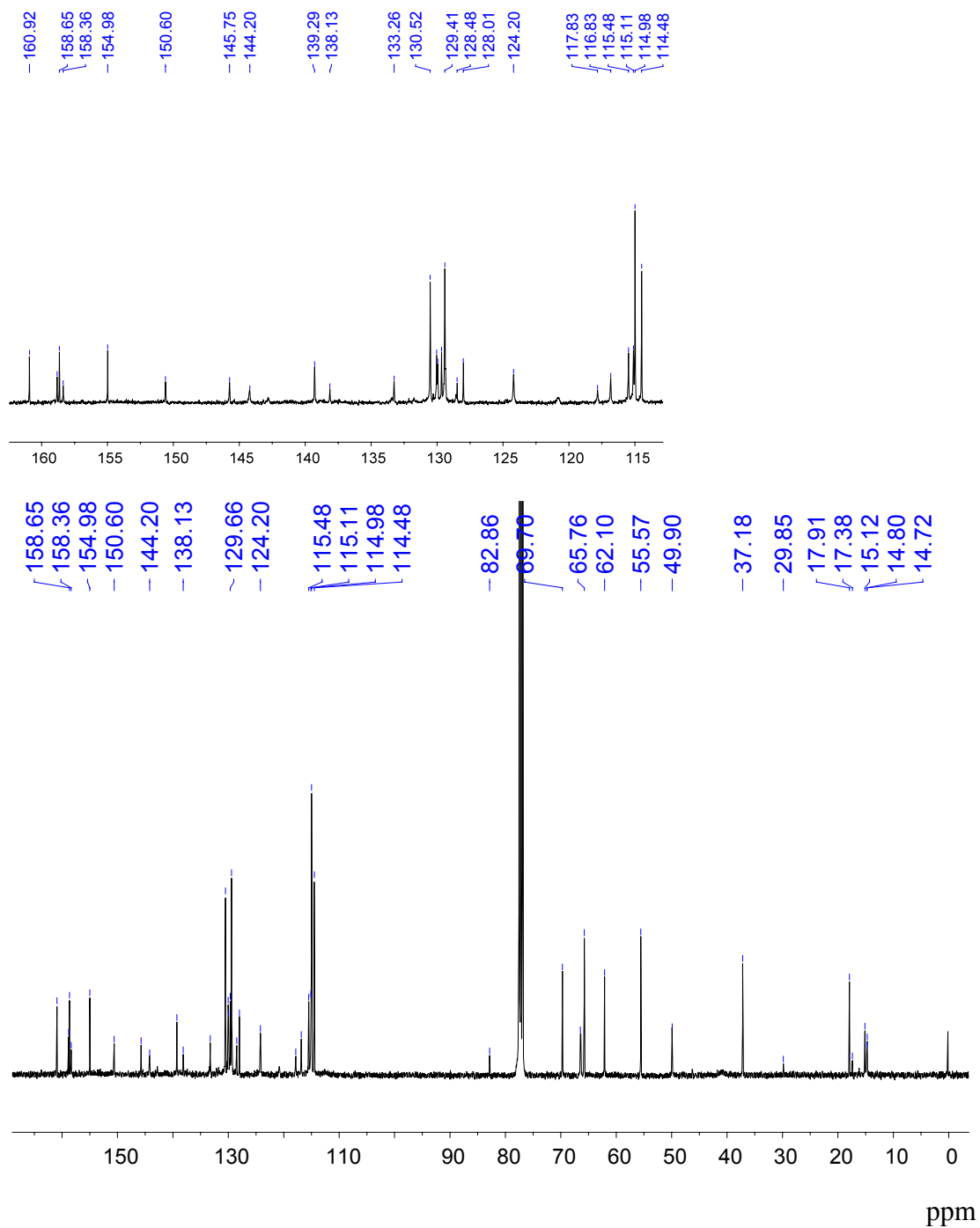


Figure S46. ^{13}C NMR of B-3-S (100 MHz, CDCl_3).

CXN-B-3-S(CHCA)
15031304 35 (0.582)

TOF LD+
1.67e3

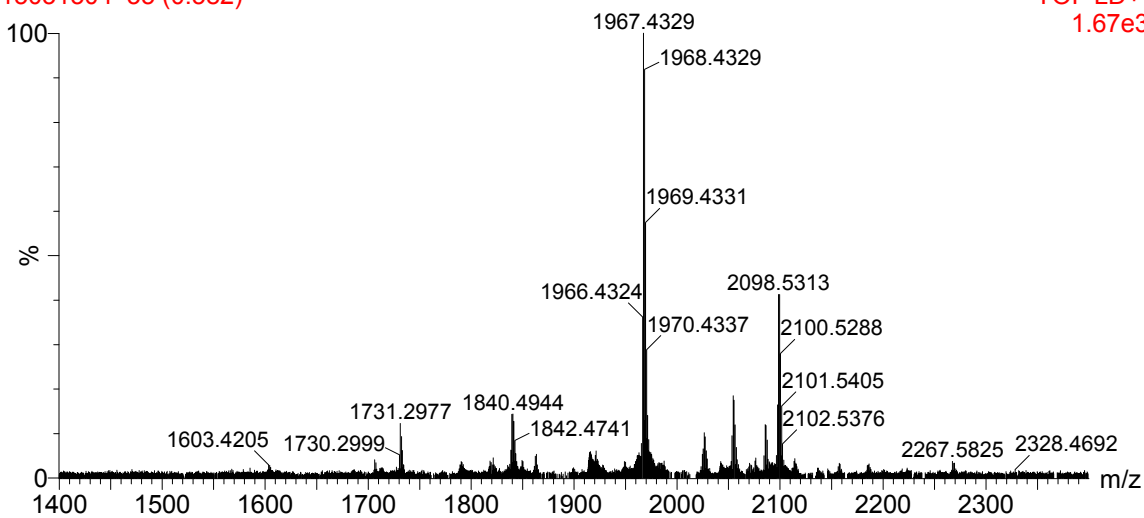


Figure S47. TOF HRMS (MALDI) of **B-3-S**.

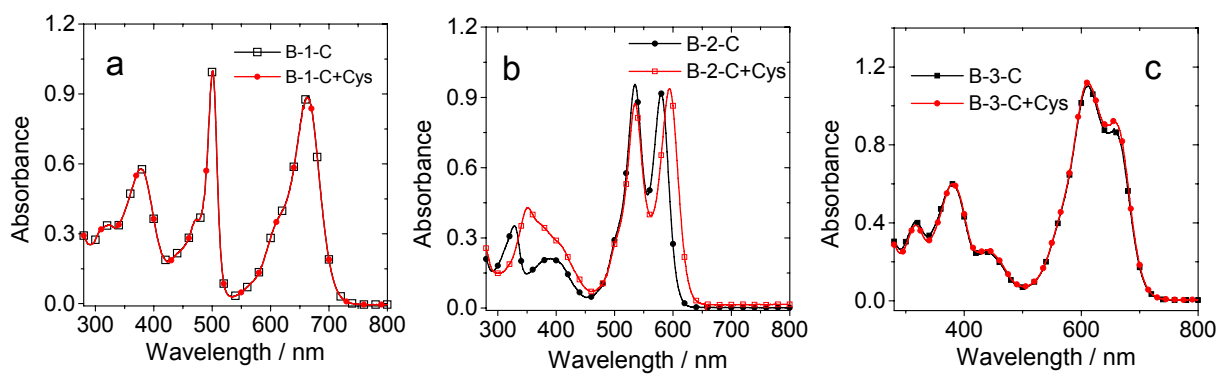


Figure S48. (a) The UV-vis absorption spectra of the **B-1-C**, **B-2-C** and **B-3-C** in the presence and absence of Cys. (a) **B-1-C**, (b) **B-2-C**, (c) **B-3-C**. In DMF/H₂O = 4/1 (v/v), pH = 7.4 (1.0×10^{-5} M; 25 °C).

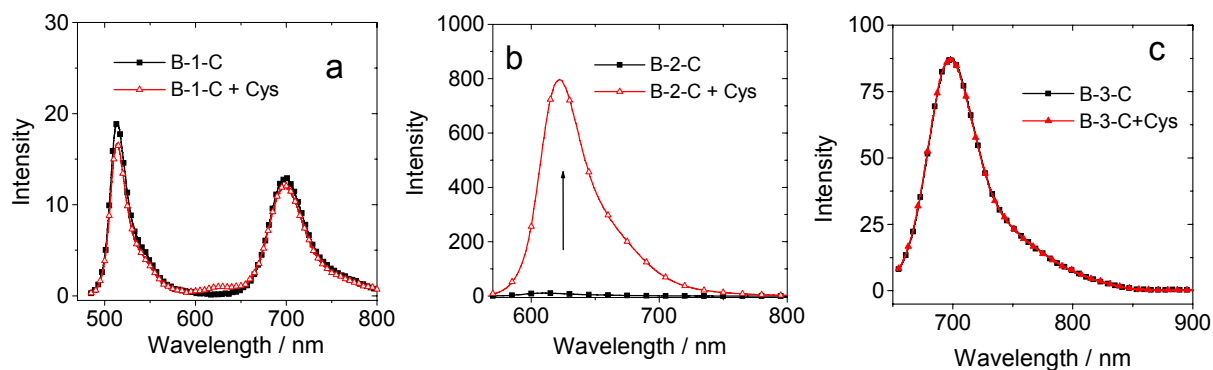


Figure S49. (a) Fluorescence emission spectra of the **B-1-C** ($\lambda_{\text{ex}} = 475$) nm and in the presence of Cys. (b) **B-2-C** ($\lambda_{\text{ex}} = 550$ nm) and in the presence of Cys. (c) **B-3-C** ($\lambda_{\text{ex}} = 650$ nm) and in the presence of Cys. pH = 7.4, In DMF/H₂O (4/1, v/v), (1.0×10^{-5} M; 25 °C).

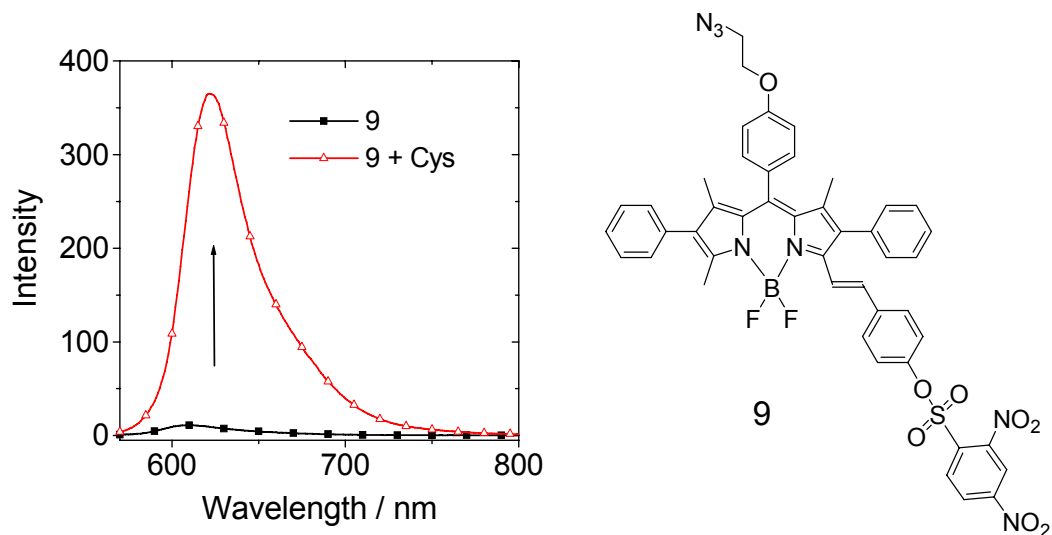


Figure S50. (a) Fluorescence emission spectra of the **9** and in presence of Cys. $\lambda_{\text{ex}} = 560$ nm. pH = 7.4, In DMF/H₂O (4/1, v/v), (1.0×10^{-5} M; 25 °C).

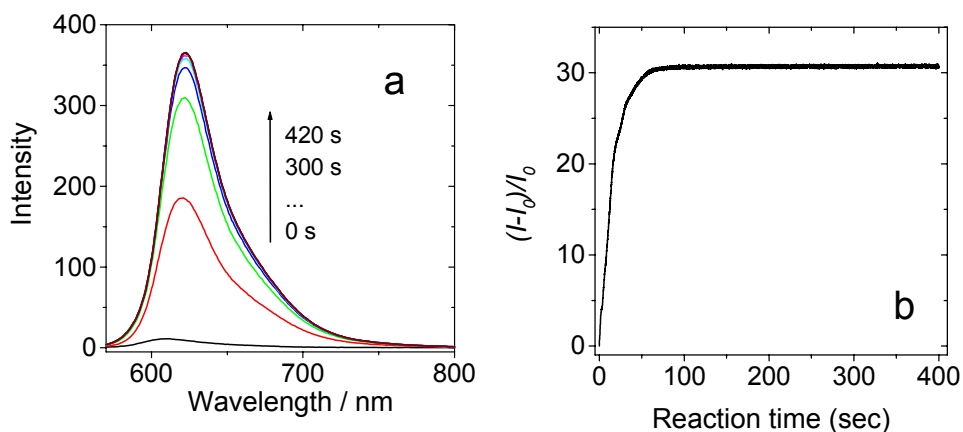


Figure S51. (a) The change of fluorescence in different time in presence of Cys for **9**, (b) The kinetics of **9** in presence of Cys (1.0×10^{-5} M), $c(\text{Cys}) = (3.0 \times 10^{-3}$ M), $\lambda_{\text{ex}} = 560$ nm, pH 7.4 In DMF/H₂O (4/1, v/v). 25 °C

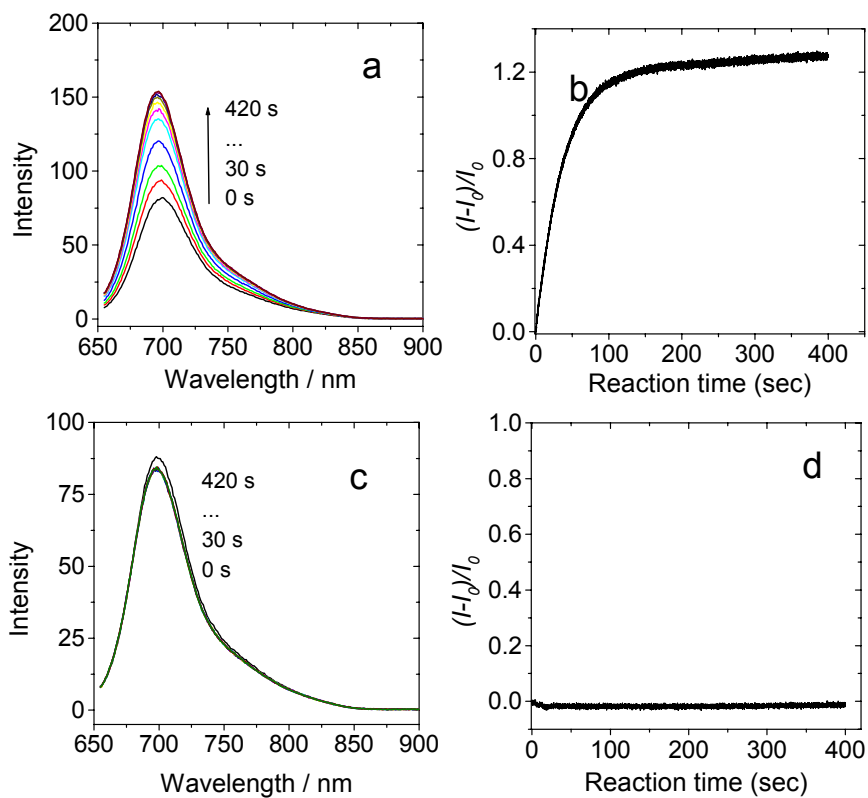


Figure S52. (a) The change of fluorescence in different time in the presence of Cys for **B-3-S** (1.0×10^{-5} M), (b) The kinetics of **B-2-S** in presence of Cys. (c) and (d) The change of fluorescence and the kinetics in different time in presence of Cys for **B-3-C** (1.0×10^{-5} M), $c(\text{Cys}) = 3.0 \times 10^{-3}$ M, $\lambda_{\text{ex}} = 650$ nm, in H₂O/DMF (v/v = 1/4), 25 °C.

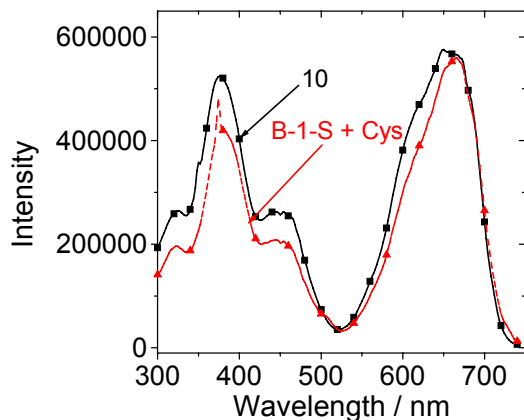


Figure S53. The fluorescence excitation spectra of **B-1-S** in the presence of cysteine and compound **10**.

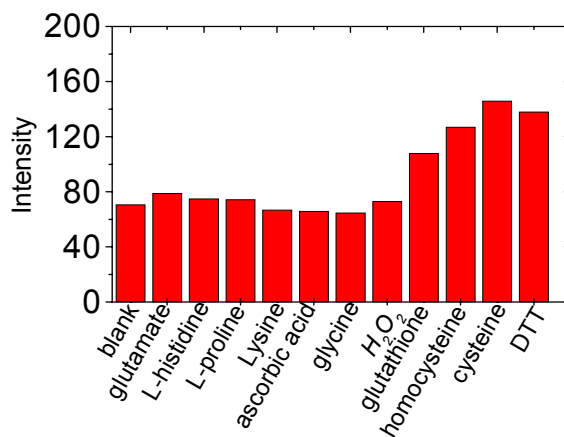


Figure S54. Response of **B-3-S** to different analytes. Relative fluorescence intensity of 10 μ M **B-3-S** at 698 nm ($\lambda_{\text{ex}} = 650$ nm) before and after incubation in the presence of 3 mM analytes at 20°C, pH 7.4, DMF/water (4:1, v/v) solution.

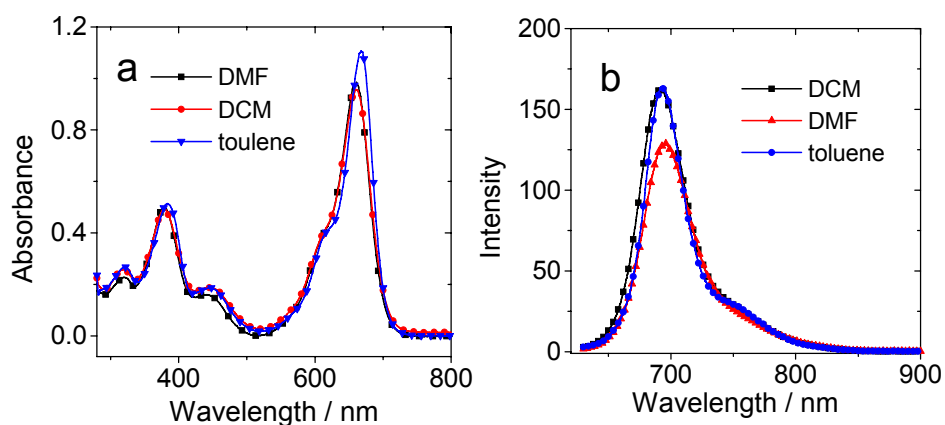


Figure S55. (a) UV-vis absorption spectra of **10** in dichloromethane (DCM), DMF and toluene. (b) Fluorescence emission spectra of the **10** in solvents with different polarity. $\lambda_{\text{ex}} = 620 \text{ nm}$ ($A = 0.48$). ($1.0 \times 10^{-5} \text{ M}$; $20 \text{ }^\circ\text{C}$).

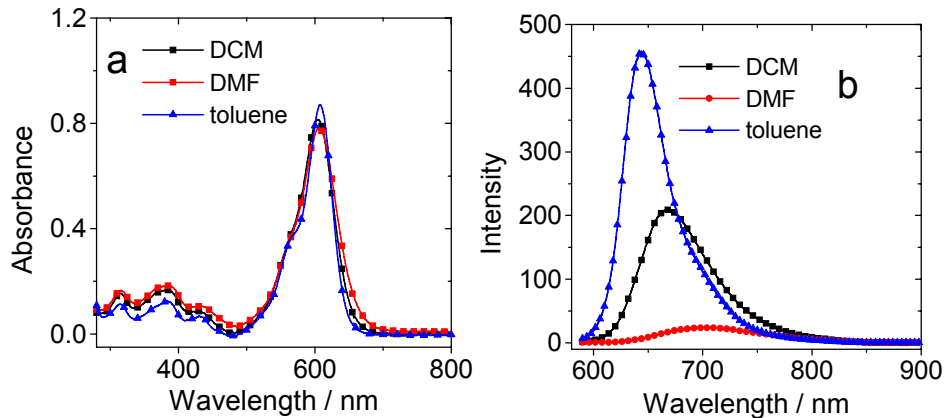


Figure S56. (a) UV/Vis absorption spectra of **11** in dichloromethane (DCM), DMF and toluene. (b) Fluorescence emission spectra of the **11** in solvents with different polarity. $\lambda_{\text{ex}} = 580 \text{ nm}$ ($A = 0.41$). ($1.0 \times 10^{-5} \text{ M}$; $20 \text{ }^\circ\text{C}$).

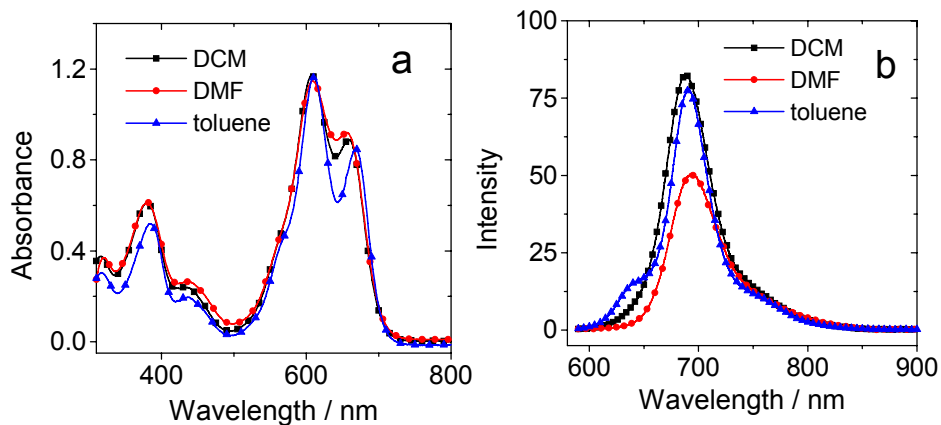


Figure S57. (a) UV-vis absorption spectra of **B-3-C** in dichloromethane (DCM), DMF and toluene. (b) Fluorescence emission spectra of the **B-3-C** in solvents with different polarity. $\lambda_{\text{ex}} = 580 \text{ nm}$ ($A = 0.67$). ($1.0 \times 10^{-5} \text{ M}$; $20 \text{ }^\circ\text{C}$).

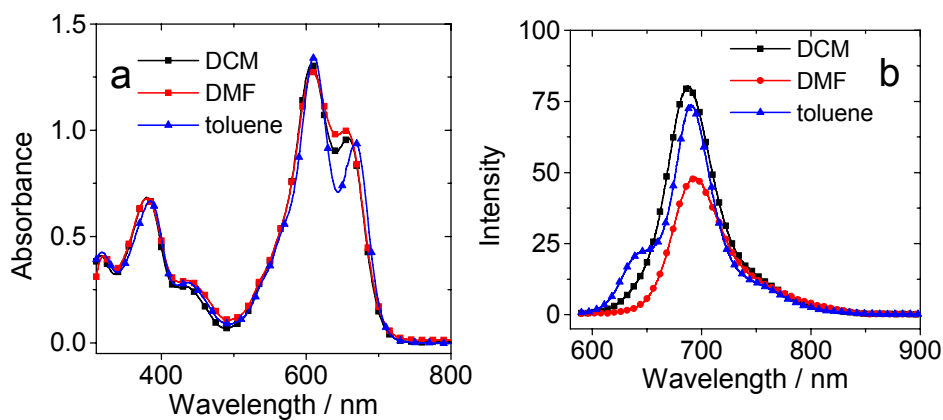


Figure S58. (a) UV/Vis absorption spectra of **B-3-S** in dichloromethane (DCM), DMF and toluene. (b) Fluorescence emission spectra of the **B-3-S** in solvents with different polarity. $\lambda_{\text{ex}} = 580 \text{ nm}$ ($A = 0.75$). ($1.0 \times 10^{-5} \text{ M}$; $20 \text{ }^\circ\text{C}$).

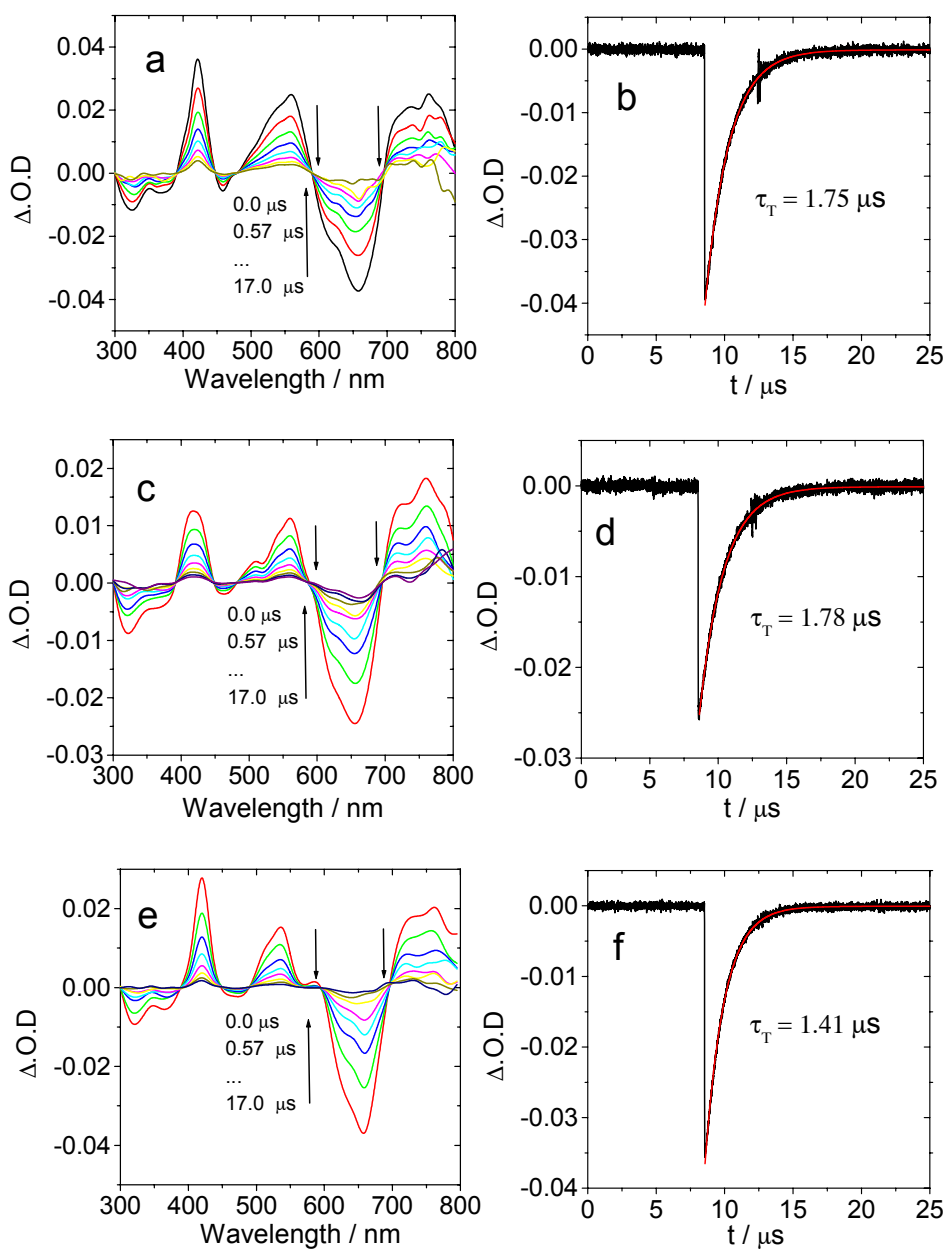


Figure S59. Nanosecond time-resolved transient difference absorption spectra of **10** (a) Transient difference absorption spectra and (b) the corresponding decay trace at 665 nm, $\lambda_{\text{ex}} = 655 \text{ nm}$. (c) Transient difference absorption spectra and (b) the corresponding decay trace at 665 nm, $\lambda_{\text{ex}} = 595 \text{ nm}$, In toluene. (e) Transient difference absorption spectra in DMF/H₂O (4/1 v/v) (f) the corresponding decay trace at 665 nm. $\lambda_{\text{ex}} = 655 \text{ nm}$. ($c = 1.0 \times 10^{-5} \text{ M}$, 25 °C).

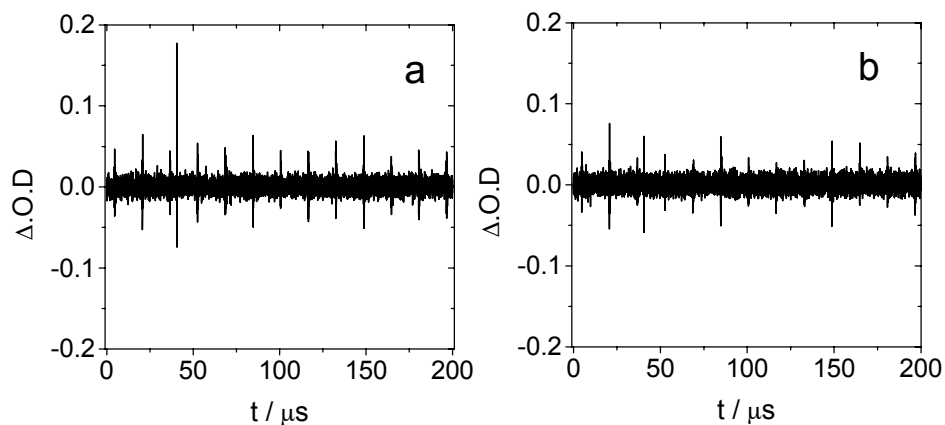


Figure S60. Nanosecond time-resolved transient difference absorption spectra of **9**. the corresponding decay trace at 595 nm, $\lambda_{\text{ex}} = 585$ nm. (a) In deaerated DMF/H₂O (b) In deaerated toluene. $c = 1.0 \times 10^{-5}$ M, 25 °C.

Conclusion: Compound **9** can not produce long lifetime triplet state under the same condition of **B-2-S**.

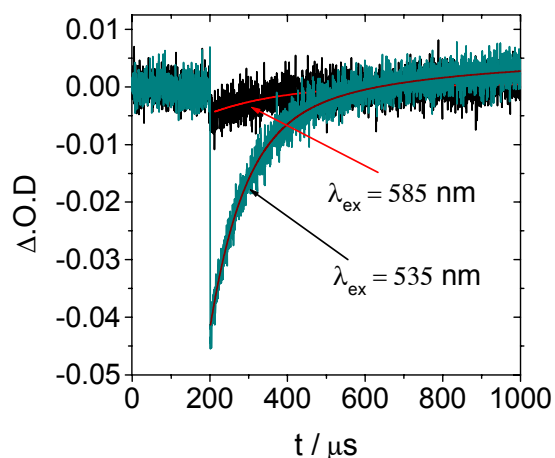


Figure S61. Nanosecond time-resolved transient difference absorption spectra of **B-2-S**. Comparison of the Δ .O.D. at the corresponding decay trace at 595 nm, different wavelength pulse laser was used. In deaerated DMF/H₂O, $c = 1.0 \times 10^{-5}$ M, 25 °C.

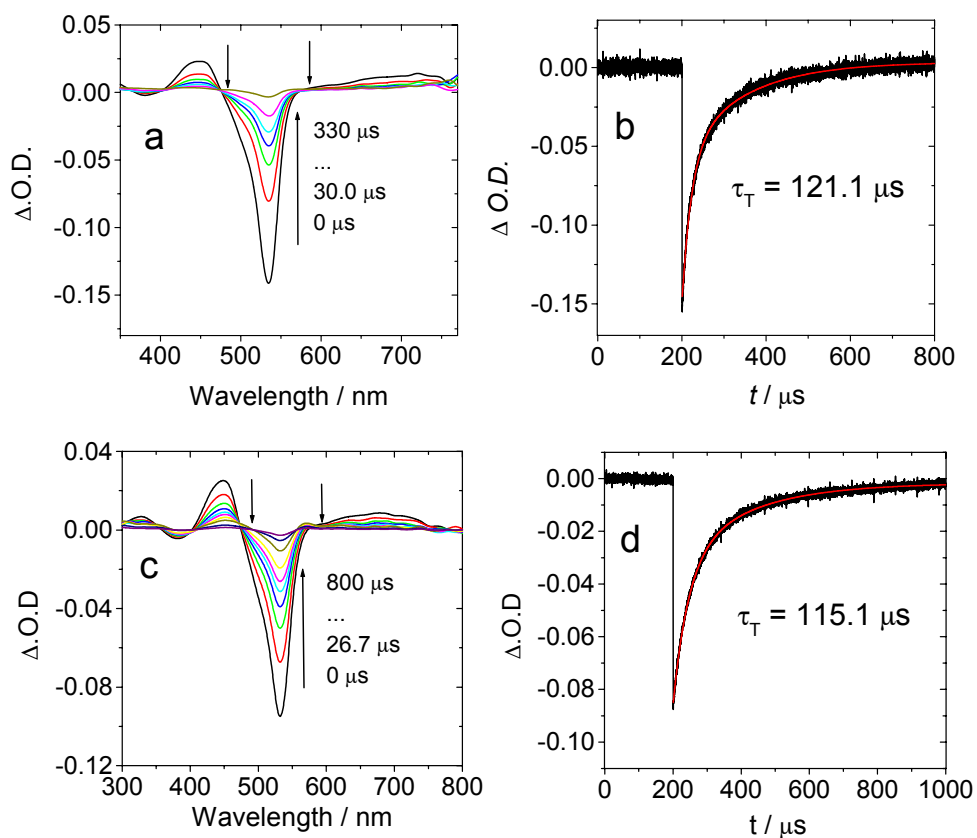


Figure S62. Nanosecond time-resolved transient difference absorption spectra of **B-4** (a) Transient difference absorption spectra in toluene and (b) the corresponding decay trace at 530 nm. In deaerated toluene. (c) Transient difference absorption spectra in toluene and (d) the corresponding decay trace at 530 nm. In deaerated DMF/H₂O = 4/1 $\lambda_{\text{ex}} = 515 \text{ nm}$, $c = 1.0 \times 10^{-5} \text{ M}$, 25 °C.

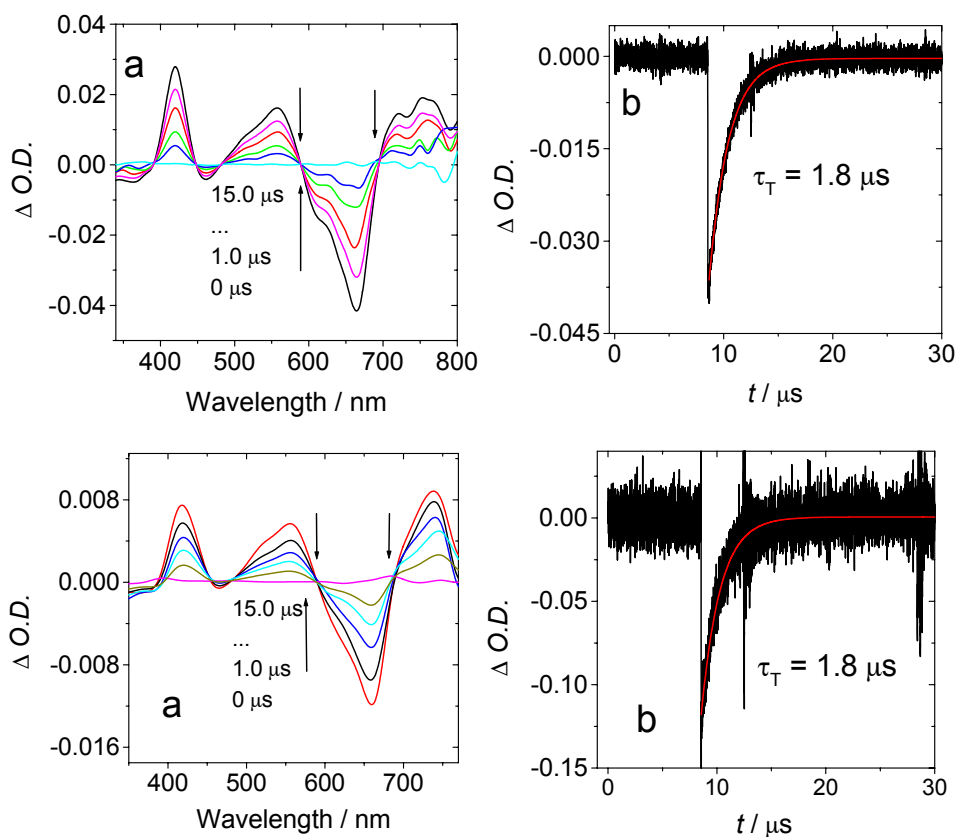


Figure S63. Nanosecond time-resolved transient difference absorption spectra of **10** (a) Transient difference absorption spectra and (b) the corresponding decay trace at 660 nm, $\lambda_{\text{ex}} = 640$ nm (c) Transient difference absorption spectra and (d) the corresponding decay trace at 660 nm, $\lambda_{\text{ex}} = 504$ nm. In deaerated toluene., $c = 1.0 \times 10^{-5}$ M, 25 °C.

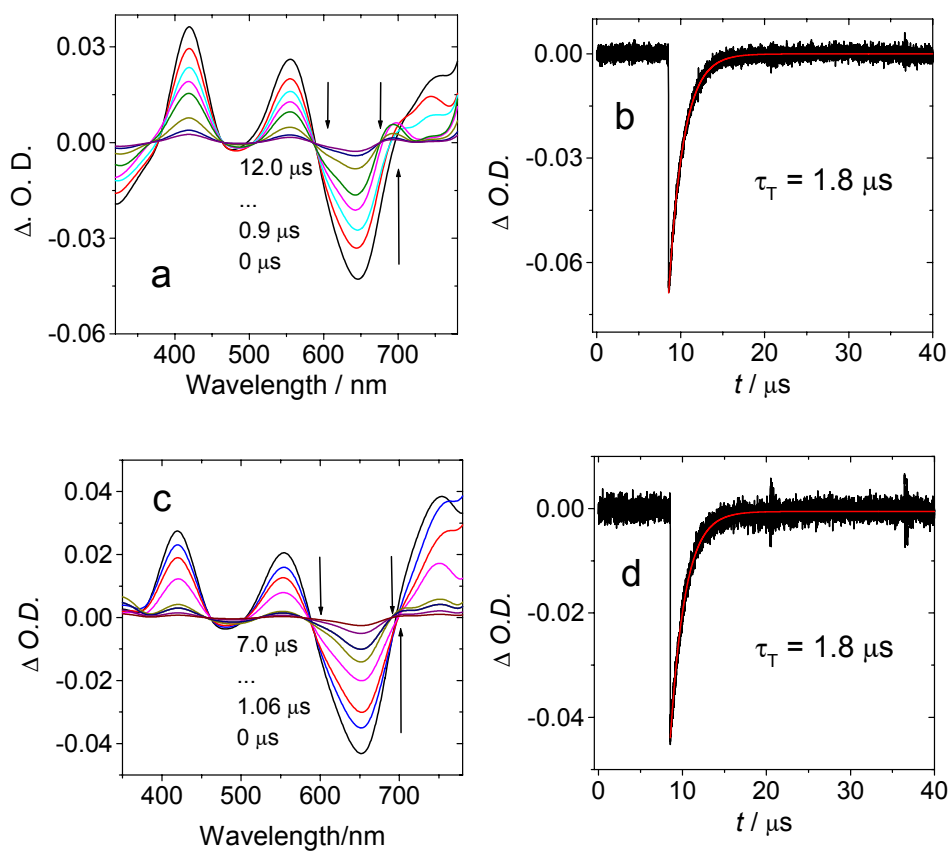


Figure S64. Nanosecond time-resolved transient difference absorption spectra of **B-1-C** (a) Transient difference absorption spectra in toluene and (b) the corresponding decay trace at 660 nm $\lambda_{\text{ex}} = 504 \text{ nm}$. (c) Transient difference absorption spectra in toluene and (d) the corresponding decay trace at 660 nm. In deaerated toluene. $\lambda_{\text{ex}} = 640 \text{ nm}$ In deaerated toluene., $c = 1.0 \times 10^{-5} \text{ M}$, 25 °C.

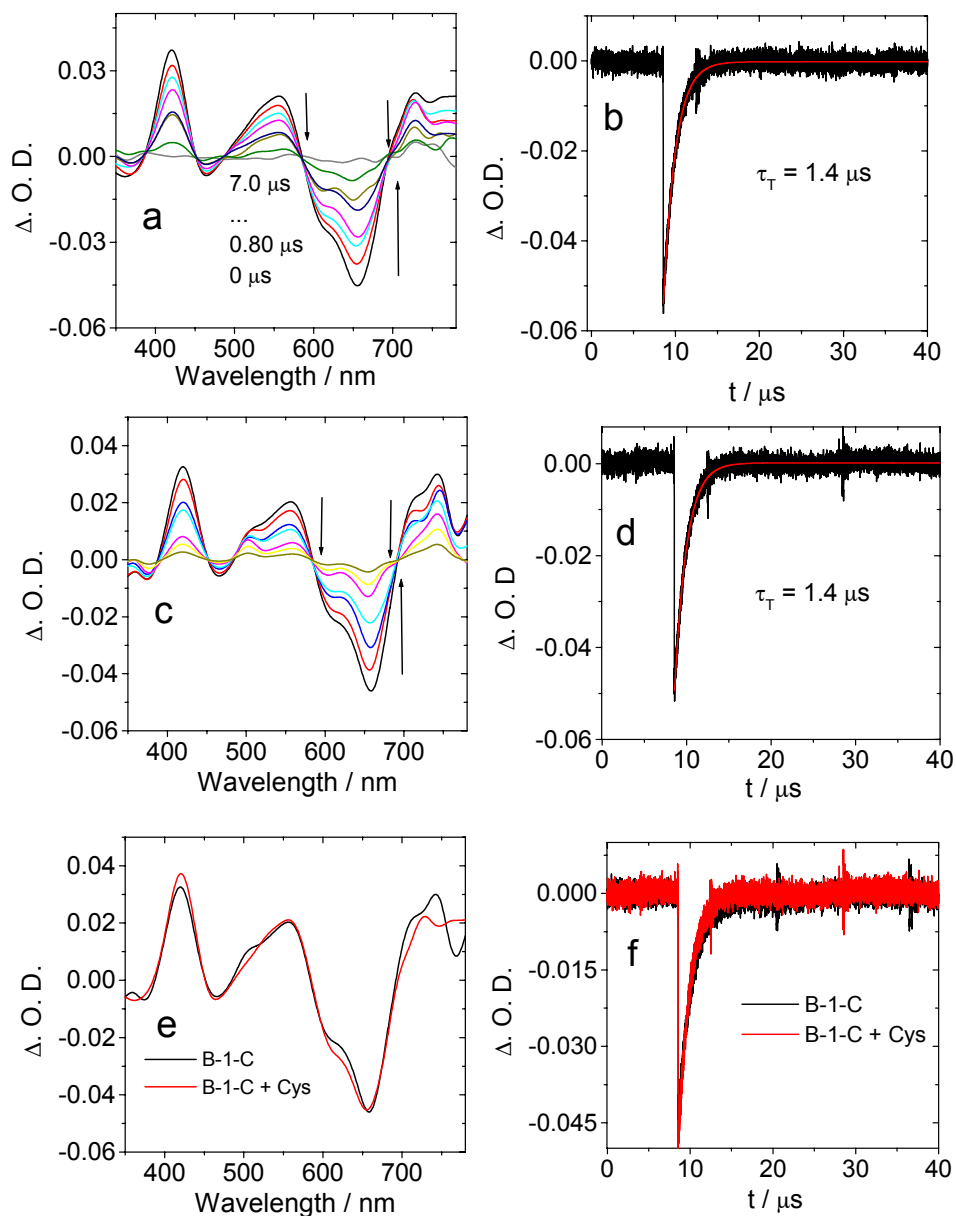


Figure S65. Nanosecond time-resolved transient difference absorption spectra of **B-1-C** (a) Transient difference absorption spectra and (b) the corresponding decay trace at 660 nm. (c) transient difference absorption spectra of **B-1-C + Cys** and (d) the corresponding decay trace at 660 nm. (e) transient difference absorption spectra of **B-1-C + Cys** and **B-1-C** in decay time is 0 μ s and (f) the corresponding decay trace at 660 nm. $\lambda_{\text{ex}} = 504 \text{ nm}$, in DMF/H₂O (4/1 v/v), $c = 1.0 \times 10^{-5} \text{ M}$, $c(\text{Cys}) = 3.0 \times 10^{-3} \text{ M}$ 25 $^{\circ}\text{C}$.

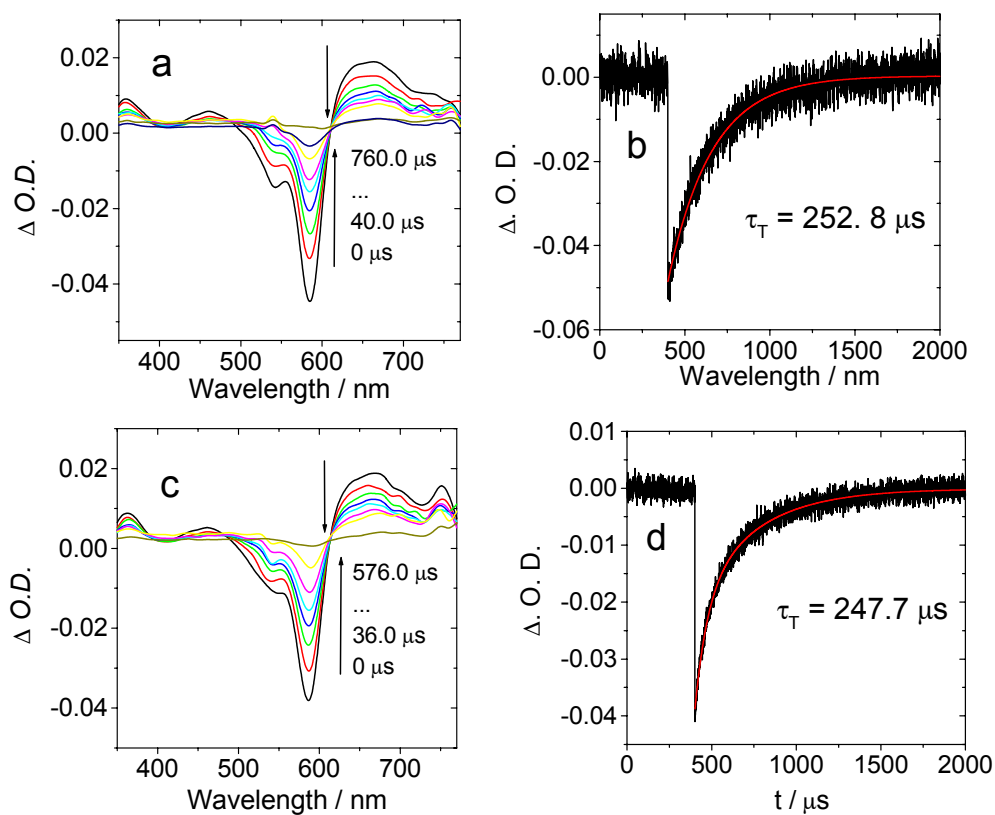


Figure S66. Nanosecond time-resolved transient difference absorption spectra of **B-2-S** and **B-2-C** (a) and (b) **B-2-S**, transient difference absorption spectra and the corresponding decay trace at 580 nm (c) and (d) **B-2-C**, transient difference absorption spectra and the corresponding decay trace at 580 nm, In deaerated toluene $\lambda_{\text{ex}} = 535 \text{ nm}$, $c = 1.0 \times 10^{-5} \text{ M}$, $25 \text{ }^\circ\text{C}$.

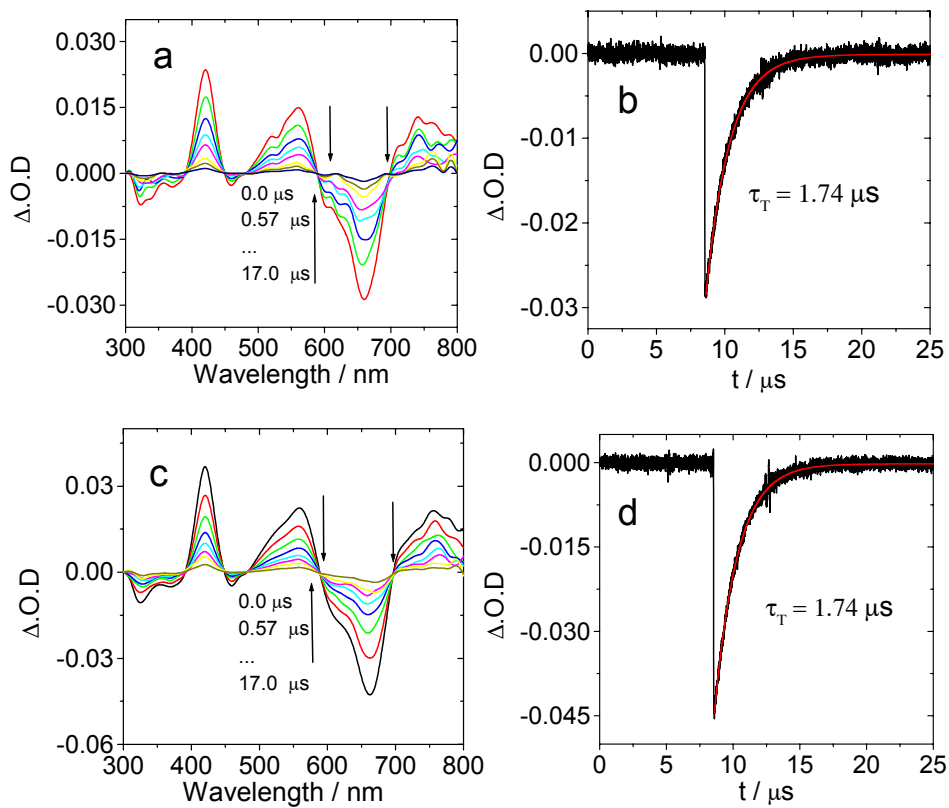


Figure S67. Nanosecond time-resolved transient difference absorption spectra of **B-3-C** (a) Transient difference absorption spectra and (b) the corresponding decay trace at 660 nm $\lambda_{\text{ex}} = 655 \text{ nm}$; (c) transient difference absorption spectra and (d) the corresponding decay trace at 660 nm. $\lambda_{\text{ex}} = 595 \text{ nm}$. In deaerated toluene, $c = 1.0 \times 10^{-5} \text{ M}$, 25 $^{\circ}\text{C}$.

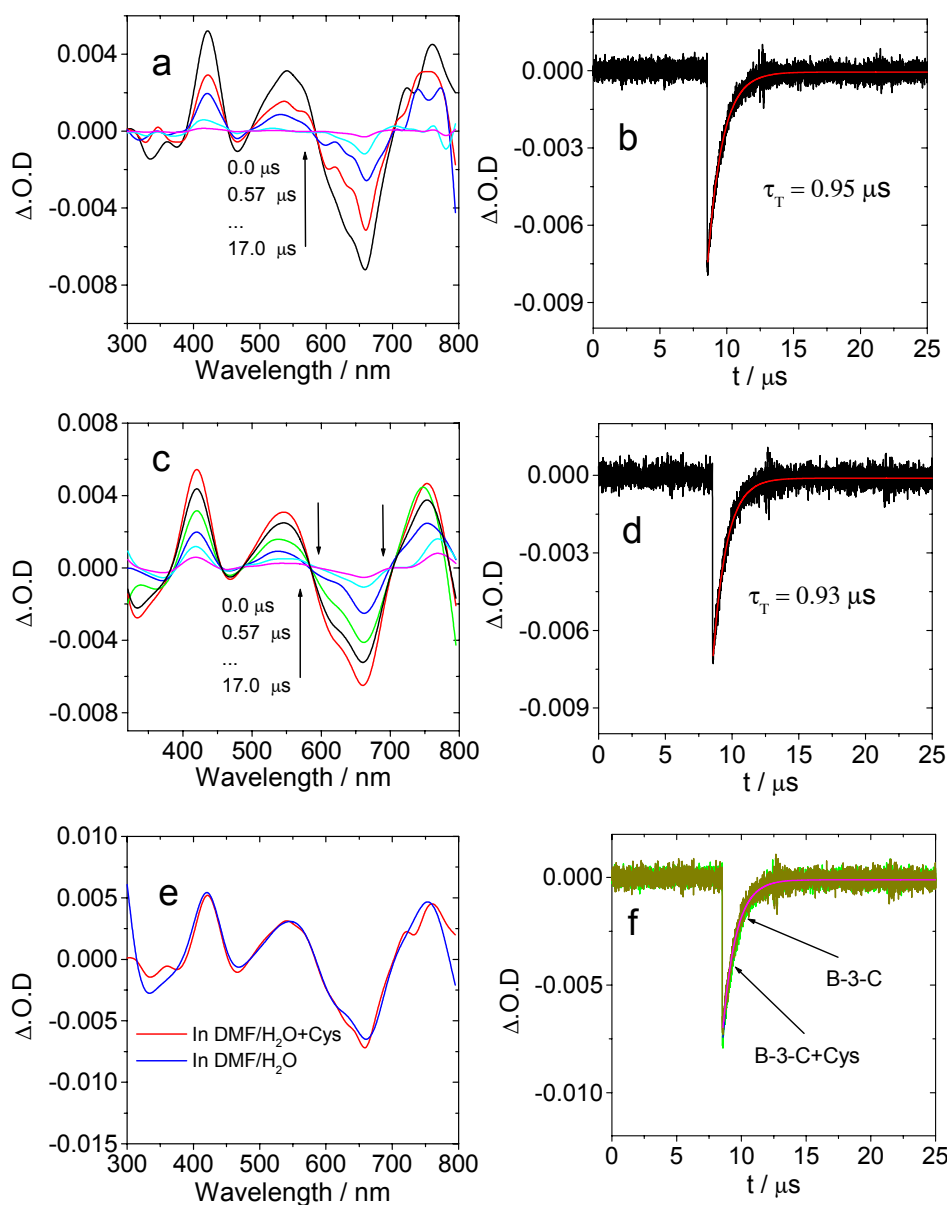


Figure S68. Nanosecond time-resolved transient difference absorption spectra of **B-3-C** (a) Transient difference absorption spectra and (b) the corresponding decay trace at 665 nm. (c) **B-3-C + Cys** transient difference absorption spectra and (d) the corresponding decay trace at 665 nm. (e) Transient difference absorption spectra in DMF/H₂O (4/1 v/v) in decay time is 0 μ s and (f) the corresponding decay trace at 660 nm. $\lambda_{\text{ex}} = 655 \text{ nm}$ In deaerated DMF/H₂O = 4/1 (v/v). $c = 1.0 \times 10^{-5} \text{ M}$, $c(\text{Cys}) = 3.0 \times 10^{-3} \text{ M}$, 25 $^{\circ}\text{C}$.

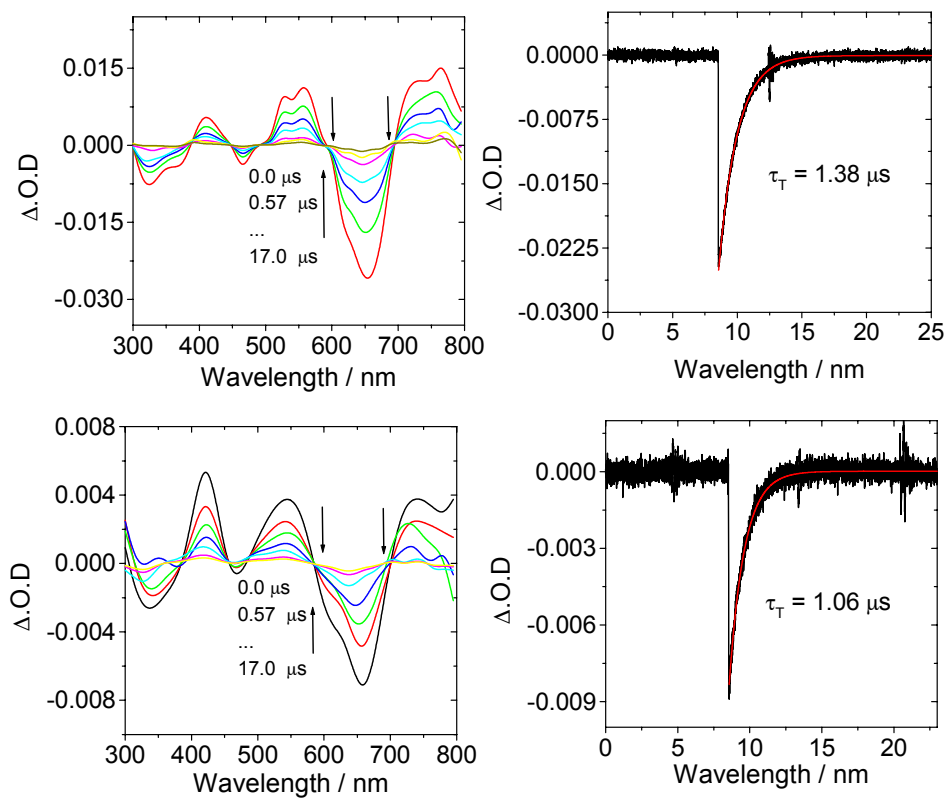


Figure S69. Nanosecond time-resolved transient difference absorption spectra of **10** and **B-3-S** in $\text{DMF}/\text{H}_2\text{O} = 4/1(\text{v/v})$ (a) **10**, Transient difference absorption spectra and (b) the corresponding decay trace at 665 nm, $\lambda_{\text{ex}} = 595 \text{ nm}$. (c) **B-3-S**, Transient difference absorption spectra and (b) the corresponding decay trace at 665 nm, $\lambda_{\text{ex}} = 595 \text{ nm}$ ($c = 1.0 \times 10^{-5} \text{ M}$, $25 \text{ }^\circ\text{C}$).

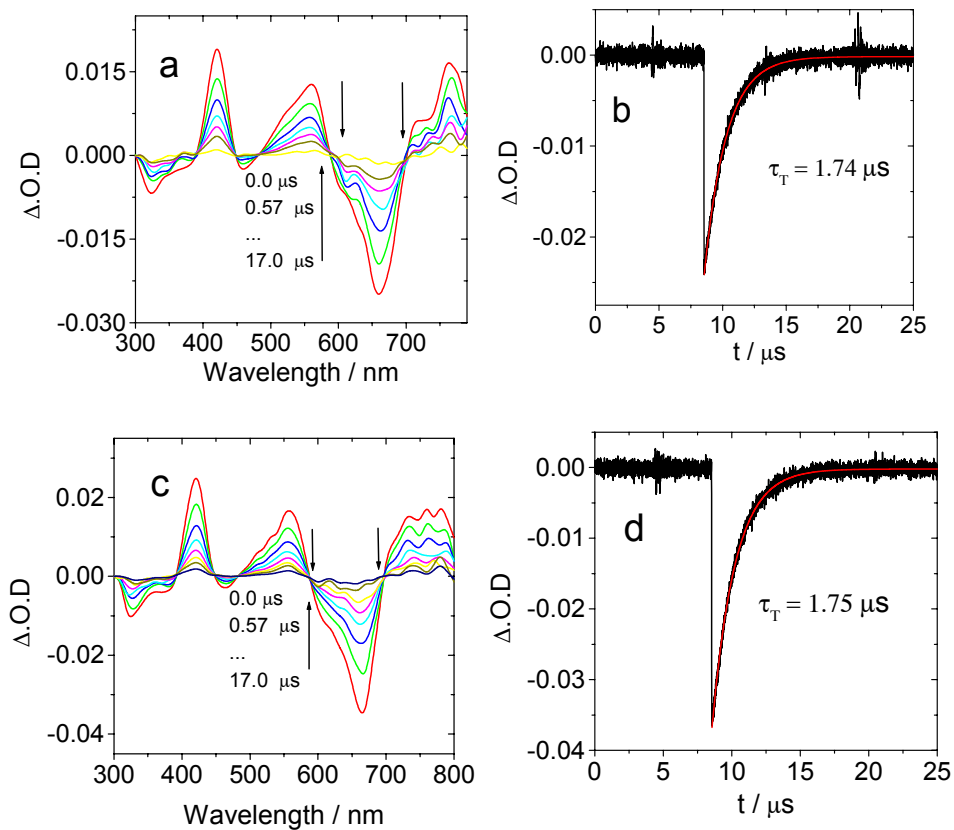


Figure S70. Nanosecond time-resolved transient difference absorption spectra of **B-3-S** (a) Transient difference absorption spectra and (b) the corresponding decay trace at 665 nm $\lambda_{\text{ex}} = 655$ nm; (c) transient difference absorption spectra and (d) the corresponding decay trace at 665 nm. $\lambda_{\text{ex}} = 595$ nm. In deaerated toluene. $c = 1.0 \times 10^{-5}$ M, 25 °C.

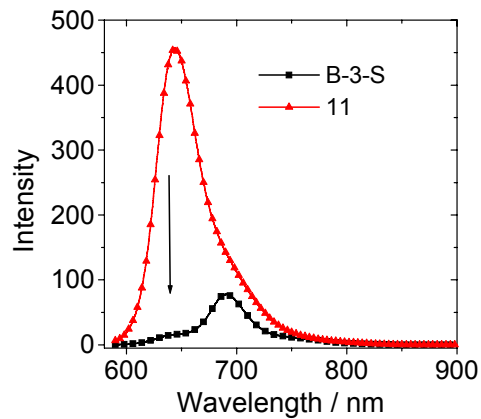


Figure S71. Fluorescence emission spectra of the **B-3-S** and **11** in toluene. $\lambda_{\text{ex}} = 580 \text{ nm}$ ($A = 0.75$). ($1.0 \times 10^{-5} \text{ M}$; $20 \text{ }^\circ\text{C}$).

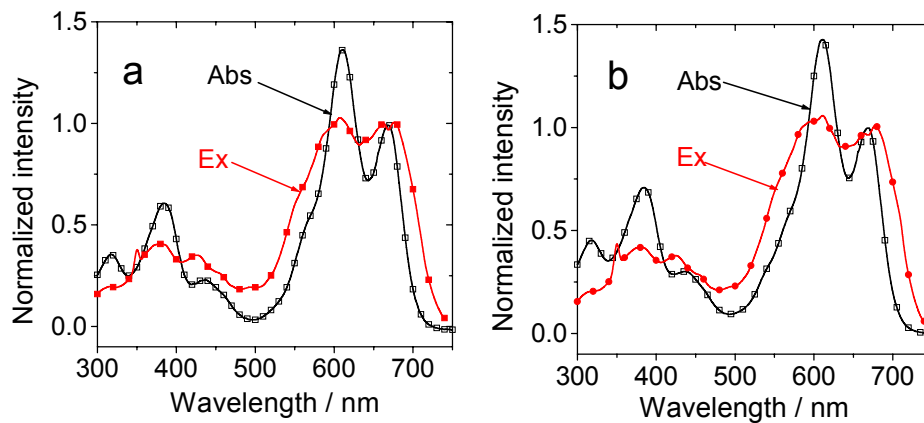


Figure S72. The fluorescence excitation spectra of **B-3-C**, **B-3-S** in toluene. (a) **B-3-C**. (b) **B-3-S**. **B-3-S** and **B-3-C** ($\lambda_{\text{em}} = 720 \text{ nm}$) $1.0 \times 10^{-5} \text{ M}$, $25 \text{ }^\circ\text{C}$.

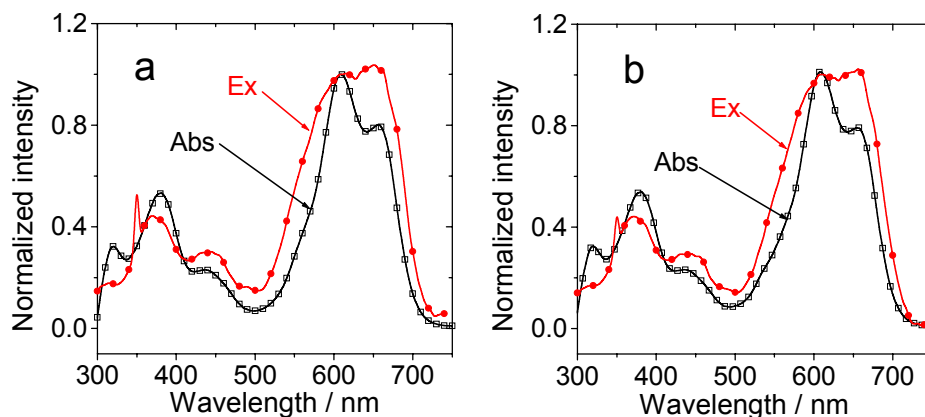


Figure S73 The fluorescence excitation spectra of **B-3-C**, **B-3-S** in DMF/H₂O = 4/1(v/v). (a) **B-3-C**. (b) **B-3-S**. **B-3-S** and **B-3-C** ($\lambda_{em} = 720$ nm) 1.0×10^{-5} M, 25 °C.

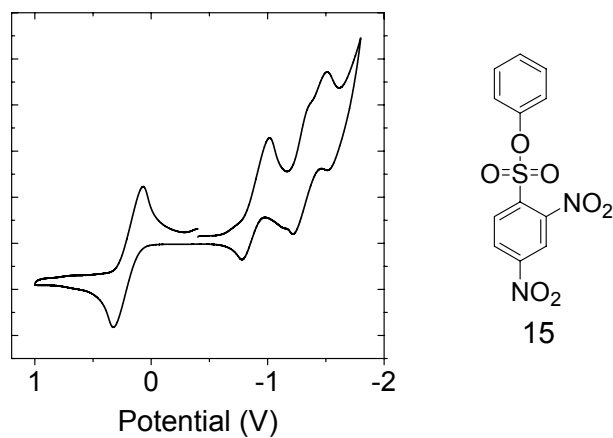


Figure S74. Cyclic voltammogram of **15** respectively. Ferrocene (Fc) was used as internal reference ($E_{1/2} = +0.64$ V (Fc⁺/Fc) vs. standard hydrogen electrode). In deaerated CH₂Cl₂ solutions and 0.10 M Bu₄NPF₆ as supporting electrode, Ag/AgNO₃ reference electrode, Scan rates: 0.1 V/s.

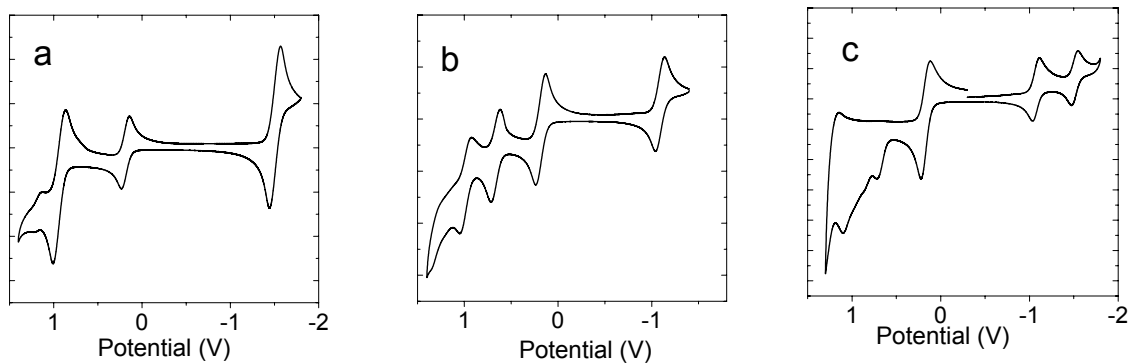


Figure S75. Cyclic voltammogram of **Bodipy**, **10** and **B-1-S** respectively. (a) **Bodipy**, (b) **10**, (c) **B-1-S**. Ferrocene (Fc) was used as internal reference ($E_{1/2} = +0.64$ V (Fc⁺/Fc) vs. standard hydrogen electrode). In deaerated CH₂Cl₂ solutions and 0.10 M Bu₄NPF₆ as supporting electrode, Ag/AgNO₃ reference electrode, Scan rates: 0.1 V/s.

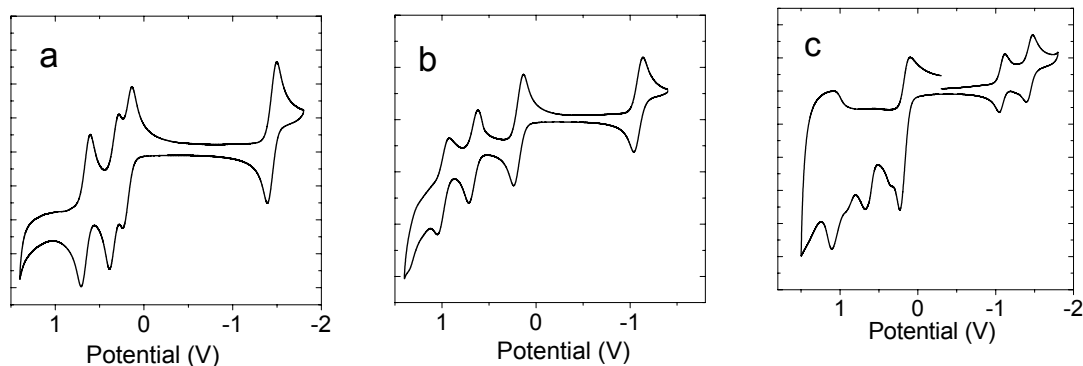


Figure S76. Cyclic voltammogram of **11**, **10** and **B-3-S** respectively. (a) **11**, (b) **10**, (c) **B-3-S**. Ferrocene (Fc) was used as internal reference ($E_{1/2} = +0.64$ V (Fc⁺/Fc) vs. standard hydrogen electrode). In deaerated CH₂Cl₂ solutions and 0.10 M Bu₄NPF₆ as supporting electrode, Ag/AgNO₃ reference electrode, Scan rates: 0.1 V/s.

The free energy changes of the electron transfer process (charge separation, CS), can be calculated with the Weller equation.

$$\Delta G^0_{CS} = e[E_{OX} - E_{RED}] - E_{00} + \Delta G_S \quad (\text{Eq. 1})$$

$$\Delta G_S = -\frac{e^2}{4\pi\epsilon_S\epsilon_0 R_{CC}} - \frac{e^2}{8\pi\epsilon_0} \left(\frac{1}{R_D} + \frac{1}{R_A} \right) \left(\frac{1}{\epsilon_{REF}} - \frac{1}{\epsilon_S} \right) \quad (\text{Eq. 2})$$

$$E_{CTS} = E_{1/2}(D^{\bullet+}/D) - E_{1/2}(A/A^{\bullet-}) + \Delta G_S \quad (\text{Eq. 3})$$

Where ΔG_S is the static Coulombic energy, which is described by Eq. 2. e = electronic charge, E_{OX} = half-wave potential for one-electron oxidation of the electron-donor unit, E_{RED} = half-wave potential for one-electron reduction of the electron-acceptor unit; note herein the anodic and cathodic peak potentials were used because in some cases the oxidation is irreversible therefore the formal potential $E_{1/2}$ cannot be derived; E_{00} = energy level approximated with the fluorescence emission wavelength (for the singlet excited state), ϵ_S = static dielectric constant of the solvent, R_{CC} = (18.0 Å) center-to-center separation distance determined by DFT optimization of the geometry, R_D (4.0 Å) is the radius of the BODIPY-based donor, R_A (4.0 Å) is the radius of the electron acceptor, ϵ_{REF} is the static dielectric constant of the solvent used for the electrochemical studies, ϵ_0 permittivity of free space. The solvents used in the calculation of free energy of the electron transfer is CH_2Cl_2 ($\epsilon = 8.9$) Based on these parameters, E_{ox} is the first peak in the anodic scan, and E_{red} is the first peak in the cathodic scan.

In CH_2Cl_2 : B-1-S, B-2-S and B-3-S, $\Delta G_S = -0.089$ eV.

In DMF/ $\text{H}_2\text{O} = 4/1$ (v/v): B-1-S, B-2-S and B-3-S, $\Delta G_S = -0.34$ eV.

(1) The S_1 state of energy donor as $E_{o,o}$

In DMF/ $\text{H}_2\text{O} = 4/1$ (v/v) :

$$\Delta G^0_{CS}(\text{B-1-S}) = e[+1.00 - (-1.07)] - 2.40 + (-0.34) = -0.68 \text{ eV}$$

$$E_{CTS}(\text{B-1-S}) = +1.00 - (-1.07) + (-0.34) = 1.73 \text{ eV}$$

$$\Delta G^0_{CS}(\text{B-2-S}) = e[+1.04 - (-0.82)] - 2.21 + (-0.34) = -0.69 \text{ eV}$$

$$E_{CTS}(\text{B-2-S}) = +1.04 - (-0.82) + (-0.34) = 1.52 \text{ eV}$$

$$\Delta G^0_{CS}(\text{B-3-S}) = e[+0.34 - (-1.09)] - 1.85 + (-0.34) = -0.76 \text{ eV}$$

$$E_{\text{CTS}}(\text{B-3-S}) = +0.34 - (-1.09) + (-0.34) = 1.09 \text{ eV}$$

In CH_2Cl_2

$$\Delta G^{\circ}_{\text{CS}}(\text{B-1-S}) = e[+1.00 - (-1.07)] - 2.41 + (-0.089) = -0.43 \text{ eV}$$

$$E_{\text{CTS}}(\text{B-1-S}) = +1.00 - (-1.07) + (-0.089) = 1.98 \text{ eV}$$

$$\Delta G^{\circ}_{\text{CS}}(\text{B-2-S}) = e[+1.04 - (-0.82)] - 2.21 + (-0.089) = -0.44 \text{ eV}$$

$$E_{\text{CTS}}(\text{B-2-S}) = +1.04 - (-0.82) + (-0.089) = 1.77 \text{ eV}$$

$$\Delta G^{\circ}_{\text{CS}}(\text{B-3-S}) = e[+0.35 - (-1.09)] - 1.85 + (-0.089) = -0.51 \text{ eV}$$

$$E_{\text{CTS}}(\text{B-3-S}) = +0.35 - (-1.09) + (-0.089) = 1.34 \text{ eV}$$

(2) The T_1 state of energy donor as $E_{o,o}$

In DMF/ H_2O = 4/1(v/v) :

$$\Delta G^{\circ}_{\text{CS}}(\text{B-1-S}) = e[+1.00 - (-1.07)] - 1.52 + (-0.34) = +0.21 \text{ eV}$$

$$\Delta G^{\circ}_{\text{CS}}(\text{B-2-S}) = e[+1.04 - (-0.82)] - 1.55 + (-0.34) = -0.032 \text{ eV}$$

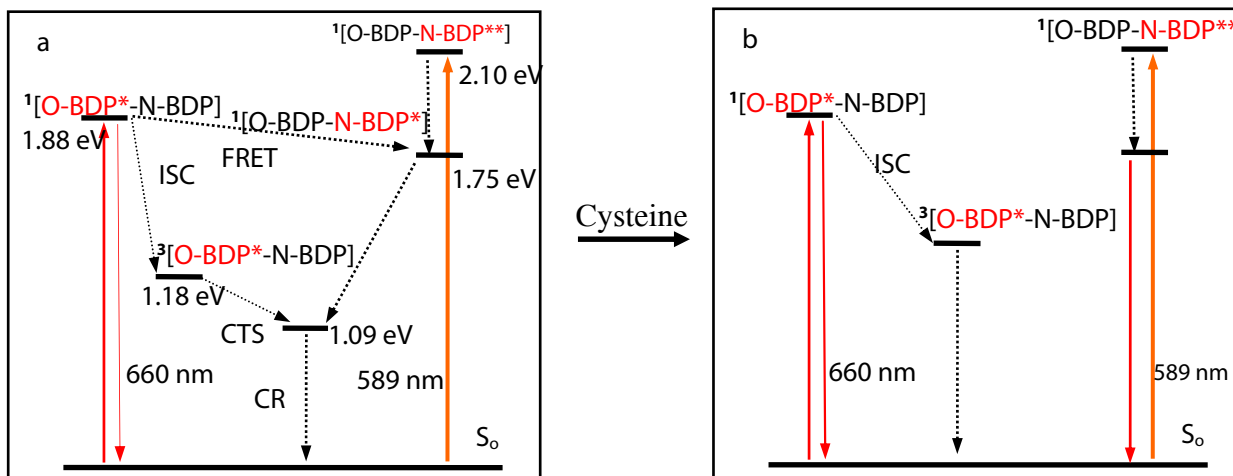
$$\Delta G^{\circ}_{\text{CS}}(\text{B-3-S}) = e[+0.34 - (-1.09)] - 1.12 + (-0.34) = -0.15 \text{ eV}$$

In CH_2Cl_2

$$\Delta G^{\circ}_{\text{CS}}(\text{B-1-S}) = e[+1.00 - (-1.07)] - 1.52 + (-0.089) = +0.46 \text{ eV}$$

$$\Delta G^{\circ}_{\text{CS}}(\text{B-2-S}) = e[+1.04 - (-0.82)] - 1.55 + (-0.089) = +0.22 \text{ eV}$$

$$\Delta G^{\circ}_{\text{CS}}(\text{B-3-S}) = e[+0.34 - (-1.09)] - 1.12 + (-0.089) = +0.10 \text{ eV}$$



Scheme S4. Simplified Jablonski diagram illustrating the photophysical processes involved in (a) **B-3-S** in the absence of Cysteine and (b) **B-3-S** in the presence of Cysteine. [O-BDP-N-BDP] stands for **B-3-S**. The component at the excited state was designated with red color and a asterisk. The number of the superscript designated either the singlet or the triplet excited state. The fluorescence and the triplet state of **B-3-S** were switched by the presence and the absence of Cysteine. Note in the absence of Cysteine, the fluorescence of **B-3-S** were quenched by charge transfer. In the presence of Cysteine, this disulfide bond is cleaved and intramolecular electron transfer disappear, as a result the fluorescence Bodipy and high singlet oxygen quantum yield was observed .

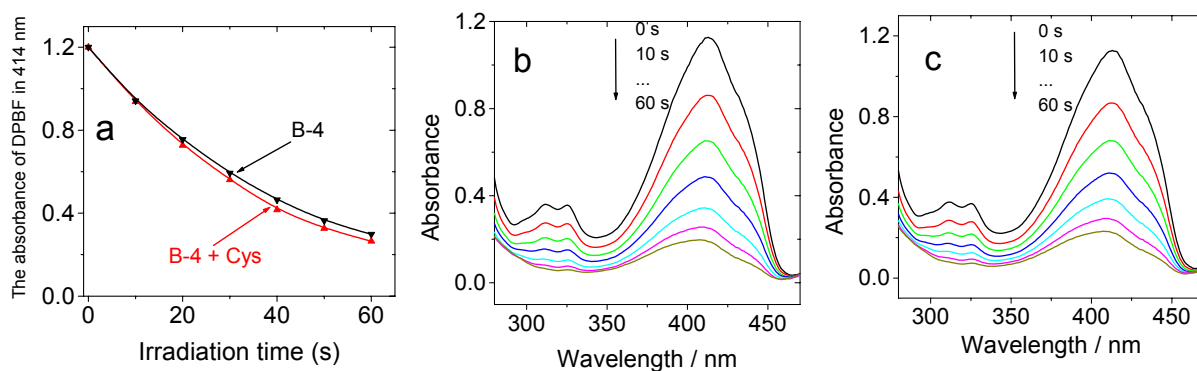


Figure S77. Switching of the singlet oxygen ($^1\text{O}_2$) photosensitizing ability of the compounds in the absence and the presence of Cysteine. The decreasing of the absorption of $^1\text{O}_2$ scavenger 1,3-diphenylisobenzofuran (DPBF) at 410 nm was monitored upon the monochromic light irradiation. UV/Vis absorption spectral changes **B-4** as photosensitizer (a) absorbance of DPBF at 410 nm changes in the absence and in the presence of Cysteine ($\lambda_{\text{ex}} = 535 \text{ nm}$). (b) in the absence of Cysteine and (c) in the presence of Cysteine. c [photosensitizers] = $1.0 \times 10^{-5} \text{ M}$ in $\text{H}_2\text{O}/\text{DMF}$ (v/v = 1/4), 25 °C.

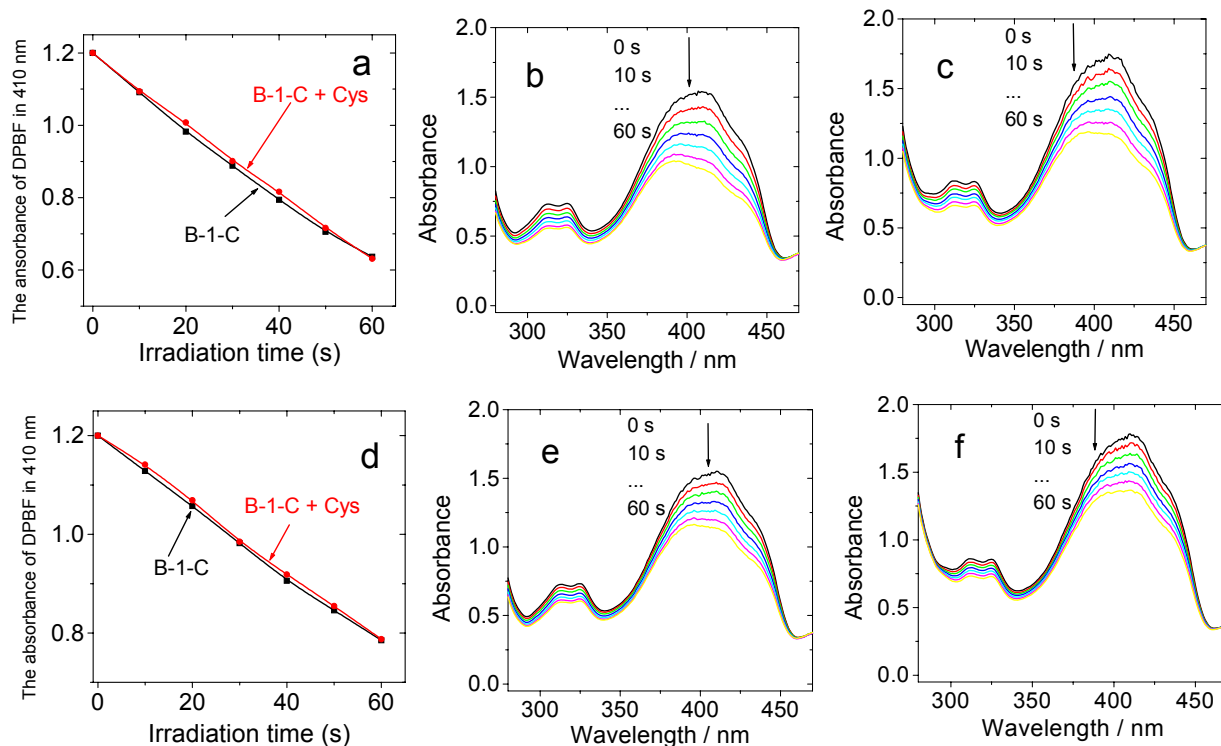


Figure S78. Switching of the singlet oxygen ($^1\text{O}_2$) photosensitizing ability of the compounds in the absence and the presence of Cysteine. The decreasing of the absorption of $^1\text{O}_2$ scavenger 1,3-diphenylisobenzofuran (DPBF) at 410 nm was monitored upon the monochromic light irradiation. UV/Vis absorption spectral changes **B-1-C** as photosensitizer (a) absorbance of DPBF at 410 nm changes in the absence and in the presence of Cysteine ($\lambda_{\text{ex}} = 504 \text{ nm}$). (b) in the absence of Cysteine and (c) in the presence of Cysteine. (d), (e) and (f) The corresponding change for **B-1-C** as photosensitizer ($\lambda_{\text{ex}} = 664 \text{ nm}$). c [photosensitizers] = $1.0 \times 10^{-5} \text{ M}$ in $\text{H}_2\text{O}/\text{DMF}$ (v/v = 1/4), $25 \text{ }^\circ\text{C}$.

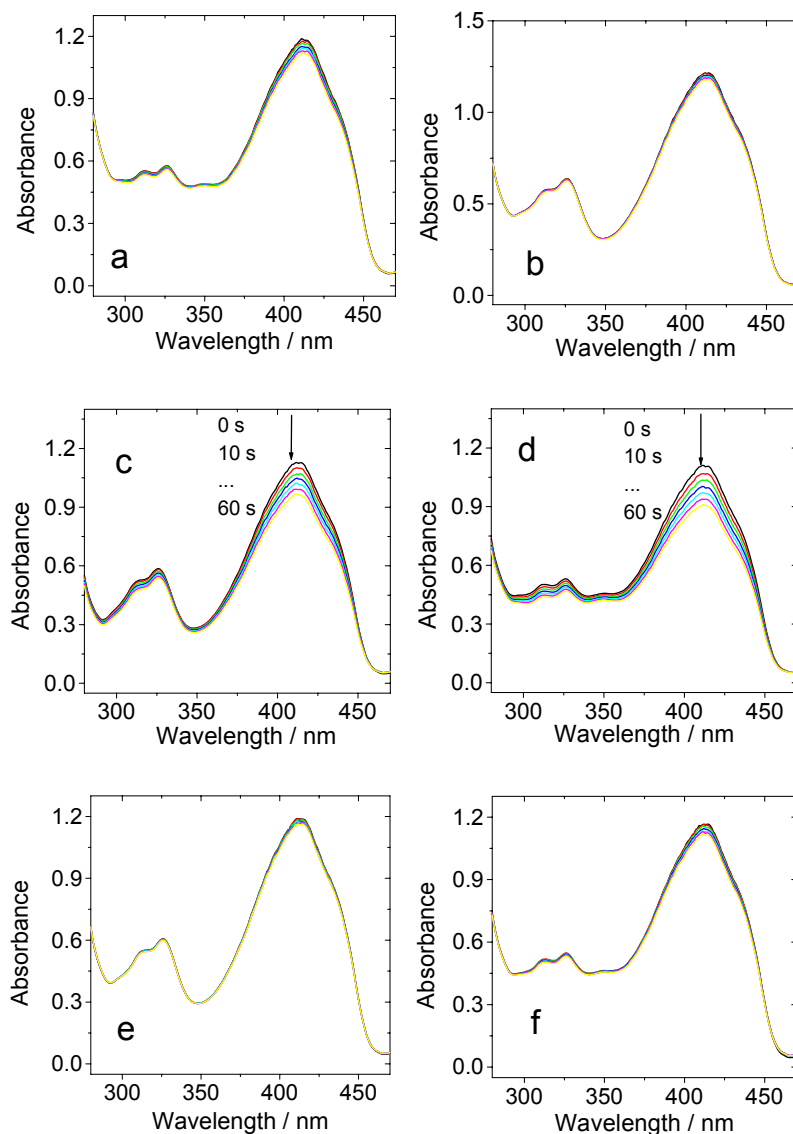


Figure S79. Switching of the singlet oxygen ($^1\text{O}_2$) photosensitizing ability of the compounds in the absence and the presence of Cysteine. The decreasing of the absorption of $^1\text{O}_2$ scavenger 1,3-diphenylisobenzofuran (DPBF) at 414 nm was monitored upon the monochromatic light irradiation. (a) and (b) UV-vis absorption spectral changes **B-2-S** as photosensitizer (a) in absence of Cysteine. (b) in the presence of Cysteine ($\lambda_{\text{ex}}=586$ nm). (c), (d), (e) and (f) **B-2-C** as photosensitizer. (c) in the absence of Cysteine and (d) in the presence of Cysteine ($\lambda_{\text{ex}}=535$ nm). (e) in the absence of Cysteine and (f) in the presence of Cysteine ($\lambda_{\text{ex}}=586$ nm).. c [photosensitizers] = 1.0×10^{-5} M, $c(\text{Cys})=3.0 \times 10^{-3}$ M, in $\text{H}_2\text{O}/\text{DMF}$ (v/v =1/4), 25 °C.

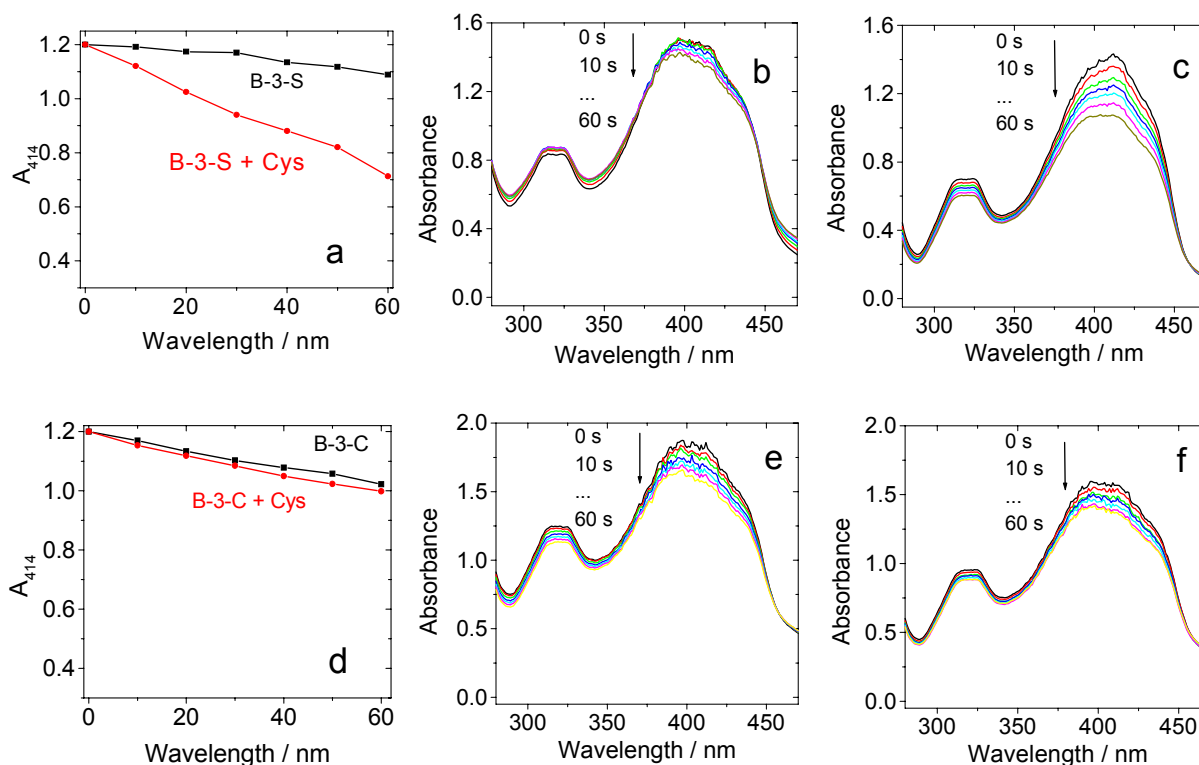


Figure S80. Switching of the singlet oxygen ($^1\text{O}_2$) photosensitizing ability of the compounds in the absence and the presence of Cysteine. The decreasing of the absorption of $^1\text{O}_2$ scavenger 1,3-diphenylisobenzofuran (DPBF) at 414 nm was monitored upon the monochromic light irradiation. UV/Vis absorption spectral changes (a), (b) and (c) **B-3-S** as photosensitizer (a) absorbance of DPBF at 414 nm changes in the absence and in the presence of Cysteine ($\lambda_{\text{ex}} = 664 \text{ nm}$). (b) in the absence of Cysteine and (c) in the presence of Cysteine. (d), (e) and (f) The corresponding change for **B-3-C** as photosensitizer ($\lambda_{\text{ex}} = 664 \text{ nm}$). c [photosensitizers] = $1.0 \times 10^{-5} \text{ M}$, c (Cys) = $3.0 \times 10^{-3} \text{ M}$, in $\text{H}_2\text{O}/\text{DMF}$ (v/v = 1/4), $25 \text{ }^\circ\text{C}$.

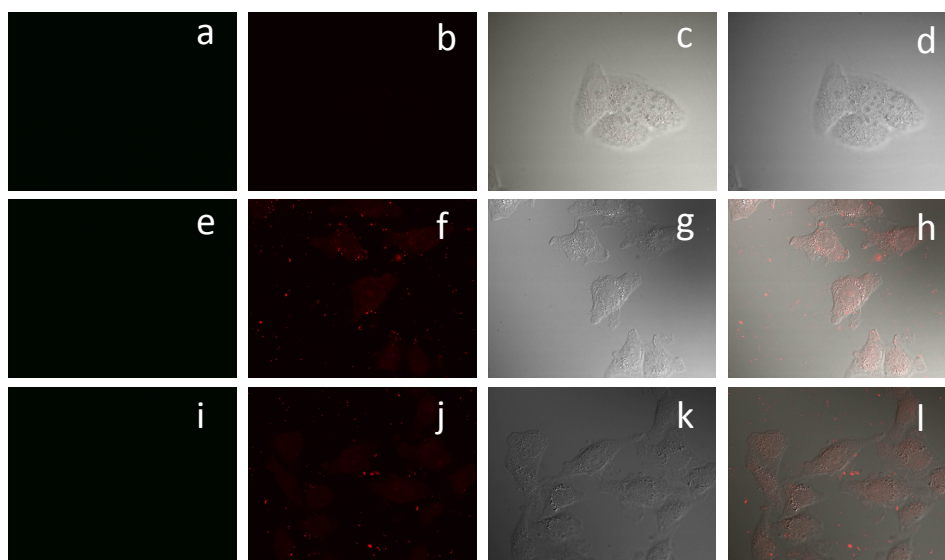


Figure S81. Confocal laser fluorescence microscopic images of HeLa cells. (a) and (b) Luminescence images of HeLa cells; (e) and (f) Luminescence images of HeLa cells incubated with **B-1-C** (25 μM) for 3 h. (i) and (j) Luminescence images of HeLa cells pretreated with *N*-methylmaleimide (0.5 mM) for 12 h and incubated with **B-1-C** (25 μM) for 3 h. (a, e, i) $\lambda_{\text{ex}} = 488 \text{ nm}$, $\lambda_{\text{em}} = 490\text{--}550\text{nm}$. (b, f, j) $\lambda_{\text{ex}} = 635 \text{ nm}$, $\lambda_{\text{em}} = 650\text{--}750\text{nm}$. the corresponding bright field images of (c, g, k); (d, h, l) are the overlay of respective luminescence and bright images.

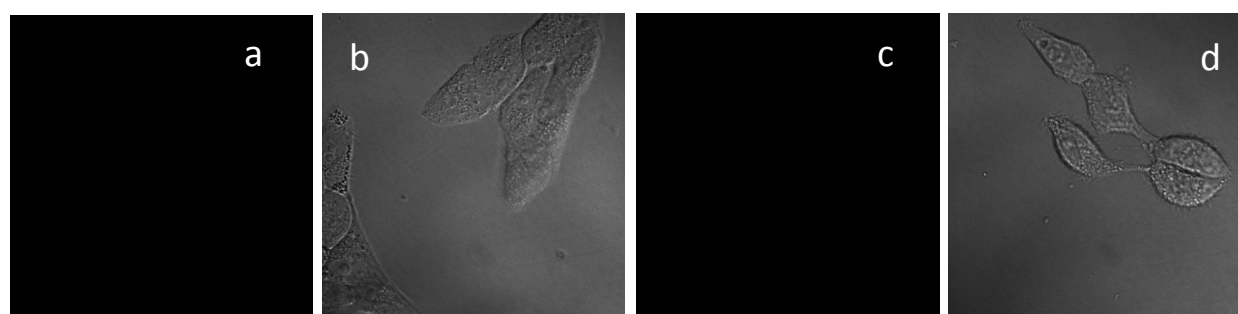


Figure S82. Confocal laser fluorescence microscopic images of the PDT effect for HeLa cells. **DCFH-DA** as singlet oxygen indicator intracellular. (a) dark field, (b) bright field, condition: no photosensitizers and no light. (c) dark field, (d) bright field, condition: **B-2-C** and no light. $c(\text{photosensitizer}) = 2.5 \mu\text{M}$, $c(\text{DCFH-DA}) = 2.0 \mu\text{M}$, $\lambda_{\text{ex}} = 488 \text{ nm}$, $\lambda_{\text{em}} = 500\text{--}550 \text{ nm}$.

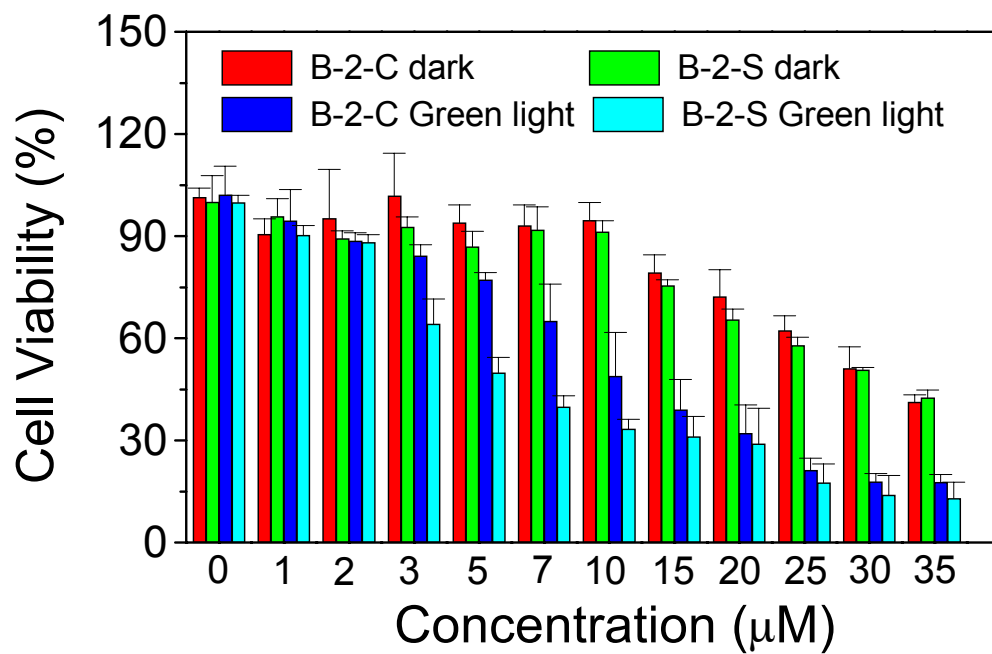


Figure S83. Comparison with the cytotoxic effects of **B-2-S** and **B-2-C** on HeLa cells in the absence of light and presence of light ($\lambda = 530 \pm 20$ nm, 5 mW/cm²), cells viability was measured by MTT assay.